THE UNIVERSITY *of* EDINBURGH

The role of 11βHSD2 in salt and water homeostasis

Louise Christine Evans

Doctor of Philosophy

Department of Molecular Physiology

The University of Edinburgh

2011

Declaration

I declare that unless otherwise stated the work in this thesis is entirely my own, and it has been composed by myself.

Louise Christine Evans

Acknowledgments

The experiments for this thesis were conducted in the Molecular Physiology Lab. I am very grateful to all of the members who helped make my PhD so enjoyable. I also acknowledge the British Heart Foundation for funding the project.

First and foremost, I would like to thank my primary supervisor, Matt Bailey, for his constant support and expert guidance throughout my PhD. Additional thanks to my secondary supervisor, John Mullins, for all of his help and advice. Exceeding this, their combined commitment to my "personal-development" is duly acknowledged: despite their methods involving emulating Machiavelli and wearing a sumo suit.

I am particularly grateful to Chris Kenyon, whose wise words resulted in some of my key experiments, and whose radiation training resulted in…time will tell. Thanks to Gill Brooker for her excellent surgical training, secondary only to her entertaining stories, and Dawn Livingstone for her q-PCR expertise. Additional thanks to Eilidh Craigie, Ali Ashek and Carl Tucker, who were always quick to provide help, chocolate and an appropriate anecdote respectively: although I suspect that some of the anecdotes were fabricated for the occasion. I gratefully acknowledge: the staff in the BRR for their assistance, particularly Will who made decaps bearable, and my committee, Bryan Conway and Megan Holmes, for their intellectual input throughout. Thanks to the two Robs: The Dr, who patiently and calmly (for the most part) guided me through the world of molecular biology, and The Physicist, whose quick wit provided stress relief when commercially available stress balls failed. Finally, special thanks to my friends and family, who, for the past three years have listened to, and feigned interest in, the highs and lows of urine collection.

Abbreviations List

11βHSD1-	11β-Hydroxysteroid Dehydrogenase Type 1
11βHSD2-	11β-Hydroxysteroid Dehydrogenase Type 2
β-gal-	β-galactosidase

A

AC-	Adenylate Cyclase
ACTH-	Adrenocorticotropic Hormone
AF-	Activation Function
AKAP-	A Kinase Anchor Protein
AME-	Apparent Mineralocorticoid Excess
AngII-	Angiotensin II
ANOVA-	Analysis of Variance
AP-	Area Postrema
ApoE-	Apolipoprotein-E
APS-	Ammonium Peroxodisulphate
AQP-	Aquaporin
ASC-	Activating Signal Co-Integrator
ASDN-	Aldosterone Sensitive Distal Nephron
ATP-	Adenosine Triphosphate
AVP-	Vasopressin

B

BK-	Big Conductance Calcium Activated Potassium Channel
BOLD-	Blood Oxygen-Level Dependent
BSA-	Bovine Serum Albumin

C

cAMP-	Cyclic Adenosine Monophosphate
CIC-K-	Voltage Gated Chloride Channel

CVLM- Caudal Ventrolateral Medulla

D

DBD DNA Binding Domain

DCT- Distal Convoluted Tubule

ddAVP- Desmopressin

D.I.- Diabetes Insipidus

DKO- 11βHSD2/ApoE Double Knockout Mice

DOCA- Desoxycorticosterone Acetate

DTT- Dithiothreitol

E

EDTA- Ethyleneiaminetetraacetic Acid

ELISA- Enzyme-Linked Immunosorbent Assay

ENaC- Epithelial Sodium Channel

ER- Endoplasmic Reticulum

ES- Embryonic Stem (Cells)

F

FE- Fractional Excretion

G

GAPDH- Glyceraldehyde 3-Phosphate Dehydrogenase

GFR- Glomerular Filtration Rate

GPCR- G-Protein Coupled Receptor

GR- Glucocorticoid Receptor

GRE- Glucocorticoid Receptor Response Element

Gs- Stimulatory G-Protein

H

HCL- Hydrochloric Acid

H+E- Hematoxylin and Eosin

HIF- Hypoxia Inducible Factor

HRE- Hormone Response Elements

HSP- Heat Shock Protein

I

I.C.V.- Intracerebroventricular

K

KRDKO- Kidney Rescue 11βHSD2$^{-/-}$/ApoE$^{-/-}$ Double Knockout Mice

L

LBD Ligand Binding Domain

M

MR- Mineralocorticoid Receptor

MRI- Magnetic Resonance Imaging

N

NaCl- Sodium Chloride

NAD- Nicotinamide Adenine Dinucleotide

NADP(H)- Nicotinamide Adenine Dinucleotide Phosphate (Reduced)

Na/K-ATPase- Sodium Potassium Adenosine Triphosphatase

NaPi- Na/Phosphate Cotransporter

NCC- Thiazide Sensitive Sodium Chloride Cotransporter

Nedd- Neural Precursor Cell Expressed Developmentally Down-Regulated Protein

NHE- Sodium Hydrogen Exchangers

NKCC2- Sodium Potassium Chloride Cotransporter

NLS- Nuclear Localization Signal

NTS- Nucleus of the Solitary Tract

O

OVLT- Organum Vasculosum Lamina Terminals

P

PGC-	Peroxisome Proliferator-Activated Receptor Gamma Coactivator
P_{Inu}-	Plasma Inulin Concentration
PKA-	Protein Kinase A
PMSF-	Phenylmethanesulfonyl Fluoride
PPIA-	Peptidylprolyl Isomerase A
PVN-	Paraventricular Nuclei of the Hypothalamus
PVDF-	Polyvinylidene Difluoride

Q

Q-PCR-	Real Time Polymerase Chain Reaction

R

RALES-	Randomized Aldactone Evaluation Study
ROMK-	Renal Outer Medullary Potassium Channel
RVLM-	Rostral Ventrolateral Medulla

S

S.C.-	Subcutaneous
SDR-	Short-Chain Alcohol Dehydrogenase/Reductase
SDS-	Sodium Dodecyl Suphate
SDS-PAGE-	Sodium Dodecyl Sulphate Polyacrylamide Gel Electrophoresis
SEM-	Standard Error of the Mean
SGK-	Serum- and Glucocorticoid Regulated Kinase
SHR-	Spontaneously Hypertensive Rats
SK-	Small Conductance Calcium Activated Potassium Channel
SON-	Supraoptic Nuclei of the Hypothalamus
Spiro-	Spironolactone
SRC-	Steroid Receptor Coactivator

SSC- Saline-Sodium Citrate

T

TEMED- Tetramethylethylenediamine

TBP- TATA Binding Protein

TONEBP- Transcription Factor Tonicity Response Enhancer Binding Protein

TUNEL- Terminal Deoxynucleotidyl Transferase dUTP Nick End Labeling

U

U_{Inu}- Urine Inulin Concentration

UOsm- Urine Osmolality

UT- Urea Transporter

UV- Urine Flow

V

V_2R- Vasopressin 2 Receptor

W

WNK- With No Lysine Kinase

Table of Contents

Abstract

11β-Hydroxysteroid Dehydrogenase Type 2 (11βHSD2) catalyses the inactivation of cortisol. In aldosterone target tissues co-expression of 11βHSD2 and mineralocorticoid receptors (MR) protects the receptor from activation by glucocorticoids. In the syndrome of Apparent Mineralocorticoid Excess, mutations in the HSD11B2 gene cause hypertension, which is thought to be driven by volume expansion secondary to sodium retention. 11βHSD2 mice are indeed hypertensive but paradoxically volume contracted, suggestive of a urine-concentrating defect. The current studies were designed to evaluate sodium and water homeostasis in 11βHSD2$^{-/-}$ mice.

11βHSD2$^{-/-}$ mice developed a severe and progressive polyuric-polydipsic phenotype. Despite basal polyuria, at <100 days 11βHSD2$^{-/-}$ mice had a functional concentration response when challenged with 24 hours water deprivation. At >180 days the exacerbated polyuria was associated with severe medullary injury in the null mice. Basal aquaporin 2 (AQP2) abundance was reduced in the 11βHSD2$^{-/-}$ mice at both <100 and >180 days. Moreover, vasopressin 2 receptor (V_2R) stimulation failed to normalize the impaired response to water deprivation in >180 day null mice. Consequently, a renal origin to the polyuria was postulated. Indeed, mice in which 11βHSD2 had been selectively targeted in the brain had a normal water turnover. A key finding from these studies is that functional deletion of 11βHSD2 in the brain, specifically the nucleus of the solitary tract (NTS), resulted in an increased salt appetite. Moreover, the mice displayed a preference for 1.5% NaCl over water.

Blockade of mineralocorticoid receptors (MR) significantly reduced NaCl intake. This is the first demonstration of an increased salt appetite in a model with normal renal function and in the absence of sodium depletion. These data implicate activation of MR on 11βHSD2 positive neurons in the NTS in the behavioural drive to consume sodium.

Chapter 1: Background

The control of body fluid homeostasis, through the regulation of intravascular blood volume and osmolality, is essential for the survival of mammals. Perturbations of plasma osmolality from a tightly regulated set point, approximately 290 mosmol/kg H_2O in humans, can have detrimental consequences, causing the loss of cellular integrity and subsequently the failure of essential physiological processes. Consequently, body water homeostasis is tightly regulated such that urinary water excretion and water intake are matched. During situations of high water intake, large volumes of dilute urine are formed, thus preventing the dilution of plasma. Conversely, during dehydration, small volumes of high osmolality urine prevent the concentration of plasma. These processes ensure that overall body water balance remains neutral. The regulation of sodium and water homeostasis is driven by complex neurohormonal systems, which through the concerted modulation of central and renal pathways ensure that balance is maintained. Aldosterone and vasopressin (AVP) have pivotal roles in these processes. Aldosterone activation of mineralocorticoid receptors (MR) increases sodium reabsorption in the distal nephron and stimulates salt-intake during sodium depletion. Increased plasma osmolality causes the central synthesis and release of AVP, which induces the renal conservation of water (Bourque, 2008). This thesis will focus on the involvement of aldosterone and AVP in the deranged salt and water homeostasis observed in 11β-hydroxysteroid dehydrogenase type 2 (11βHSD2) null mice.

1.1. 11βHSD2 protects MR from activation by glucocorticoids

1.1.1. Mineralocorticoid Receptor

The MR is a member of the nuclear hormone receptor family, which consists of approximately fifty receptors, all of which are ligand-activated transcription factors. In common with other members of the family, MR consists of four structurally distinct domains: the N-terminal domain, the DNA-binding domain, a hinge region and a ligand-binding domain (Pippal and Fuller, 2008). In the absence of ligand, MR is maintained in a transcriptionally inactive state through interactions between the ligand-binding domain and chaperone proteins such as heat shock protein 90 (hsp90). Whilst held in this inactive conformation, MR is capable of ligand but not DNA binding (Couette *et al*., 1998, Edwards, 2000). Ligand binding to the ligand-binding domain induces conformational changes within the region's alpha helical structure, resulting in the dissociation of chaperone proteins and the exposure of the nuclear localization signal (NLS). Consequently, ligand-activated MR translocates to the nucleus (Fejes-Toth *et al*., 1998, Walther *et al*., 2005). Central to the ligand-dependent activation of MR is a helical sequence referred to as activation function 2 (AF-2), located at the carboxyl-terminal of the ligand-binding domain (Glass and Rosenfeld, 2000). Ligand-induced conformational changes facilitate the binding of AF-2 to transcription coactivators, such as activating signal co-integrator 2 (ASC-2), steroid receptor coactivator 1 (SRC-1) and peroxisome proliferator-activated receptor gamma coactivator 1 alpha/beta (PGC-1α/β) (Hultman *et al*., 2005). Although such coactivators have no intrinsic affinity for DNA, their binding to the ligand-binding domain induces and enhances MR transcriptional activity (Hermanson *et al*., 2002). The ligand-binding domain is also involved in MR receptor dimerization. The DNA-

binding domain is located towards the centre of the MR, and contains eight cysteine residues, which bind to two zinc ions, forming zinc fingers. These interactions are fundamental in the stabilization of the DNA-binding domain (Berg *et al*., 2002), with the first zinc finger binding to the minor grove of MR target DNA and the second aiding receptor dimerization (Viengchareun *et al*., 2007). Following activation, dimeric MR binds to hormone response elements (HREs) located within the promoter regions of its target genes. Once bound to DNA, MR acts as a molecular scaffold for gene transcription machinery, thus facilitating the process (Viengchareun *et al*., 2007). In addition to AF-2 located at the carboxyl-terminal of MR, regions within the N-terminal domain (AF-1a and AF-1b) are also involved in transcription and transrepression. As with AF-2, these regions modulate MR activity through the recruitment of, and interaction with, cofactors (Pascual-Le Tallec and Lombes, 2005). The ligand-binding domain of MR bares a high degree of homology to the ligand-binding domain of the glucocorticoid receptor (GR) (Figure 1.1). Consequently, glucocorticoids bind with the same affinity as mineralocorticoids (Arriza *et al*., 1987). In addition to regulating transcription, MR cofactors are also thought to confer aldosterone specificity upon the receptor. However, in aldosterone target tissues, MR specificity is primarily conferred by its co-expression with the enzyme 11β-Hydroxysteroid Dehydrogenase Type 2 (11βHSD2).

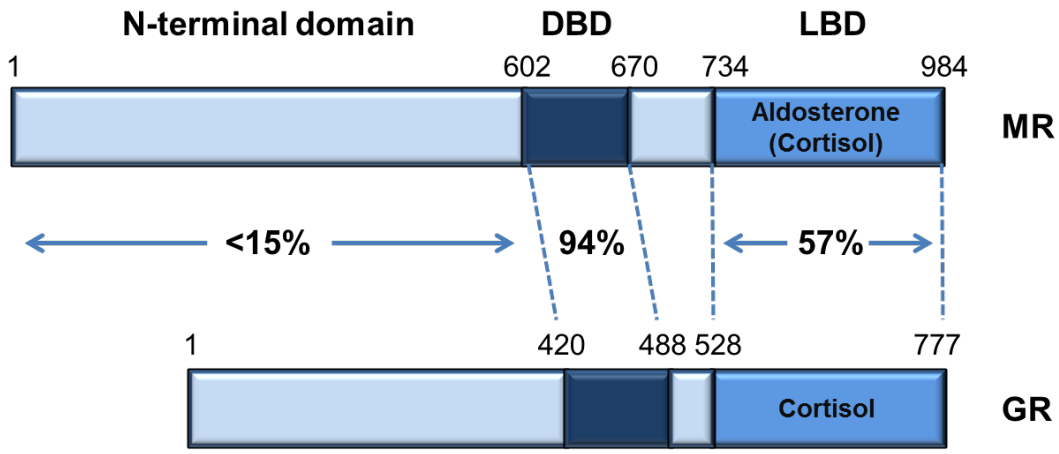

Figure 1.1: Schematic diagram illustrating the amino acid sequence homology between the mineralocorticoid receptor (MR) and the glucocorticoid receptor (GR). DBD, DNA binding domain. LBD, ligand binding domain. Adapted from (Pippal and Fuller, 2008).

The importance of MR in sodium homeostasis is highlighted by gene targeting experiments to "knockout" functional expression of the receptor. MR null mice displayed a severe sodium wasting phenotype and consequently died within two weeks of birth. An impaired excretory response to amiloride implicated loss of the epithelial sodium channel (ENaC) in the phenotype (Berger *et al*., 1998). In contrast, spatially regulated deletion of MR in the principal cells of the late connecting tubule and collecting duct did not result in natriuresis. Since plasma aldosterone levels were significantly elevated in the null mice it was postulated that upregulation of ENaC in the late distal convoluted tubule (DCT2) compensated for the downstream loss of the channel. However, when challenged with a low sodium diet the mice were unable to remain in balance despite further increases in plasma aldosterone,

suggesting that ENaC in DCT2 was not sufficient to compensate in this situation (Ronzaud *et al*., 2007). Temporal induction of MR deletion in the late connecting tubule and collecting duct resulted in the same phenotype, confirming that the impaired sodium handling was the result of MR deletion rather than developmental changes resulting from the absence of the receptor (Ronzaud *et al*., 2011).

1.1.2. 11βHSD2 confers aldosterone specificity on MR

In Vitro both aldosterone and cortisol have equal affinities for MR (Arriza *et al*., 1987) nevertheless in normal physiological conditions the receptors are selectively activated by aldosterone. This selectivity results from pre-receptor glucocorticoid metabolism by the isozymes of 11βHSD in target tissues (Stewart *et al*., 1987, Funder *et al*., 1988). Two isoforms of 11βHSD have been cloned, 11βHSD1 and 11βHSD2. Both enzymes are members of the short-chain alcohol dehydrogenase/reductase (SDR) family, but are encoded by distinct genes (*HSD11B1* and *HSD11B2*) and have a low sequence homology. 11βHSD1 functions primarily as a reductase *in vivo*, converting inactive cortisone to cortisol (11β-dehydrocorticosterone to corticosterone in rodents). Reductase activity is dependent on NADP(H) cofactor binding. Generation of cortisol by 11βHSD1 is involved in the regulation of GR activation (Paterson *et al*., 2005).

HSD11B2 is a five-exon gene located on chromosome 16 in humans (chromosome 8 in mice), which encodes the 405 amino acid protein 11βHSD2. 11βHSD2 is an NAD-dependent dehydrogenase that regulates cortisol inactivation, catalyzing its

conversion to the inactive 11-keto metabolite cortisone (corticosterone to 11-dehydrocorticosterone in rodents) (Figure 1.2) (Agarwal *et al*., 1995, Albiston *et al*., 1994).

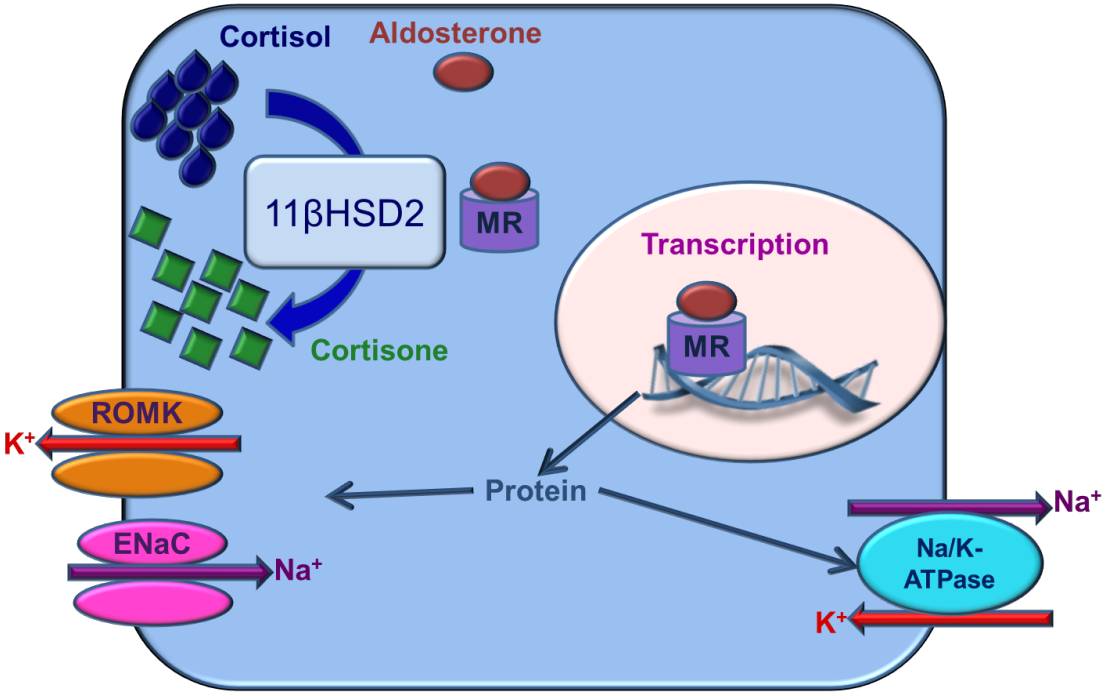

Figure 1.2: Inactivation of cortisol by 11βHSD2. 11βHSD2 converts cortisol to cortisone (corticosterone to 11-dehydrocorticosterone in rodents). Since cortisone has no affinity at MR this ensures aldosterone specific activation in target tissues. ROMK, potassium channel. ENaC, epithelial sodium channel. Na/K-ATPase, sodium potassium adenosine triphosphate.

Despite the low sequence homology between members of the SDR family the protein structures of the enzymes are highly conserved (Tsigelny and Baker, 1995). Consequently, much of the information about 11βHSD2 structure has been gained from homology modeling, predominantly using the x-ray crystal structure of 11βHSD1 as a template (Yamaguchi *et al*., 2011a). The secondary structure of 11βHSD2 consists of 6 parallel β-sheets flanked by 3 α-helices (Yamaguchi *et al*., 2011a) (Figure 1.3). NAD binds to a highly conserved Gly89XXXGly93XGly95 motif located within the ligand-binding site of 11βHSD2. The conserved glycines are essential for the attraction of NAD (Yamaguchi *et al*., 2011b), with their substitution resulting in the loss of enzyme function (Weiner and Hurley, 2005). Cofactor binding is stabilized through the formation of hydrogen bonds with Asp91, Phe94, Tyr232 and Thr267 in the ligand-binding site (Yamaguchi *et al*., 2011b, Yamaguchi *et al*., 2011a). Cortisol also binds to the ligand-binding site (Yamaguchi *et al*., 2011a). 11βHSD2 enzymatic activity is dependent on a conserved YXXXK motif. Site directed mutagenesis demonstrated that the mutation of either Tyr-179 of Lys-183 within the motif abrogated enzyme activity (Obeid and White, 1992). Through inactivation of cortisol, 11βHSD2 confers aldosterone selectivity and protects MR from activation by glucocorticoids (Funder *et al*., 1988).

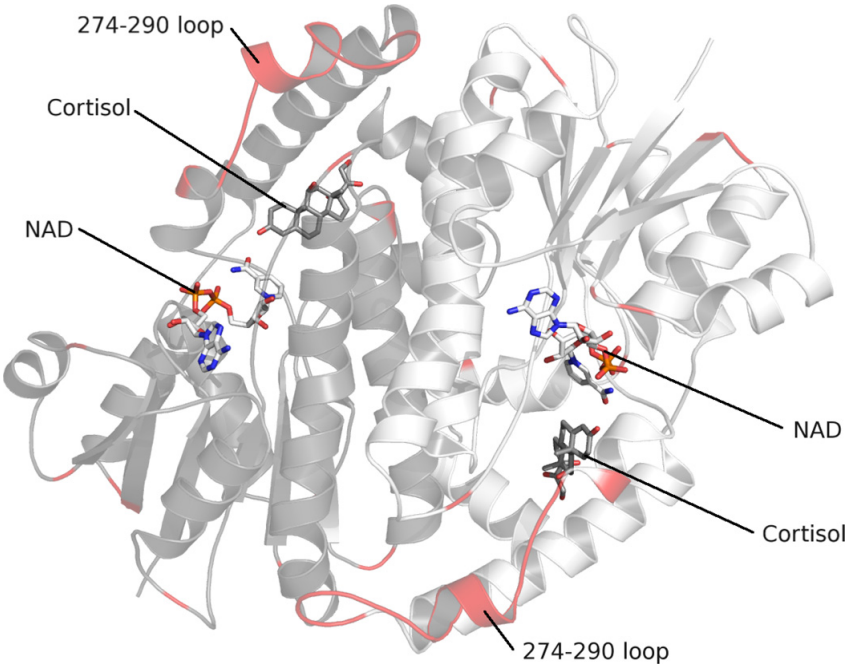

Figure 1.3: 3-dimensional model of dimeric 11βHSD2. The two monomers are shown in dark grey and white. NAD is shown with carbons-white, cortisol is grey. Other atoms: oxygen-red, nitrogen-blue, phosphorus-orange. Portions with reported modelling problems are shown in red. Figure taken from (Manning *et al*., 2010)

1.1.3. Localisation of 11βHSD2

Given its role in protecting MR from activation by glucocorticoids, expression of 11βHSD2 is enriched in aldosterone target tissues. Within the cell 11βHSD2 is localized to the endoplasmic reticulum (ER) (Odermatt *et al*., 1999). Epitope-tagging the N and C terminal of 11βHSD2 enabled the determination of the enzyme's orientation in the ER. The catalytic C-terminal was shown to be cytoplasmic, whereas the N-terminal transmembrane anchor faced the lumen (Odermatt *et al*., 1999). Algorithmic modeling was used to predict the membrane topology of 11βHSD2, which was proposed to consist of three transmembrane helices originating at the luminal N-terminal (Obeyesekere *et al*., 1997). In the absence of 11βHSD2 MR has a diffuse intracellular expression. In contrast, coexpression with 11βHSD2 resulted in the localization of MR to the ER. The close proximity between enzyme and receptor was shown to be essential for the conferment of aldosterone selectivity on MR. When co-expressed with 11βHSD2 aldosterone but not cortisol induced nuclear translocation of MR (Odermatt *et al*., 2001). Fundamentally, the discrete location of 11βHSD2 in regions of the kidney and brain involved in salt and water homeostasis enables aldosterone regulation of extracellular fluid status, which would otherwise be prevented by the promiscuous occupation by glucocorticoids of MR.

1.1.3.1. Expression in the kidney

In the kidney expression of 11βHSD2 is restricted to the distal nephron. The aldosterone sensitive distal nephron (ASDN), so termed because 11βHSD2 expression ensures aldosterone specific activation of MR, initiates at the start of the

DCT2. Immunohistochemical evaluation has enabled the localization of 11βHSD2 along the murine nephron to be determined. 11βHSD2 mRNA expression was primarily detected in the principal cells of the connecting tubule and collecting duct. Additionally, low levels of mRNA were detected in the terminal DCT (Campean *et al*., 2001). Consequently, it was postulated that in the murine nephron the connecting tubule and collecting duct are the major regions of aldosterone signaling, with the terminal DCT playing a secondary role. Further evaluation utilized mice in which the enzyme cre-recombinase was placed under the control of the 11βHSD2 promoter. The cre mice were subsequently crossed with mice in which β-galactosidase activity was driven by cre-recombination (ROSA26). Therefore tissues with active cre-recombinase, and therefore expressed 11βHSD2, were positive when X-gal stained. X-gal staining was most abundant in the connecting tubule and collecting duct, and absent in the proximal tubules and glomeruli. No 11βHSD2 expression was detected in the DCT (Naray-Fejes-Toth and Fejes-Toth, 2007). Together these data suggest that in the murine kidney expression of 11βHSD2 is predominant in the connecting tubule and collecting duct, with little to no expression in the DCT. Similarly, immunohistochemical staining has demonstrated the abundant expression of 11βHSD2 in the principal cells of the connecting tubule and collecting duct in human tissue (Kyossev *et al*., 1996, Hirasawa *et al*., 1997). However, in contrast to the results from murine kidneys, these studies also demonstrated the expression of 11βHSD2 in the thick ascending limb of the loop of Henle (Kyossev *et al*., 1996, Hirasawa *et al*., 1997), suggesting species differences in the expression profiles. Indeed 11βHSD2 activity has also been detected in the thick ascending limb of the rabbit nephron (Bonvalet *et al*., 1990). Notably, 11βHSD2

expression is consistently absent from more proximal regions of the tubule, regardless of species. Consequently, the distal nephron is involved in the aldosterone-mediated fine-tuning of sodium excretion, which is critical in the regulation of blood pressure and fluid homeostasis.

1.1.3.2. Expression in the brain

In the central nervous system expression of 11βHSD2 is wide spread during embryogenesis (Diaz *et al*., 1998, Holmes *et al*., 2006b). During development overexposure to glucocorticoids can have deleterious effects on neuronal development, resulting in the inhibition of proliferation, migration and differentiation. Prenatally, the broad distribution of 11βHSD2 prevents neuronal damage by ensuring that local glucocorticoid concentrations are kept low. In adult mice the expression of 11βHSD2 is restricted to the nucleus of the solitary tract (NTS) (Holmes *et al*., 2006b), although a more diverse distribution has been described in other species (Roland *et al*., 1995, Robson *et al*., 1998, Geerling *et al*., 2006b). 11βHSD2-positive neurons within the NTS are active in sodium-deprived, but not replete rats, implicating them in the response to sodium deficiency (Geerling *et al*., 2006a). Additionally, the NTS has been proposed as a site of integration for afferents involved in the regulation of cardiovascular function, specifically arterial baroreceptor afferents (Reviewed in (Boscan et al., 2002).

1.1.3.3. Other sites of expression

In addition to the kidney and brain, 11βHSD2 is also highly expressed in the placenta where it protects the foetus from overexposure to maternal glucocorticoids. Reductions in placental 11βHSD2 activity result in reduced birth weight (Stewart *et al*., 1995, Dave-Sharma *et al*., 1998). Moreover, overexposure to glucocorticoids *in utero* can program detrimental effects postnatally, including hypertension, renal damage and altered tubular sodium handing (Dagan *et al*., 2007, Ortiz *et al*., 2003). This illustrates the importance of glucocorticoid metabolism by placental 11βHSD2 during fetal development.

Expression of 11βHSD2 has also been documented in the vasculature and bone. 11βHSD2 is implicated in the response to vasoactive agents. However, although augmented vasoconstriction in response to noradrenaline was recorded in aortae isolated from 11βHSD2$^{-/-}$ mice bred on an MF1 background (Hadoke *et al*., 2001) the results were not reproduced when the mice were backcrossed onto a C57Bl/6 background (Bailey *et al*., 2008). Therefore the role of 11βHSD2 in the modulation of vascular constriction is unclear. Within the bone 11βHSD2 modulation of glucocorticoid levels is thought to ensure appropriate formation and maintenance. Mice in which 11βHSD2 is overexpressed in osteoblasts have a reduced bone mass, illustrating the importance of regulated glucocorticoid signaling in bone development (Yang *et al*., 2010).

1.2. 11βHSD2 and the renal regulation of sodium and water balance

In normal physiological conditions the human kidneys filter in the order of 180 l of water per day at the glomerulus, of which approximately 99.4% is reabsorped by the renal tubules. Despite this large reabsorption, there is no active transport of water within the nephron: rather its movement is driven solely by the reabsorption of solute. In contrast to plasma, filtrate entering the tubule is largely protein free. The glomerular filtration barrier, which consists of three components; the capillary endothelial cells, the basement membrane and podocytes, mediates the exclusion of protein from the filtrate. The barrier filters on the basis of charge and size; consequently, large negatively charged molecules such as albumin are excluded from the luminal fluid. Accordingly, glomerular disease can be characterized by the presence of protein in the urine (D'Amico and Bazzi, 2003).

1.2.1. The proximal tubule

The majority (65%) of filtrate reabsorption occurs in the proximal tubule, with the movement of water secondary to that of sodium and other osmolytes. The movement of sodium from the luminal fluid into the cell is mediated by a battery of sodium-coupled exchanges, predominantly sodium-hydrogen exchangers (NHE) expressed on the apical membrane (Figure 1.4). Consequently, the influx of sodium largely occurs in exchange for the secretion of hydrogen. Two isoforms of NHE have been identified on the apical membrane: NHE3, which is highly expressed in adults and NHE8, the predominant form in neonates. It is thought that a developmental switch between NHE8 and NHE3 occurs during the postnatal renal maturation process (Becker *et al*., 2007). As in other regions of the nephron, the electrochemical

gradient required for the movement of sodium into the cell is generated by Na/K-ATPases located on the basolateral membrane. The basolateral membrane of the proximal tubule is highly invaginous, bringing membrane bound Na/K-ATPases into close proximity with intracellular mitochondria. This maximizes the surface area and energy supply and facilitates the mass reabsorption that occurs in this region (Thomas, 2008).

60-70% of filtered water is reabsorbed in the proximal tubule and is mediated by aquaporin-1 (AQP1) and aquaporin-7 (AQP7) channels. AQP1 is located on both the apical and basolateral membranes of the cells (Nielsen *et al*., 1993b). AQP1 null mice were shown to have an impaired concentration response: following a 36-hour water deprivation challenge they developed severe dehydration and in extreme cases unresponsiveness (Ma *et al*., 1998). Although AQP1 is also expressed on the descending thin limb of the loop of Henle, free flow micropuncture experiments confirmed extensive impairment of osmotic water permeability in the proximal tubule of AQP1 null mice, substantiating AQP1 as the main pathway for the reabsorption of water in this region of the nephron (Schnermann *et al*., 1998). AQP7, located on the apical membrane of the proximal tubule, also contributes to the reabsorption of water, although to a much lesser extent than AQP1. Based on measurements of the water permeability of isolated brush border membrane vesicles from AQP7 null mice, AQP7 accounted for ~10% of water reabsorption (Sohara *et al*., 2005). The remaining ~10% of proximal tubule water reabsorption occurs paracellularly. Since in this region the movement of water and solute are

inextricably linked, fluid leaving the proximal tubule is approximately isosmotic to plasma despite the daily reabsorption of approximately 120 l of water.

Since the proximal tubule is devoid of 11βHSD2 (Kyossev *et al*., 1996, Naray-Fejes-Toth and Fejes-Toth, 2007) it is not a major site for aldosterone regulation.

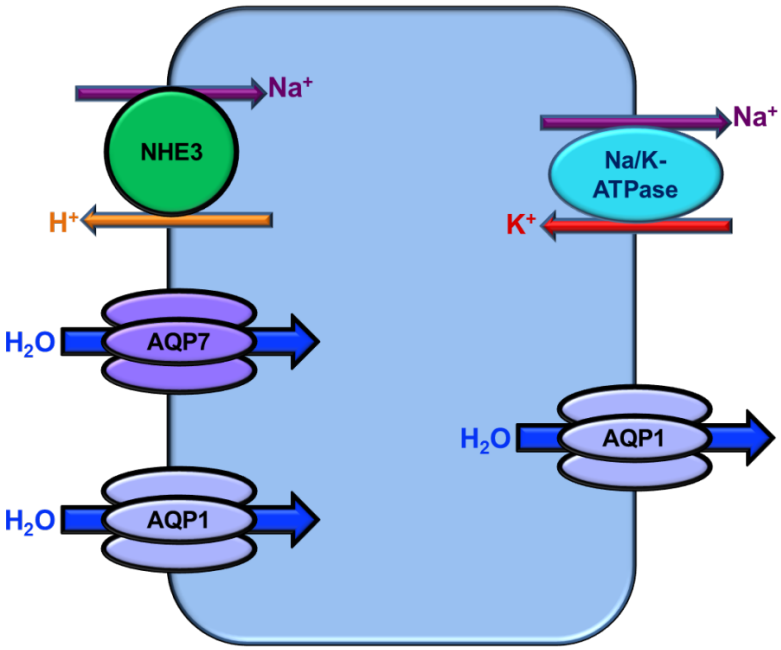

Figure 1.4: Proximal tubule cell. NHE3, sodium-hydrogen exchanger 3. AQP1, aquaporin 1. AQP7, aquaporin 7. Na/K-ATPase, sodium potassium adenosine triphosphatase.

1.2.2. The loop of Henle

1.2.2.1. The loop of Henle generates a medullary gradient

As the nephron leaves the cortex and descends into the renal medulla, the reabsoption of water and sodium are separated due to the selective permeabilities of the ascending and descending limbs of Henle. In the ascending limb, solutes are transported from the luminal fluid into the interstitium by the concerted action of the furosemide-sensitive sodium-potassium-chloride cotransporter (NKCC2) on the apical membrane, and Na/K-ATPase on the basolateral membrane. Sodium, potassium and chloride are transported from the luminal fluid into the cell via NKCC2 in a ratio of 1:1:2 (Brenner and Rector, 2004). The majority of the potassium transported into the cell returns to the luminal fluid via apical membrane potassium channels encoded by ROMK, one with a conductance of 30-pS (SK) and another of 70-pS (ROMK) (Wang, 1994, Lu *et al*., 2004). Therefore, although the concentration of potassium in the luminal fluid is substantially lower than that of sodium, the recycling of potassium prevents it from limiting sodium transport. Consequently, the limiting factor in sodium reabsorption in the ascending limb is the delivery of fluid from the proximal tubule. Increased sodium reabsorption in the proximal tubule results in reduced sodium delivery to the ascending limb, and therefore limits the generation of the cortico-medullary osmotic gradient. This results in an attenuated osmotic gradient across the collecting duct, and therefore an impaired ability to concentrate urine (Schrier, 2003). The movement of sodium from the luminal fluid into the cell is dependent on a favourable sodium gradient; consequently, the concentration of sodium within the cell must be kept low. As in the proximal tubule, the sodium gradient is generated by the active extrusion of

sodium from the cell by Na/K-ATPase located on the basolateral membrane. Moreover, since NKCC2 generates a relatively high concentration of chloride in the cell, it also moves down its gradient, out of the cell, via basolateral membrane chloride channels (CIC-K1 in the thin- and CIC-K2 in the thick-ascending limb (Uchida *et al*., 1993, Adachi *et al*., 1994). Consequently, this sequence of events causes the accumulation of NaCl in the medullary interstitium. Since the ascending limb is impermeable to water, these processes lead to the generation of a relatively hyperosmotic interstitium and hypoosmotic tubular fluid (Figure 1.5).

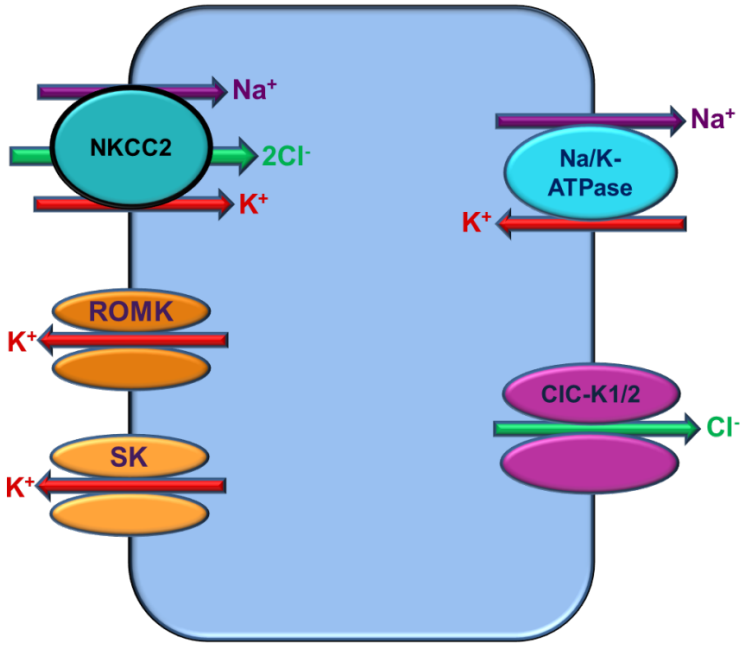

Figure 1.5: Ascending limb loop of Henle cell. NKCC2, furosemide-sensitive sodium-potassium-chloride cotransporter. ROMK, renal outer medullary potassium channel. SK, small conductance calcium activated potassium channel. Na/K-ATPase, sodium potassium adenosine triphophatase. CIC-K, voltage gated chloride channel.

The ascending limb is also a major site of divalent cation reabsorption. In this region 60% of filtered magnesium and 20% of filtered calcium is reabsorbed paracellularly, driven by the substantial transepithelial voltage gradient predominantly generated by NKCC2. The evaluation of isolated perfused tubules established that transepithelial voltages in the ascending limb range from 3-10mV dependent on the species and flow rate (Burg, 1982). The importance of this voltage gradient in divalent cation reabsorption was illustrated in isolated perfused thick ascending limbs. Voltage clamp experiments demonstrated that calcium and magnesium reabsorption were negligible in the absence of a transepithelial voltage (Bourdeau and Burg, 1979, Shareghi and Agus, 1982). Since intra-luminal furosemide increased urinary calcium and magnesium in micropuncture experiments, (Quamme, 1981) and decreased the transepithelial voltage in isolated perfused tubules (Burg et al., 1973), the pivotal role of NKCC2 in paracellular cation transport was confirmed.

1.2.2.2. Countercurrent multiplication

It is of note that individual cells in the wall of the ascending limb are only capable of sustaining an osmotic gradient of approximately 200 mosmol/kg H_2O. This means that at any transverse plane along the medulla the difference between the osmolality of the fluid in the ascending limb and in the interstitium is restricted to 200 mosmol/kg H_2O. However, within the medulla a substantially larger longitudinal osmotic gradient exists, extending from the cortico-medullary boundary to the tip of the papilla. This gradient is generated by countercurrent multiplication, a process dependent on the anatomical arrangement of the loop of Henle (Figure 1.6) (Lote, 2000, Brenner and Rector, 2004, Guyton and Hall, 2000).

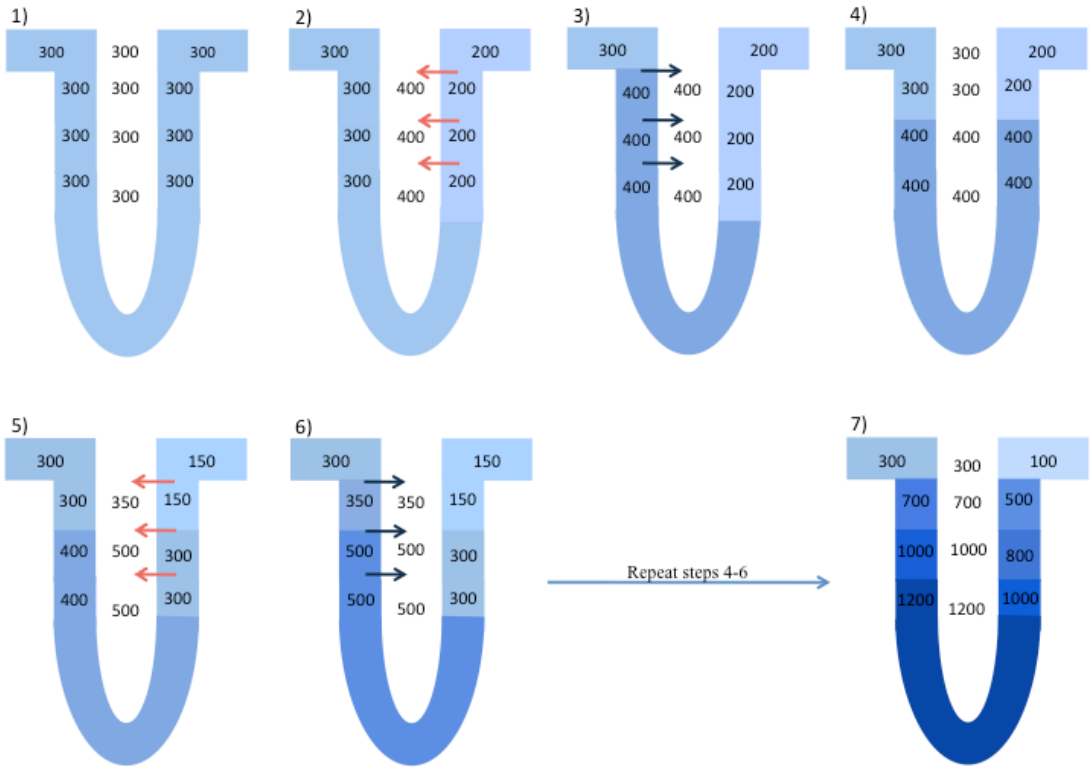

Figure 1.6: Countercurrent multiplication in the loop of Henle. Figure adapted from (Guyton and Hall, 2000). Values are in mOsm. Pink arrows represent the transport of Na from the ascending limb into the interstitium. Blue arrows represent the movement of water from the descending limb into the interstitium.

The descending limb of the loop of Henle, (which lies parallel to the ascending limb but has a countercurrent tubular flow), has a relatively low permeability to sodium but a high permeability to water due to the constitutive presence of AQP1 channels on both the apical and basolateral membranes (Nielsen *et al*., 1995b). Fluid entering the descending limb from the proximal tubule is isosmotic to plasma. As this fluid descends into the medulla, water translocates from it, through AQP1 channels, into the relatively hyperosmotic interstitium generated by the ascending limb. The reabsorption of water continues until an osmotic equilibrium has been achieved. Consequently, fluid in the descending limb is hyperosmotic relative to that in the ascending limb, but isosmotic with the interstitium. As the hyperosmotic fluid enters the ascending limb, NaCl is again transported from it into the interstitium, further augmenting its osmolality and decreasing that of the tubular fluid. This cycle of events continues and the longitudinal gradient through the medulla is established. Therefore, countercurrent multiplication allows a small transverse osmotic difference (a single-osmotic effect of 200 mosmol/kg H_2O) to be multiplied into a large longitudinal osmotic gradient. The maximum osmolality achieved along the gradient is dependent on the length of the loop of Henle, with osmolalities of 1400 mosmol/kg H_2O being achieved at the tip of long loops in humans (Brenner and Rector, 2004). In rodents osmolalities of over 3000 mosmol/kg H_2O are frequently reached at the tip of papillae, enabling the production of more concentrated urine (Kwon *et al*., 2009). Moreover, the separation of solute and water in the loop of Henle means that fluid leaving the ascending limb and entering the DCT is hypoosmotic relative to plasma, with the degree of hypoosmoticity dependent on the length of the loop.

Although the accumulation of NaCl in the interstitium is fundamental in the concentration of urine, the resultant hypertonic environment imposes severe stress on the cells within the renal medulla. In order to maintain integrity, and a constant intracellular environment, cells within the medulla generate organic osmolytes, such as sorbitol. Accumulation of compatible osmolytes increases intracellular osmolality, allowing the maintenance of intracellular volume and ultimately preventing hypertonicity induced cell death. Central to this response is the transcription factor tonicity-responsive enhancer binding protein (TONEBP) (Woo *et al*., 2002). During hypertonicity TONEBP mRNA and protein abundance increase. This leads to the increased transcription of a battery of genes involved in the generation of compatible osmolytes, including aldose reductase, which catalyses the conversion of glucose to sorbitol (Lopez-Rodriguez *et al*., 2004, Cai *et al*., 2005, Miyakawa *et al*., 1999). The central role of TONEBP in the maintenance of medullary integrity has been illustrated in TONEBP null mice. In mice deletion of TONEBP resulted in the impaired regulation of osmoprotective genes. Consequently the mice the developed severe meduallary atrophy (Lopez-Rodriguez *et al*., 2004).

1.2.2.3. The contribution of urea to the medullary gradient

The accumulation of NaCl in the medulla is pivotal in the generation of the medullary osmotic gradient. However, the concentration of NaCl only accounts for approximately half of the medullary hyperosmoticity. The remainder is largely attributable to urea. Since plasma concentrations of urea are relatively low, approximately 5 mmol/L in humans (Hinwood, 1992) and 9 mmol/L in mice (Zhao *et al*., 2006), renal recycling mechanisms exist to establish and maintain high

concentrations of urea within the inner medulla. The pivotal recycling pathway involves the movement of urea between the terminal inner medullary collecting duct and the thin ascending limb of the loop of Henle. Urea is freely filtered at the glomerulus; therefore the concentration entering the proximal tubule is equal to that of the plasma. 50% of filtered urea is reabsorbed in the proximal tubule, moving by passive diffusion down its concentration gradient into the medulla. As the nephron descends through the medulla it passes through increasing concentrations of interstitial urea. Consequently, urea moves from the interstitium back into the luminal fluid within the descending limb of the loop of Henle. Luminal fluid entering the ascending limb of the loop of Henle has a urea concentration approximately equal to that of plasma. Regions of the nephron distal to the descending limb are relatively impermeable to urea. Since water is reabsorbed from the collecting duct, the concentration of urea in the luminal fluid increases as the nephron descends back through the medulla. Consequently, the concentration of urea in the luminal fluid in the inner medullary collecting duct can be 50 times greater than that of plasma. In the mouse kidney urea is reabsorbed from the inner medullary collecting ducts though urea transporter A1 (UT-A1) on the apical membrane and urea transporter A3 (UT-A3) on basolateral plasma membrane (Fenton *et al*., 2002). Since the ascending limb of the loop of Henle and the inner medullary collecting duct are virtually contiguous, urea reabsorbed from the collecting duct re-enters the ascending limb of the loop of Henle via the interstitium. The low blood flow through the medulla ensured by countercurrent exchange within the vasa recta, means that large concentrations of urea are retained in the interstitium. Therefore the recycling of urea further increases the osmolality of the interstitium.

Moreover, the high concentration of urea within the interstitium prevents the induction of osmotic diuresis, which would otherwise be required to excrete the large quantities of urea in the urine (Reviewed in (Fenton et al., 2006).

1.2.2.4. Countercurrent exchange maintains the osmotic gradient

Once established, the cortico-medullary osmotic gradient is maintained by the unique hairpin arrangement of the capillaries within the medulla. The descending vasa recta originate from juxtamedullary efferent arterioles. Consequently, the sodium concentration of blood entering the medulla is approximately equal to that of plasma, 140 mmol/l. Like other capillaries within the body the vasa recta have a high permeability to both solutes and water; therefore as the capillaries pass through the medulla the osmolality of the blood equilibrates with that of the interstitium. As the vasa recta descend into the medulla solutes (mainly sodium and urea) diffuse down their concentration gradient from the interstitium into the blood. In addition water leaves the blood through AQP1 channels (Nielsen *et al*., 1995b). At the tip of the papilla the concentration of blood within the vasa recta is approximately equal to that of the interstitium. In contrast, as the vasa recta ascend towards the cortex the osmolality of the interstitium becomes progressively less. Consequently, solutes are reabsorbed into the interstitium, and water moves into the blood. Hence the anatomical arrangement of the vasa recta "traps" solute within the medulla and preserves the osmotic gradient. Moreover, countercurrent exchange provides a mechanism by which blood can move into and out of the medulla without disrupting the osmotic gradient (Brenner and Rector, 2004).

1.2.2.5. The effect of AVP on the loop of Henle

Through the stimulation of NaCl reabsorption in the thick ascending limb, AVP increases the effects of countercurrent multiplication and enhances AVP induced urine concentration in the collecting duct. The effects of AVP in the thick ascending limb are mediated by the activation of vasopressin 2 receptors (V_2R). *In situ* hybridization demonstrated V_2R mRNA expression along the thick ascending limb (Mutig *et al*., 2007). Abundance was highest in the inner medullary stripe and declined progressively as the tubules ascended through the cortex. Activation of V_2R causes the increased reabsorption of NaCl through the stimulation of the NKCC2. Administration of desmopressin (ddAVP) to adult mice resulted in an approximately 2-fold increase in the abundance of phosphosphorylated NKCC2. Since the phosphorylated NKCC2 localized at the apical membrane of the thick ascending limbs it was postulated that AVP regulation of NKCC2 was similar to that of AQP2, with AVP stimulating exocytosis and consequently increased membrane expression (Gimenez and Forbush, 2003). Indeed it was subsequently shown that as with AQP2, AVP induced exocytosis of NKCC2 was cAMP dependent, and could be blocked by the administration of a protein kinase A (PKA) inhibitor (Caceres *et al*., 2009).

1.2.2.6. The effect of corticosteroids on the loop of Henle

Studies in adrenalectomized rats demonstrated that the removal of the adrenal hormones resulted in reduced sodium reabsorption in the loop of Henle. Reabsorption was increased to near control levels by aldosterone but not dexamethasone, implicating the mineralocorticoid in the modulation of sodium

transport in the loop of Henle (Stanton, 1986). Recently, immunohistochemical analysis has demonstrated significant expression of MR in the thick ascending limb (Ackermann *et al*., 2010); however, since the region of the nephron does not robustly express 11βHSD2 (Bujalska *et al*., 1997), and therefore does not form part of the ASDN, the physiological relevance of these findings is uncertain. Indeed it was demonstrated that in intact rats the cellular localization of MR in the thick ascending limb is determined by glucocorticoids. Aldosterone was only capable of inducing nuclear translocation of MR in absence of endogenous corticosterone (Ackermann *et al*., 2010).

1.2.3. The distal convoluted tubule

1.2.3.1. The distal convoluted tubule further dilutes filtrate

5-10% of sodium reabsorption occurs in the DCT. This region of the nephron can be divided into two sections: DCT1 the initial segment in which the majority of sodium reabsorption is driven by the thiazide-sensitive transporter (NCC); and DCT2 the late segment which also expresses ENaC. DCT2 marks the start of the ASDN since it is the first region of the tubule in which MR and 11βHSD2 are coexpressed (Bostanjoglo *et al*., 1998). Again, in this section of the nephron the gradient required for the movement of sodium is driven by Na/K-ATPases located in the basolateral membrane. In DCT1 Na reabsorption occurs though NCC and is an electroneutral process. In the absence of an electrochemical gradient the secretion of potassium through ROMK and BK in this region is minimal (Brenner and Rector, 2004). Therefore, in DCT1 the majority of potassium secretion is mediated by K/Cl-

cotransporters, predominantly in situations when luminal Cl is low or bicarbonate excretion is high (Amorim *et al*., 2003). In DCT2 ENaC mediates reabsorption of sodium. The reabsorption of sodium through ENaC results in the depolarization of the apical membrane and the generation of the electrochemical gradient required for potassium secretion. Consequently in normal conditions the majority of potassium secretion occurs in DCT2, through ROMK and BK potassium channels expressed on the apical membrane (Figure 1.7). In this region the rate of potassium secretion is dependent in on the reabsorption rate of sodium through ENaC and the activity- and expression- of ROMK at the apical membrane (Meneton *et al*., 2004). Since DCT does not express AQPs it permeability to water is low. Consequently, the dilution of urine is this region is attributable to the reabsorption of sodium.

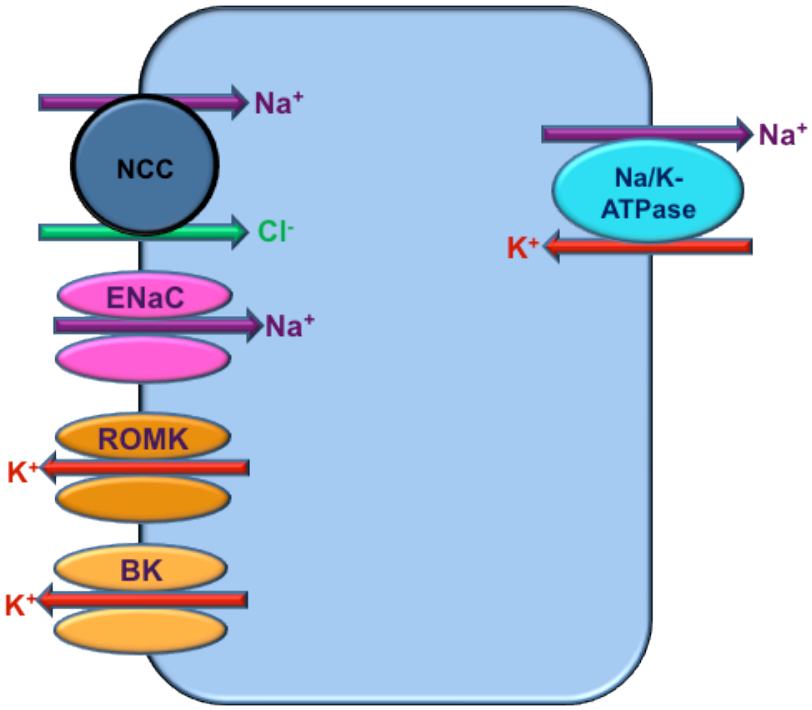

Figure 1.7: Late distal convoluted tubule cell. NCC, thiazide sensitive sodium chloride cotranspoter. ENaC, epithelial sodium channel. ROMK, renal outer medullary potassium channel. BK, big conductance calcium activated potassium channel. Na/K-ATPase, sodium potassium adenosine triphosphatase

1.2.3.2. The effect of AVP on the distal convoluted tubule

Substantial V_2R mRNA expression has been demonstrated in the DCT (Mutig *et al*., 2007). The physiological role of AVP in the DCT was demonstrated in Brattleboro rats, a model devoid of endogenous AVP. In these rats chronic ddAVP administration resulted in increased NCC protein abundance (Ecelbarger *et al*., 2001a). Subsequently it was shown that ddAVP stimulation of V_2R resulted in increased NCC phopsphorylation and apical membrane expression (Mutig *et al*., 2010, Pedersen *et al*., 2010). Plasma levels of AVP are elevated during hypovolemia, when increased water reabsorption is desired. However, since the DCT has a low permeability to water, and as such contributes to urinary dilution, it seems counterintuitive that sodium reabsorption in this region is increased in situations of high plasma osmolality. It has been postulated that as in the ascending limb, sodium reabsorption from the DCT increases the medullary osmotic gradient, thereby facilitating AVP-induced water reabsorption from the collecting duct (Pedersen *et al*., 2010).

1.2.3.3. The effect of corticosteroids on the distal convoluted tubule

The primary role of aldosterone in the DCT is the modulation of ENaC, through the regulation serum- and glucocorticoid-regulated kinase 1 (SGK-1) and the neural precursor cell expressed developmentally down-regulated protein (Nedd) type 4-2, an E3 ubiquitin ligase. SGK-1 is expressed in several regions throughout the nephron (glomerulus, proximal tubule and distal nephron), however it is only in the ASDN where its expression is regulated by aldosterone (Pearce *et al*., 2000). Studies in rats demonstrated that physiological doses of aldosterone induced the upregulation

of SGK-1 expression 30-60 minutes post administration. This increase was associated with decreased urinary sodium excretion, suggesting SGK-1 stimulated increased sodium reabsorption in the distal nephron. Moreover, administration of a glucocorticoid receptor antagonist demonstrated that the effects of aldosterone were mediated by the activation of MR (Bhargava *et al*., 2001). Initial evidence for the role of SGK-1 in regulation of ENaC expression came from studies in *Xenopus* oocytes. Co-expression of SGK-1 with ENaC increased the ENaC mediated sodium current approximately 7-fold, relative to expression of ENaC alone. Since SGK-1 alone had no effect on sodium transport it was concluded that its effect was mediated through increased ENaC activity (Chen *et al*., 1999). This conclusion was further substantiated through the evaluation of SGK-1 knockout mice. Although the mice were phenotypically normal when receiving a standard sodium diet (2.5g Na^+/kg), when challenged with sodium restriction (0.15g Na^+/kg) they displayed an impaired ability to appropriately conserve sodium. Consequently, they had an attenuated blood pressure and glomerular filtration rate in spite of elevated plasma aldosterone levels (Wulff *et al*., 2002). Despite its pivotal role in the control of ENaC mediated sodium reabsorption, SGK-1 is not thought to phosphorylate the channel directly; rather its posttranslational effects are mediated by the phosphorylation and subsequent inhibition of Nedd4-2. The α, β and γ subunits of ENaC contain a PY motif in their carboxyl-terminal domains. These motifs are the point of interaction for Nedd4-2, which ubiquitinates the channel, targeting it for internalization and lysosomal degradation. Since ubiquitination is central in the membrane retrieval of ENaC, this causes its accumulation at the apical membrane (Debonneville *et al*., 2001, Staub *et al*., 1996).

In addition, glucocorticoids regulate α ENaC transcription through the activation of a glucocorticoid receptor response element (GRE) in the genes promoter region. In contrast to the posttranslational modification, modulation of transcription occurs independently of SGK-1 activation (McTavish *et al.*, 2009).

Since 11βHSD2 is not expressed in DCT1 the region is insensitive to aldosterone (Campean *et al*., 2001). Therefore aldosterone modulation of NCC is restricted to DCT2. *In vivo* microperfusion studies demonstrated that both mineralocorticoids and glucocorticoids are capable of NCC modulation. Both aldosterone and dexmethasone replacement in adrenalectomized rats resulted in increased NCC mediated sodium reabsorption (Velazquez *et al*., 1996). Moreover the effects were shown to be the result of increased channel expression. Additionally, aldosterone has been shown to modulate the serine theronine kinase with-no-lysine 4 (WNK4). WNK4 inhibits NCC mediated sodium reabsorption by reducing trafficking of the channel to the plasma membrane (Yang *et al*., 2003, Wilson *et al*., 2003). The inhibition NCC trafficking is likely mediated by WNK4 phosphorylation of the channel since catalytic inhibition of the kinase prevented the suppression of NCC activity (Wilson *et al*., 2003). Aldosterone is thought to remove the inhibitory effects of WNK4 on NCC through the activation of SGK-1. In oocytes SGK-1 was shown to phosphorylate WNK4 and consequently increase the activity of NCC (Rozansky *et al*., 2009). Therefore, aldosterone stimulation of SGK-1 would result in increased NCC activity. In addition to removing the inhibitory effects of WNK4, chronic administration of aldosterone to has been shown to increase NCC protein

expression (Kim *et al*., 1998). These data illustrate that aldosterone can augment sodium reabsorption DCT2 via the regulation of NCC and ENaC.

1.2.4. The collecting duct

1.2.4.1. The collecting duct regulates the fine tuning of urine concentration

The generation of the longitudinal osmotic gradient in the medulla is fundamental to the modulation of urine concentration in response to changes in plasma osmolality. This fine-tuning of urine concentration occurs in the collecting duct and is regulated by AVP. AVP acts to increase the water permeability of the collecting duct in both the short and long term. In the short term, AVP induces the translocation of AQP2 from intracellular vesicles to the apical membrane (Nielsen *et al*., 1995a). This response occurs rapidly, with increase water permeability measurable 5-30 minutes after exposure to peritubular AVP (Kuwahara and Verkman, 1989, Wall *et al*., 1992). Chronic AVP stimulation, as occurs during 24-hour water deprivation challenges, causes the increased expression of AQP2 in the collecting duct (Nielsen *et al*., 1993a). *In vitro* this was shown to be mediated by the increased transcription of AQP2 (Matsumura *et al*., 1997).

1.2.4.2. The effect of AVP on the collecting duct

In the principal cells of the collecting duct AVP binds to the G-protein coupled receptor (GPCR) V_2R, located on the basolateral membrane (Figure 1.8).

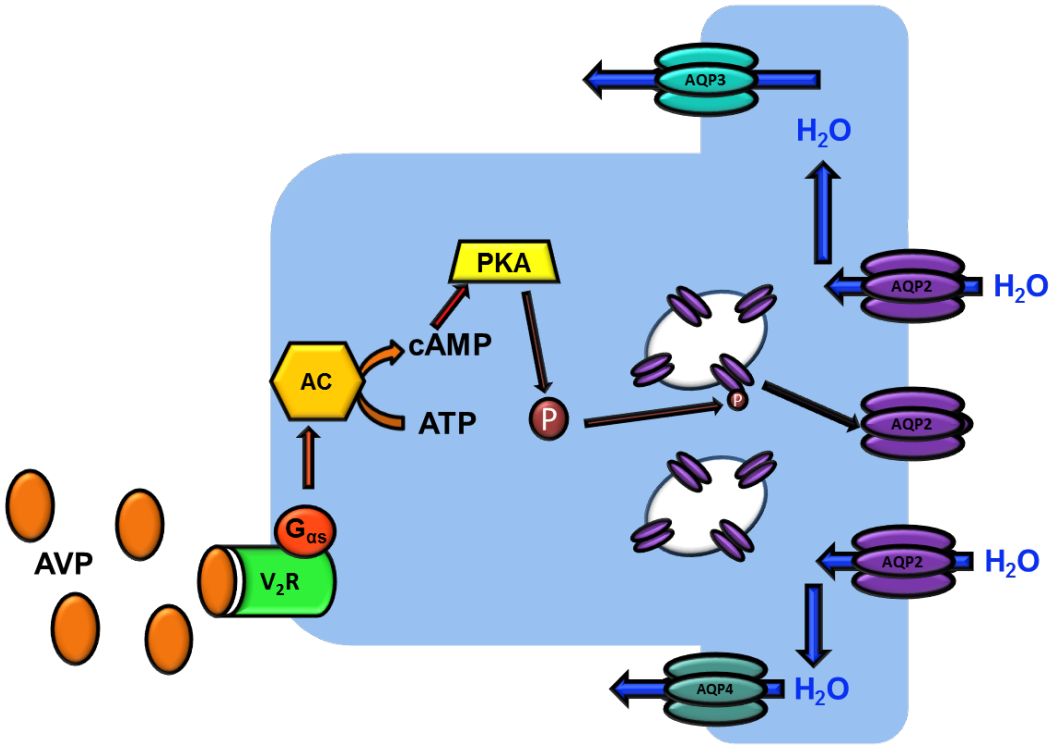

Figure 1.8: Vasopressin activation of V_2R increases apical AQP2. AVP, vasopressin. V_2R, vasopressin 2 receptor. AC, adenylate cyclase. ATP, adenosine triphosphate. cAMP, cyclic monophosphate. PKA, protein kinase A. P, phosphorylated. AQP2, aquaporin 2. AQP3, aquaporin 3. AQP4, aquaporin 4.

Activation of these receptors causes the stimulatory G-protein, Gs, to translocate to, and activate, adenylate cyclase. Activation of adenylate cyclase causes an increased synthesis of cAMP from intracellular ATP and consequently the activation of PKA (Boone and Deen, 2008, Fushimi *et al*., 1997). In addition, the regulatory subunits of PKA in the collecting duct are also bound to the PKA anchoring protein 18δ (AKAP18δ). AKAP18δ anchors PKA in AQP2 expressing intracellular vesicles, allowing the regulated and spatially orchestrated phosphorylation of AQP2 following AVP binding to V_2R (Henn *et al*., 2004). In 1993 when Fushimi *et al*., cloned and characterized AQP2 in the rat collecting duct they identified a cAMP dependent PKA phosphorylation site (Fushimi *et al*., 1993). Further analysis using site-directed mutagenesis demonstrated that PKA phosphorylation of Ser-256, stimulated translocation of AQP2 from intracellular vesicles to the apical membrane (Fushimi *et al*., 1997). Moreover, the PKA inhibitor H89 prevented AVP-induced translocation (Katsura *et al*., 1997). Consequently, it was postulated that AVP-induced phosphorylation of Ser-256 by PKA was essential for apical membrane expression of AQP2. In view of these data, it was somewhat surprising that intracellular AQP2 was shown to be phosphorylated in the kidneys of hydrated rats (Nishimoto *et al*., 1999). This finding was resolved by Kamsteeg *et al*., who demonstrated that the phosphorylation of three out of four monomers of tetrameric AQP2 was required for its apical membrane expression (Kamsteeg *et al*., 2000). Although these studies were originally performed in *Xenopus* oocytes, the importance of Ser-256 in AQP2 regulation was recently corroborated *in vivo*, using a mouse model of congenital progressive hydronephrosis. In these mice a single base change resulted in the substitution of Ser-256 to Leu-256, which rendered the residue nonphosphorylatable.

As a result AQP2 did not accumulate at the apical membrane and the mutant mice developed severe polyuria and hydronephrosis (McDill *et al*., 2006). Following its translocation to the apical membrane, AQP2 enables water to move down its osmotic gradient into the cell. Aquaporin-3 (AQP3) and aquaporin-4 (AQP4) channels located on the basolateral membrane then allow the movement of water from the cells into the interstitium. Although both AQP3 and AQP4 are constitutively expressed on the basolateral membrane, AQP3 expression is increased following chronic AVP stimulation, as occurs during water deprivation challenges (Ecelbarger *et al*., 1995, Terris *et al*., 1996). Conversely, water deprivation and chronic AVP stimulation have no effect on AQP4 expression (Terris *et al*., 1996). Once plasma osmolality has been restored, circulating levels of AVP decrease, and AQP2 endocytosis predominate over exocytosis (Knepper and Nielsen, 1993).

The reabsorption of urea from the inner medullary collecting duct is increased by AVP. In situations of antidiuresis, the increased reabsorption of urea into the interstitium facilitates the concentration of urine. Evaluation of inner medullary collecting ducts isolated from UT-A1/3 knockout mice demonstrated the absence of AVP sensitive urea transport (Fenton *et al*., 2004). Therefore UT-A1 and UT-A3 mediate AVP sensitive urea reabsorption in the inner medullary collecting duct. The fundamental role of urea recycling in urine concentration was confirmed by the demonstration of polyuria in UT-A1/3 null mice when on a normal protein diet. Since polyuria was abolished by protein restriction, it was proposed that in the absence of urea recycling, diuresis was required to excrete the high luminal concentrations of urea (Fenton *et al*., 2004).

1.2.4.3. The effect of corticosteroids on the collecting duct

In addition to AVP, the other major hormonal regulator of the collecting duct is aldosterone. Aldosterone stimulation increases sodium reabsorption through its action at the MR, which upon ligand binding acts as a transcription factor. Consequently, aldosterone's action at MR located in the principal cells of the collecting duct causes the increased transcription of proteins involved in sodium reabsorption. Such proteins included the α, β and γ subunits of ENaC, and the α_1 and β_1 subunits of Na/K-ATPase and SGK-1. Since 90% of filtered sodium is reabsorbed in regions prior to the collecting duct, aldosterone's action in this region of the nephron is responsible for the fine-tuning sodium excretion (Brenner and Rector, 2004).

In the collecting duct the movement of sodium is a two-step process, sodium enters the cell via ENaC located on the apical membrane, it is then actively pumped into the interstitium by Na/K-ATPases located on the basolateral membrane. The entry of sodium through ENaC is the rate-limiting step. Aldosterone regulation of sodium reabsorption occurs in two phases. Initially (1-4 hours post stimulation) the effects are predominantly mediated by SGK-1, whereas in the later phase (>4 hours post stimulation) increased expression of Na/K-ATPase and ENaC becomes the primary mechanism (McCormick *et al*., 2005). The regulation of ENaC in the collecting duct is as previously described for the DCT (Section 1.2.3).

Additionally, aldosterone had been shown to modulate the expression of AQP2 in the collecting duct. *In vitro* administration of aldosterone was shown to have biphasic effect on AQP2 expression. Following AVP stimulation, aldosterone initially caused a reduction in AQP2 protein expression, whereas prolonged treatment resulted in increased AQP2 abundance. The effects of aldosterone on AQP2 were blocked by MR antagonism, implicating the activation of the receptor in the response. In contrast concurrent administration of aldosterone with AVP resulted in a reduction in AQP2 mRNA expression at all of the time points. These data suggest that the long-term effects of aldosterone on AQP2 protein abundance occurred independently of changes in mRNA expression and were rather mediated by increased mRNA translation. Since aldosterone had no effect on AQP2 protein expression in the absence of AVP it was postulated to play a modulatory role, acting to buffer the effects of AVP (Hasler *et al*., 2003).

1.3. 11βHSD2 and the central regulation of sodium and water balance

The kidneys modulate water and sodium excretion in order to maintain plasma osmolality at a set point of ~290 mosmol/kg H_2O. To enable this, plasma osmolality must be detected and information relayed to the kidneys. Moreover, extra-renal mechanisms such as thirst and/or salt appetite, also act to normalize water balance and plasma osmolality.

1.3.1. AVP synthesis and release

1.3.1.1. Central control of AVP release

Changes in plasma osmolality are primarily detected by osmoreceptors located in the *organum vasculosum lamina terminals* (OVLT), a region of the brain not protected by the blood brain barrier, thus enabling a rapid response to perturbations in osmolality. The osmoreceptors are extremely sensitive: a 1% increase in plasma osmolality results in a rapid increase in plasma AVP concentration (Dunn *et al*., 1973). Electrophysiological approaches confirmed the involvement of the OVLT in osmosensation. Application of hyperosmotic fluid to isolated OVLT neurons evoked membrane depolarization; moreover there was a linear correlation between osmolality and firing rate (Ciura and Bourque, 2006). Additionally, functional magnetic resonance imaging in humans demonstrated that infusion of hypertonic saline resulted in activation of the third ventricle (illustrated by an increased blood-oxygen-level dependent (BOLD) signal), which contains the OVLT, and the sensation of thirst (Egan *et al*., 2003).

To be classified as osmoreceptors, activation of osmosensitive neurons must trigger a functional response, which acts to normalize plasma osmolality, for example the secretion of AVP. Lesions of the OVLT abolished the correlation between plasma osmolality and AVP release (Thrasher *et al*., 1982). Neurons from the OVLT have been demonstrated to project to both the supraoptic- and paraventricular- nuclei of the hypothalamus (SON and PVN respectively) (Camacho and Phillips, 1981). Additionally, the neurons that project from the OVLT to the SON are activated by hypertonic fluid (Nissen *et al*., 1993). As a result, changes in plasma osmolality are detected by the osmoreceptors in the OVLT, and relayed to the SON and PVN where AVP is synthesized.

AVP, a nine amino acid cyclic peptide, is produced in magnocellular neurosecretory cells located within the PVN and SON of the hypothalamus (Harding *et al*., 1995) (Figure 1.9). Evaluation of AVP-secreting cells within the SON of rats demonstrated increase neuron firing in response to augmented plasma osmotic pressure. Moreover there was a linear correlation between plasma osmotic pressure and the firing rate of AVP cells, indicative of the controlled and graded release of AVP in response to increased plasma osmolality. Reducing plasma osmotic pressure by water loading reduced neuron firing (Brimble and Dyball, 1977), suggestive of basal AVP release during resting conditions, enabling a rapid response to perturbations in plasma osmolality. Once synthesized, the AVP precursor is stored in membrane bound vesicles, which are transported along axons to the posterior pituitary, in which AVP is stored and then subsequently released into circulation.

Considerable levels of AVP accumulate within the posterior pituitary, such that basal secretion could be maintained for a month without additional synthesis. During dehydration these stores deplete rapidly; after approximately three days of water deprivation stored AVP levels would have reduced to about 90% (Laycock, 2010). Consequently, the rate of AVP synthesis and delivery to the posterior pituitary must increase to match demand. In response to dehydration, AVP mRNA expression increases followed by augmented protein synthesis, processes that take approximately two hours to complete. Therefore large AVP stores in the posterior pituitary are required for the rapid and sustained response to dehydration. Since the posterior pituitary is not protected by the blood brain barrier AVP is released directly through fenestrations into the circulation (Zingg *et al*., 1986, Gainer *et al*., 1977).

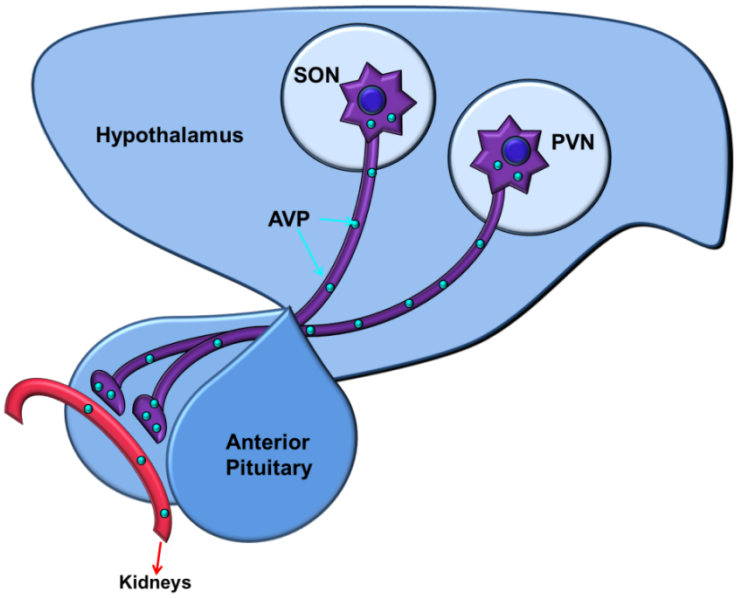

Figure 1.9: AVP is synthesized in the hypothalamus and then released into circulation by the posterior pituitary. SON, supraoptic nuclei of the hypothalamus. PVN, paraventricular nuclei of the hypothalamus. AVP, vasopressin.

1.3.1.2. The effect of corticosteroids on AVP release

Glucocorticoids are involved in the regulation of AVP synthesis and release. Hyperadrenocorticism is associated with an impaired release of AVP in response to plasma hypertonicity (Biewenga *et al*., 1991). Moreover, postmortem analysis of patients who had been receiving glucocorticoid therapy showed an attenuation of AVP immunoreactive neurons in their PVN and SON relative to controls (Erkut *et al*., 1998). The AVP gene contains a GRE. Binding of GR to this region caused a reduction in AVP promoter activity and consequently attenuated levels of AVP (Kim *et al*., 2001). These data support an inhibitory role for glucocorticoids in the regulation of AVP. In contrast, non-suppressible AVP release has been documented in experimental models of glucocorticoid deficiency (Boykin *et al*., 1978, Saito *et al*., 2000).

1.3.2. Thirst

In conjunction with reduced water excretion, increased water intake, through the stimulation of thirst, also acts to normalize augmented plasma osmolality. As with AVP secretion, the sensation of thirst is triggered by the activation of osmoreceptors located in the OVLT. Small increases in plasma osmolality (1-2%) elicit thirst, which continues to increase in parallel with plasma hypertonicity. In addition to altered plasma osmolality, water intake is also stimulated by changes in blood volume, and blood pressure.

The role of the OVLT in the initiation of fluid intake was demonstrated by lesion studies, in which the destruction of the region reduced water consumption in response to increased plasma osmolality (Thrasher *et al*., 1982). Given that water intake is terminated prior to the restoration of plasma osmolality a feed-forward mechanism is implied, such that the anticipation of rehydration prevents excessive fluid consumption. Such a mechanism was demonstrated in dehydrated dogs: fluid intake stopped prior to the dilution of plasma (Thrasher *et al*., 1981). These data suggest first that the act of drinking, rather than fluid intake *per se*, regulates thirst: and second that osmoreceptors located outside of the brain detect water intake. In line with this hypothesis, the NTS and the area postrema (AP) receive vagal inputs from the abdominal viscera (Norgren and Smith, 1988). In rats the destruction of these neuronal fibres resulted in the over consumption of water (Curtis and Stricker, 1997).

Volume contraction also stimulates water intake, indeed the loss of blood in the absence of plasma hypertonicity initiates fluid consumption and AVP release (Stricker and Sved, 2000). Fluid intake in response to hypovolemia is initiated in part in response to neuronal inputs from cardiac baroreceptors. Afferents from baroreceptors project to the NTS, triggering fluid intake. Destruction of cardiac baroreceptors prevented water intake in response to reduced venous return in dogs (Quillen *et al*., 1990). Similarly, the placement of an arterial balloon, which prevented the detection of hypovolemia, blunted water intake in rats (Kaufman, 1984). However, despite this, in rats the destruction of the NTS did not prevent water intake or AVP secretion induced by volume contraction (Schreihofer *et al*.,

1994). These data suggest that although baroreceptor activation is involved in the initiation of thirst, it is not essential for the response to volume contraction.

Finally, thirst is also stimulated by hypotension. The administration of β-adrenoreceptor agonists to rats caused a significant reduction in blood pressure and a concominant increase in water intake (Lehr *et al*., 1967).

1.3.3. Salt appetite

1.3.3.1. Salt appetite: the innate drive to consume sodium

Sodium is the predominant extracellular cation and therefore the main determinant of plasma osmolality. As such its intake and excretion must be tightly regulated in order to maintain balance. The excretion of sodium is largely mediated by the kidneys, whereas the motivation to consume sodium ("salt appetite") is driven by complex central circuits which respond to both hypovolemia and sodium depletion. Wilkins and Richter obtained clinical evidence for the existence of an intrinsic salt appetite in 1940. Their seminal case study described a child suffering from adrenal insufficiency. As a result of the condition he synthesized low levels of aldosterone and was unable to conserve sodium renally. To compensate for the unregulated loss of sodium he developed an augmented salt appetite, actively seeking and ingesting high levels of the mineral. When admitted to hospital and placed on a regular diet the child died (Wilkins and Richter, 1940), illustrating that the maintenance of sodium balance is essential for survival.

Experimentally, salt appetite is modeled by inducing sodium depletion, commonly through adrenalectomy (which causes renal sodium wasting) (Fregly and Waters, 1966) or sodium deprivation challenges (Liedtke *et al*., 2011). The trigger for increased sodium intake is not, however, hyponatremia but rather volume contraction; indeed reductions in plasma sodium in the absence of volume contraction do not stimulate sodium appetite. In contrast to the thirst response to hypovolemia, which occurs within hours of volume contraction, the onset of salt appetite is relatively delayed, sometimes occurring days after the stimulus, and often over corrects the deficit (Geerling and Loewy, 2008).

1.3.3.2. The effect of corticosteroids on salt appetite.

The involvement of adrenal hormones in salt appetite was elucidated from investigations in adrenalectomized rats. Removal of the adrenal gland resulted in death, unless the rats were given a sodium-supplemented diet. When given access to salt solution and water the rats chose to drink vast quantities of the sodium solution. Therefore, they were able to intrinsically compensate for the renal inability to conserve sodium (Richter, 1936). Subsequently, it was proved that the salt appetite stimulated by adrenalectomy was a consequence of sodium deficiency. Adminstration of aldosterone, to restore renal sodium reabsorption, reduced NaCl intake in adrenalectomized rats. There was, however, a U shaped correlation between NaCl intake and the dose of aldosterone administered. Minimum consumption was observed at the concentration of aldosterone closest to the rate at which it is secreted from the adrenal gland of intact rats. At this concentration it could be postulated that sodium balance was restored. However, at

supraphysiological doses aldosterone stimulated NaCl consumption (Fregly and Waters, 1966). Aldosterone is the only hormone that has been demonstrated to selectively stimulate salt intake: unlike other hormones, e.g. angiotensin II (angII), it has minimal effects on water intake (Geerling and Loewy, 2006). Despite this, the demonstration that supraphysiological concentrations are required to induce sodium ingestion (Fregly and Waters, 1966) suggests that aldosterone acts to increase sodium appetite, rather than being the primary stimulus for it. This hypothesis is corroborated by the demonstration that glucocorticoids and intracerebroventricular (i.c.v.) angII exacerbated aldosterone's effect (Ma *et al*., 1993, Fluharty and Epstein, 1983)

1.3.3.3. The role of 11βHSD2 in salt appetite.

MR are located on the neurons of the NTS. The coexpression of 11βHSD2 ensures that the receptors are selectively activated by the mineralocorticoid. Recent work suggests that 11βHSD2-positive neurons in the NTS play a key role in the central response to sodium deficiency. Firstly, 11βHSD2 neurons were shown to be active in sodium-deprived but not replete rats (Geerling *et al*., 2006a). *In vivo* investigations into the role of 11βHSD2 in salt appetite have been hampered by the inability to selectively inhibit the enzyme in the NTS. Therefore, although subcutaneous glycyrrhizic acid (to inhibit 11βHSD2) resulted in augmented salt appetite in rats (Cooney and Fitzsimons, 1996), it is impossible to discern whether the intake was secondary to altered renal sodium handling. Increased salt appetite has been documented in a patient with a partial loss of 11βHSD2 activity. Significantly, the increased salt intake was postulated to exacerbate the potentially

mild hypertensive effects of attenuated enzyme activity in the kidney (Ingram *et al*., 1996).

1.4. The Syndrome of Apparent Mineralocorticoid Excess

1.4.1. Clinical loss of 11βHSD2.

In humans the loss of 11βHSD2 function causes the syndrome of apparent mineralcorticoid excess (AME). Characterized by features associated with hyperaldosteronism and augmented activation of MR (salt-dependent hypertension, hypokalemic alkalosis and plasma volume expansion), AME was first described by Werder *et al*., in 1974 (Werder E *et al*., 1974). Paradoxically, sufferers also exhibited hypoaldosteronism (Ulick *et al*., 1979) suggesting the involvement of non-aldosterone mediated activation of MR. Polyuria has also been documented (Stewart *et al*., 1996). Subsequent evaluation demonstrated that the severity of the condition could be augmented by cortisol administration and improved by dexamethasone, a synthetic glucocorticoid with negligible activity at MR (Stewart *et al*., 1988). Based on these data it was postulated that AME resulted from the illicit occupation and activation of MR by glucocorticoids due to defective 11βHSD2. Genetic analysis of patients suffering from AME confirmed that *HSD11B2* was mutated. To date >35 different genotypes have been identified, the mutations of which, (with the exception of L114,Δ6nt, R74G and P75,Δ1nt), are all located on exons 3, 4 and 5 of *HSD11B2* (Draper and Stewart, 2005, Morineau *et al*., 2006) (Figure 1.10). In 1990 a second variant of AME (AME type 2) was described (Ulick *et al*., 1990). Sufferers of this condition presented with a milder phenotype and a delayed onset of hypertension,

which typically developed in early adulthood (Li *et al*., 1998). In these patients mutations in *HSD11B2* resulted in only partial reductions in 11βHSD2 enzyme activity. This has led to the classification of AME as a continuum disorder (Li *et al*., 1998) with the extent of the enzyme deficiency correlating with the severity of the phenotype.

In addition to being congentital disease AME can be acquired, typically by the overconsumption of licorice and carbenoxolone (an antiulcer drug). Since glycrrhizic acid (the active component of licorice) and carbenoxolone inhibit 11βHSD2, abuse of these substances results in hypertension and hypokalemia (Mantero *et al*., 1996).

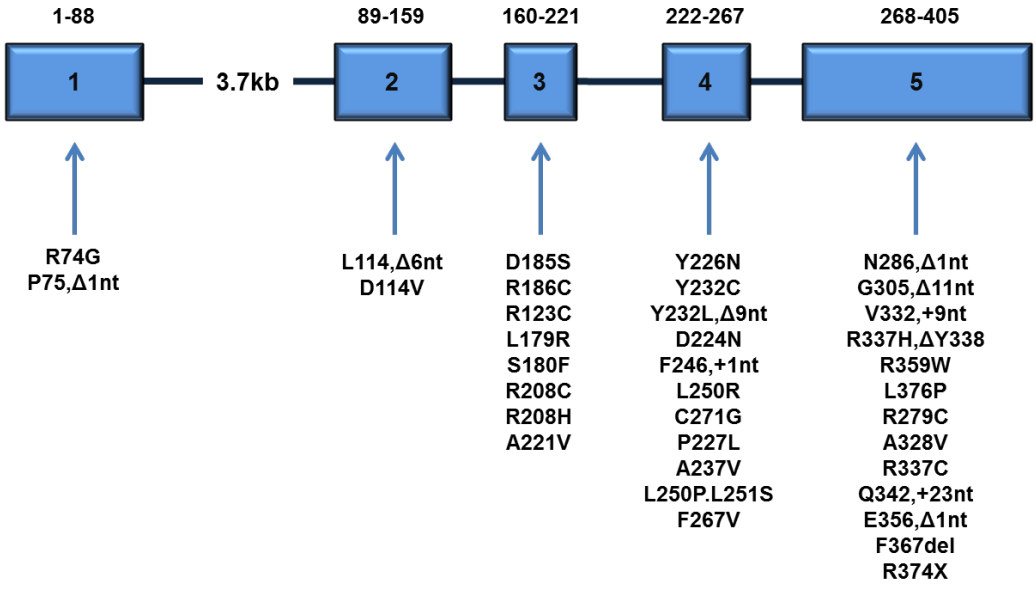

Figure 1.10: Schematic of the HSD11B2 gene mutations causative in AME. The five exons are represented by boxes, the introns are lines. Numbers above the exons are the amino acid numbers. Adapted from (Morineau *et al*., 2006)

1.4.2. Experimental evaluation of the origins of AME

Attempts to resolve the effects of loss of 11βHSD2 function into specific organ function (brain/kidney) have compared the effects of i.c.v. and subcutaneous (s.c.) drug delivery. I.c.v. infusion of aldosterone induced hypertension in unilaterally nephrectomized rats. Moreover, the concentrations required to increase blood pressure were significantly lower than those needed when aldosterone was administered s.c. The pressor effects of aldosterone were attenuated by MR antagonism, implicating the receptor in the response (Gomez-Sanchez and Gomez-Sanchez, 1986). Similarly, i.c.v. carbenoxolone (to inhibit 11βHSD2 in the brain) increased blood pressure in rats and the hypertensive effects of oral carbenoxolone were prevented by the concurrent i.c.v. infusion of an MR antagonist (Gomez-Sanchez and Gomez-Sanchez, 1992). Given that MR antagonism prevented the hypertensinogenic effects of carbenoxolone, it is likely that the increased blood pressure reflects reduced protection of MR by 11βHSD2 in the brain. Despite these data, the fact that blood pressure was normalized in an AME patient by kidney transplantation (Palermo *et al*., 2000) suggests that the hypertension was renal in origin.

In addition, s.c. but not i.c.v. aldosterone was shown to induce polyuria in unilaterally nephrectomized rats (Gomez-Sanchez, 1986). Similarly, i.c.v. carbenoxolone, to inhibit 11βHSD2 in the brain, did not alter urine flow in rats, whereas oral administration resulted in a two-fold increase. In support of a renal origin to the polyuria, the increased urine flow was not normalized by the i.c.v. administration of an MR antagonist (Gomez-Sanchez and Gomez-Sanchez, 1992).

However, caution must be taken when interpreting these data given the unselective nature of carbenoxolone, which also inhibits 11βHSD1 (Hult *et al*., 1998).

1.4.3. A mouse model of AME

Although evaluation of AME sufferers has provided useful information regarding the consequences of defective 11βHSD2, investigations are hampered by 1) the rarity and severity of the disease and 2) the limits of clinical experiments in patients. Less than 100 cases of AME have been documented worldwide, making large clinical investigations of the disorder unfeasible. Moreover, the condition is predominantly found in children, often with fatal manifestations, (Mantero *et al*., 1996) further limiting clinical studies. Therefore, research into the consequences of mutated *HSD11B2* has been greatly aided by the development of genetically modified mice.

Homologous recombination permits the discrete targeting of genes within a genome. In past two decades this technology has been used to generate "knockout" mice, in which the gene of interest is rendered functionally inactive. Consequently, the *in vivo* function of the gene product can be evaluated (Figure 1.11). This technique was used to generate 11βHS2D2$^{-/-}$ mice.

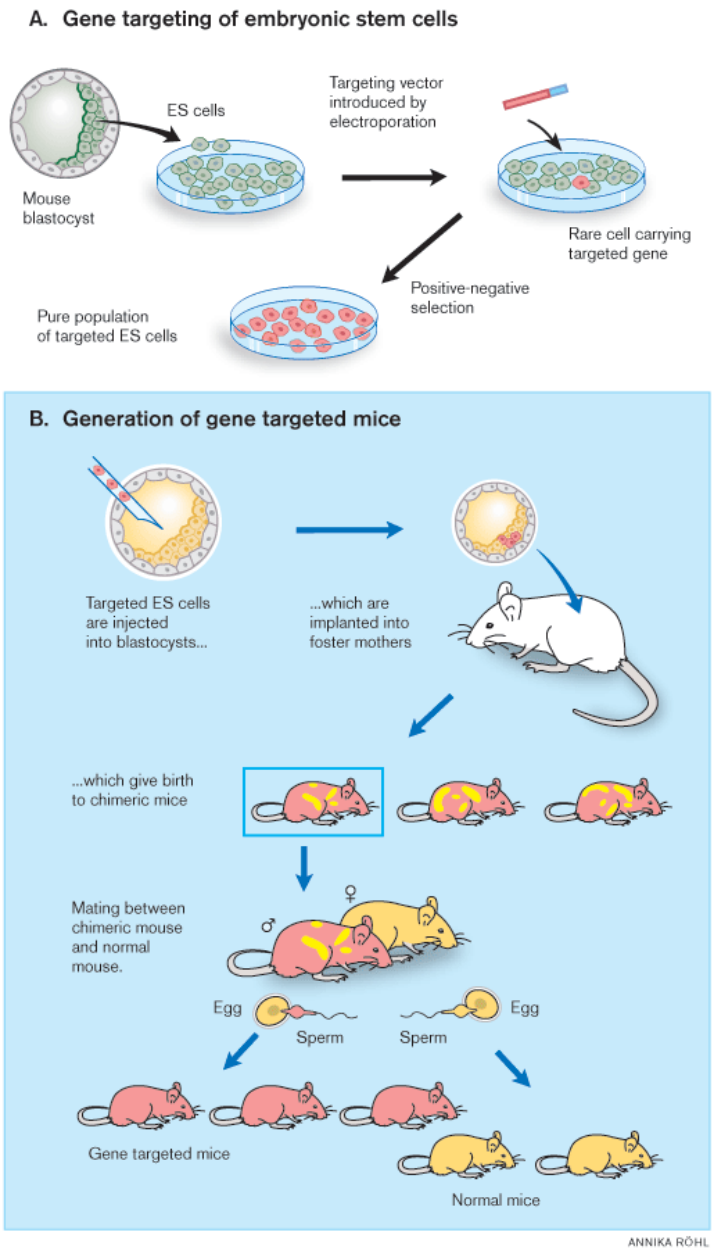

Figure 1.11: Gene targeting in mice. Electroporation is used to introduce the targeting vector in embryonic stem (ES) cells. In a few cells homologous recombination will occur such that the mutation is transferred into the genome. Cells in which homologous recombination has occurred are identified using positive-negative selection. Blastocysts containing the targeted cells are then implanted in the foster mother, the offspring of which are chimeric. Crossing of the chimeric mice with wildtype mice leads to the generation of gene targeted mice. Figure taken from (Hansson, 2007)

Mice in which 11βHSD2 have been deleted provide an excellent experimental model of AME, having many of the clinical features of the disease (hypertension, hypokalemia and polyuria) (Bailey *et al*., 2008, Kotelevtsev *et al*., 1999). Neonatal mortality was observed in the null mice, ~50% died within two days of birth. The mice had a low urinary sodium/potassium ratio, suggesting that increased urinary potassium excretion contributed to the hypokalemia. To evaluate whether the altered electrolyte handling was attributable to increased glucocorticoids the effect of dexamethasone was assessed. Dexamethasone, which suppresses corticosterone, normalized urinary sodium/potassium ratios. The involvement of glucocorticoids in the phenotype was confirmed by the observation urinary sodium/potassium ratios returned to the basal level following corticosterone replacement. Consequently, overactivation of MR was postulated to contribute to the phenotype. Structural changes within kidney were also described, notably hypertrophy and hyperplasia within the distal tubule. Since chronic sprionolactone did not normalize the renal structure, the involvement of non-MR stimulated pathways in the damage was postulated. Notably, heterozygous mice were phenotypically normal (Kotelevtsev *et al*., 1999).

Additionally, time course investigation has provided insights into the etiology of the hypertension observed in AME (Bailey *et al*., 2008). Initially the augmented blood pressure was renal in origin, driven by increased ENaC activity and impaired sodium excretion. However, at later time points sodium excretion was normalized in correlation with decreased ENaC activity. The observation that urinary excretion of

catecholamines was increased in 11βHSD2$^{-/-}$ mice, and that antagonism of α1-adrenoreceptor normalized blood pressure, implicated sympathetic overdrive in the hypertension.

A key finding from this study was the separation of water and sodium retention in the model (Bailey *et al*., 2008). Although the mice were hypertensive at all time points, they were also paradoxically volume contracted. The uncoupling of sodium and water retention was indicative of a urine-concentrating defect, indeed the mice were polyuric, producing high volumes of low osmolality urine.

1.5. Aim of PhD

The studies detailed in this thesis were undertaken to evaluate water and sodium turnover in 11βHSD2$^{-/-}$ mice. It was hypothesized that loss of enzyme in the activity the kidney would result in the derangement of water and sodium excretion. In addition the evaluation of mice in which *hsd11b2* had been selectively targeted in the brain and kidney allowed the separation of central and renal effects of 11βHSD2.

Chapter 2: Evaluation of Renal Water and Electrolyte Handling in Conscious 11βHSD2$^{-/-}$ Mice

2.1. Introduction

The syndrome of Apparent Mineralocorticoid Excess is characterized by glucocorticoid-mediated activation of MR, as a result of impaired 11βHSD2 function. Cardinal features of the condition include hypokalemia, hypoaldosteronism and hypertension. Although 11βHSD2 is expressed in several tissues throughout the body, including the brain and vascular endothelium, it is postulated that the hypertension in the condition is renal in origin, driven by the impaired renal excretion of sodium (van Uum *et al*., 1998, Ferrari and Krozowski, 2000).

In the kidney, as in other aldosterone target tissues, 11βHSD2 acts to protect the MR from activation by glucocorticoids. In the principal cells of the distal nephron activation of MR causes the increased activity of ENaC and Na/K-ATPase, and consequently increased sodium reabsorption. Therefore, it is postulated that in AME hypertension is driven by sodium retention and the concurrent volume expansion (Ferrari and Krozowski, 2000). This hypothesis is in accord with the Guytonian view of the blood pressure regulation, summarized in Figure 2.1. In this model the retention of sodium causes the retention of fluid, volume expansion and consequently increased cardiac output. As a result of this, peripheral resistance increases, causing an increase in mean arterial blood pressure. In an attempt to normalize blood pressure, urinary sodium excretion is increased (referred to as pressure natriuresis) resulting in reduced extracellular blood volume and therefore blood pressure.

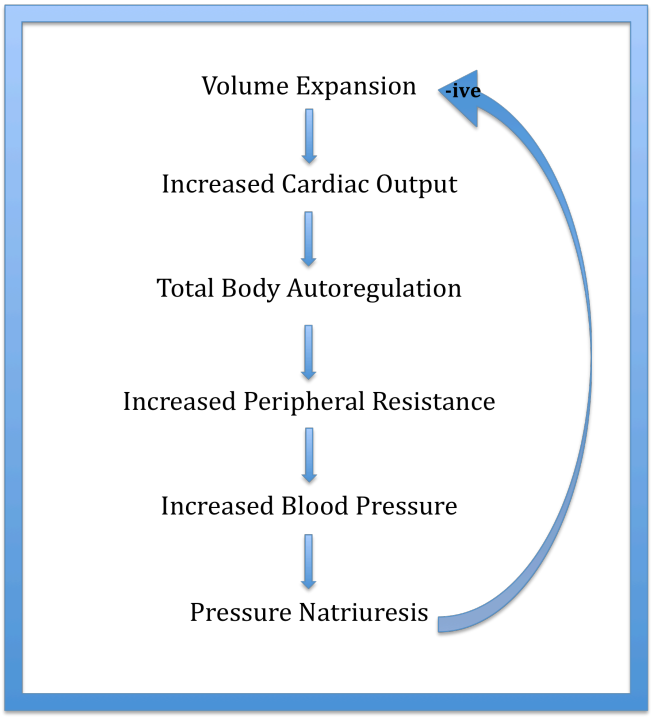

Figure 2.1: The Guytonian view of blood pressure regulation, (adapted from (Bongartz *et al*., 2005).

Clinically, the confirmation of the molecular mechanisms involved in the development of hypertension in AME has been hampered by the rarity of the disease. Nevertheless, the limited data available do support a renal component to the augmented blood pressure. Firstly, the urinary sodium/potassium concentration ratio was suppressed in a patient with AME, indicative of augmented sodium retention and potassium excretion. These data are cohesive with the effects of MR stimulation in the distal nephron. Indeed, since dexamethasone increased, and hydrocortisone decreased, the urinary sodium/potassium concentration ratio, glucocorticoid

activation of MR was implicated in the phenotype. The impaired renal handling of sodium and potassium in the patient resulted in hypokalemia and hypertension (Stewart *et al*., 1988). Secondly, blood pressure and plasma potassium concentrations were normalized by a kidney transplantation operation in a patient with AME (Palermo *et al*., 2000), suggesting that in this instance hypertension was the result of impaired renal function.

Identification of the molecular mechanisms causative in AME has been facilitated by the generation of *hsd11b2* null mice (Kotelevtsev *et al*., 1999). When originally bred on an MF1 background the phenotype of the 11βHSD2$^{-/-}$ mice was shown to closely parallel the clinical condition: hypertension, hypokalemia and suppressed plasma aldosterone levels were observed. Moreover, the urinary sodium/potassium ratio was attenuated in the null mice and could be normalized by dexamethasone, suggestive of glucocorticoid mediated over-activation of MR in the distal nephron. However, the high neonatal mortality in the model, when maintained on an MF1 background, prevented the more thorough evaluation of the mechanisms involved in the impaired renal electrolyte handling. Subsequently, the mice were backcrossed onto a C57Bl/6 background, which resulted in a milder phenotype and increased survival. This enabled the more detailed evaluation of mechanisms causative in AME.

Temporal evaluation of the progression of hypertension in the 11βHSD2$^{-/-}$ mice provided key insights into its development. Although sodium retention and increased ENaC function were reported at early time points (35 and 60 days) this did

not persist. At 80 days decreased ENaC function and natriuresis were observed, suggesting that at this age hypertension was not the result of sodium retention. Moreover, volume contraction was observed in the null mice at all points assessed, suggestive of a urine-concentrating defect, and the uncoupling of sodium and water retention at early time points (Bailey *et al*., 2008). Although it is likely that a transient volume expansion is causative in the development of hypertension at the time points prior to those assessed, at the point of evaluation a new steady state of volume contraction was observed, suggesting that alternative mechanisms contribute to the sustainment of hypertension.

Therefore, the studies detailed in this chapter were designed to evaluate the effect of *hsd11b2* deletion on the renal handling of water, sodium and potassium in conscious mice. Initial experiments confirmed that the polyuric phenotype, previously observed in the 11βHSD2$^{-/-}$ when bred on an MF1 background, persisted on an inbred C57Bl/6 background. A key aim was to establish whether the deranged water handling was progressive, and whether the ability to concentrate urine in response to a water deprivation challenge was impaired. Finally, a detailed evaluation of electrolyte excretion was performed to provide an insight into the renal handling of sodium and potassium in conscious 11βHSD2$^{-/-}$ mice.

Hypothesis

1. Global deletion of 11βHSD2 results in a urine-concentrating defect.
2. Loss 11βHSD2 function in the kidney results in polyuria, with polydipsia arising as a secondary consequence in order to maintain balance.

2.2. Methods

2.2.1. Animals

Experiments were performed on male C57Bl/6 and 11βHSD2$^{-/-}$ mice aged <100 and >180 days (representing mice aged 50-70 and 180-250 days respectively). These time points were selected on the basis of pilot histopathological analysis (performed by Dr David Brownstein, data not shown). Since the 11βHSD2$^{-/-}$ mice used in these studies were generated from null-null crosses, wildtype littermates were not available for comparison. Therefore, throughout the studies detailed, C57Bl/6 mice were used as controls given that this is the background strain of the null mice (n=4-7 throughout).

2.2.2. Metabolic cage studies

Mice were individually housed in metabolic cages (model 3600M021, Tecniplast Ltd, UK) for the duration of the experiments under 12-hour light and dark cycles in a room with controlled temperature (~23°C) and humidity (~25%). Throughout the study mice had free access to powdered rodent maintenance (RM1) diet (0.7% potassium and 0.3% sodium, Special Diet Services Ltd, UK) and water, unless otherwise specified.

2.2.2.1. Evaluation of basal renal function and urine concentrating ability

Following 3-4 days acclimatization, baseline measurements of body weight, urine output, food and water intake were made over 4 days, after which water was

removed for 24 hours to assess urine concentrating ability. Following a 1 week recovery period, a second 24-hour water deprivation was performed, immediately prior to which the synthetic V_2R agonist desmopressin (ddAVP; 1μg/kg s.c, Sigma-Aldrich, UK) was administered.

2.2.2.2. Evaluation of the response to acute V_2R stimulation

The origin of the polyuria was evaluated in separate cohorts of mice. Following a 3-4 day acclimatization period, baseline measurements were made over 4 days, during which time the mice had *ad libitum* access to food and water. Throughout this period urine output and water intake were measured at 6 and 24 hours on each day. On the fifth day mice were treated with ddAVP (1μg/kg s.c.). Urine output and water intake were measured at 6 and 24 hours post administration. Additional experiments were performed to control for the effects of s.c. injection (30μl saline s.c.).

2.2.2.3. Evaluation of the response to water restriction

To evaluate the contribution of polydispsia to the polyuria, water restriction studies were performed. After acclimatization and baseline measurements, as described in section 2.2.1.1, 11βHSD2$^{-/-}$ mice were presented with a restricted water intake (5ml/24hr) over a 4 day period. This volume was selected based on the consumption of aged matched C57Bl/6 mice in the study detailed in 2.2.1.1.

2.2.3. Analysis

Urine volume (UV) was determined gravimetrically, assuming a density equal to that of water; urine flow rates are expressed as ml/24hr. Water intake was calculated similarly. Water balance was calculated by subtracting the average daily urine flow rate (ml/24hr) from the average daily water intake (ml/24hr). Cumulative water balance, expressed in ml, was the sum of the individual daily water balances over the 4-day baseline period. Daily consumption of food (g/24hr) was used to calculate sodium intake, which was expressed in mmol/24hrs.

Urinary sodium and potassium concentrations were measured using flame photometry (Model BWB-1 Performance Plus Flame Photometer, Spectonic Analytical Instruments, UK) or an electrolyte analyzer (AVI 9180 Electrolyte analyzer, Roche, UK). For flame photometry 200µl of urine was mixed with 9800µl diluent solution (1ml diluent (approximately 1% w/v Brij-35, BWB Technologies, UK) in 1000ml deionised water) prior to analysis. Four point standard curves were generated using sodium and potassium standard solutions (BWB Technologies, UK) and used for electrolyte quantification. For the electrolyte analyzer, urine samples were diluted 1 in 5 in deionised water and then 1 in 3 in 120mM NaCl. Cumulative sodium balance over the 4-day baseline period was calculated in a similar fashion to water balance. Sodium excretion was subtracted from sodium intake and balance expressed in mmol/24hrs.

Urine osmolality was measured in a 40µl sample by freezing point depression (Osmometer, OM801, Vogel, Germany).

Urinary calcium, magnesium and phosphate were measured by the Clinical Analysis Core Service at the University of Edinburgh, using commercially available colourmetric assays. Urinary aldosterone was measured by Dr Emad Al-Dujaili using a previously described ELISA (Al-Dujaili *et al*., 2009).

2.2.4. Statistics

Data are presented as means ± standard error of the mean (S.E.M.) except for cumulative data, which are medians ± range. Statistical significance was evaluated using a one-way ANOVA and Tukey post-test, or a Kruskal-Wallis test with Dunn's post-test as appropriate to compare significance between groups.

2.3. Results

2.3.1. Water homeostasis in 11βHSD2$^{-/-}$ mice

2.3.1.1. Basal water handling and urine concentrating ability

To examine the effect of *hsd11b2* deletion on water turnover, water intake and urine flow were evaluated in <100 and >180 day old mice. At <100 days 11βHSD2$^{-/-}$ mice drank significantly more water (Figure 2.2.A) and produced significantly more urine (Figure 2.2.B) than aged matched C57Bl/6 controls. Urine osmolality was significantly lower in the <100 day 11βHSD2$^{-/-}$ mice than the <100 day C57Bl/6 mice (Figure 2.2.C). The elevated water turnover meant that cumulative water balance was significantly higher in the 11βHSD2$^{-/-}$ than the C57Bl/6 mice at <100 days (Figure 2.2.D).

At >180 days, the null mice displayed exacerbated polyuria (Figure 2.2.B) and polydipsia (Figure 2.2.A). 24-hour urine flow was four times greater in 11βHSD2$^{-/-}$ mice the age matched C57Bl/6 controls (Figure 2.2.B). Polyuria was associated with a significant polydipsia (Figure 2.2.A); and consequently the mice maintained a cumulative water balance not significantly different from the C57Bl/6 controls (Figure 2.2.D). Throughout the baseline period, both 11βHSD2$^{-/-}$ and C57Bl/6 mice remained in a positive water balance. This likely reflects insensible water losses, such as the evaporation that occurs during respiration. Using the methods detailed it was not possible to measure insensible water losses. Urine osmolality was lower in the >180 day 11βHSD2$^{-/-}$ mice than the age matched C57Bl/6 mice, suggesting an

impaired urine concentrating ability (Figure 2.2.C). Consequently, urine-concentrating ability was assessed using a 24-hour water deprivation challenge.

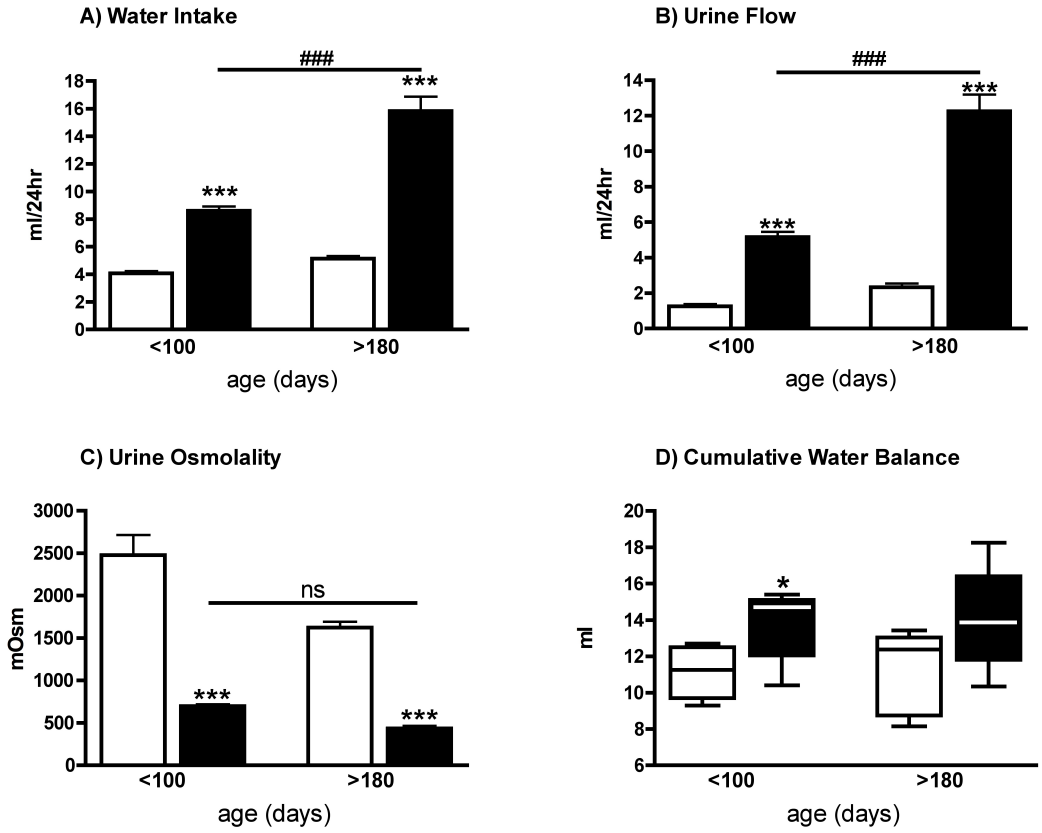

Figure 2.2: Water turnover in C57Bl/6 (white) and 11βHSD2$^{-/-}$ (black) mice aged <100 and >180 days. (A) Water intake. (B) Urine Flow. (C) Urine Osmolality. (D) Cumulative Water Balance calculated over the four-day baseline period. Data are means ± S.E.M. except for (D) which are medians ± range. Statistical analysis was performed using a one-way ANOVA with Tukey post-test (A, B, C) or Kruskal-Wallis test with Dunn's post-test (D) as appropriate. ***P<0.001, **P<0.01, *P<0.05, compared to age matched controls. ###P<0.001 compared to younger mice within the same genotype.

At <100 days 11βHSD2$^{-/-}$ mice concentrated their urine to the same extent as age matched C57Bl/6 controls, with no significant difference between urine flow (Figure 2.3.A) or urine osmolality (Figure 2.3.B). In corroboration with a functional concentration response, weight loss (used as an indicator of body fluid loss) and water balance were not significantly different between the two groups at this age (Figures 2.3.C and 2.3.D).

In contrast, at >180 days urine concentrating ability was impaired in 11βHSD2$^{-/-}$ mice. Urine flow rate remained significantly higher (Figure 2.3.A), and osmolality significantly lower (Figure 2.3.B) than the C57Bl/6 controls during the water deprivation challenge. 11βHSD2$^{-/-}$ mice at this age lost significantly more weight (Figure 2.3.C) and water balance was more significantly negative (Figure 2.3.D) reflective of a net fluid loss.

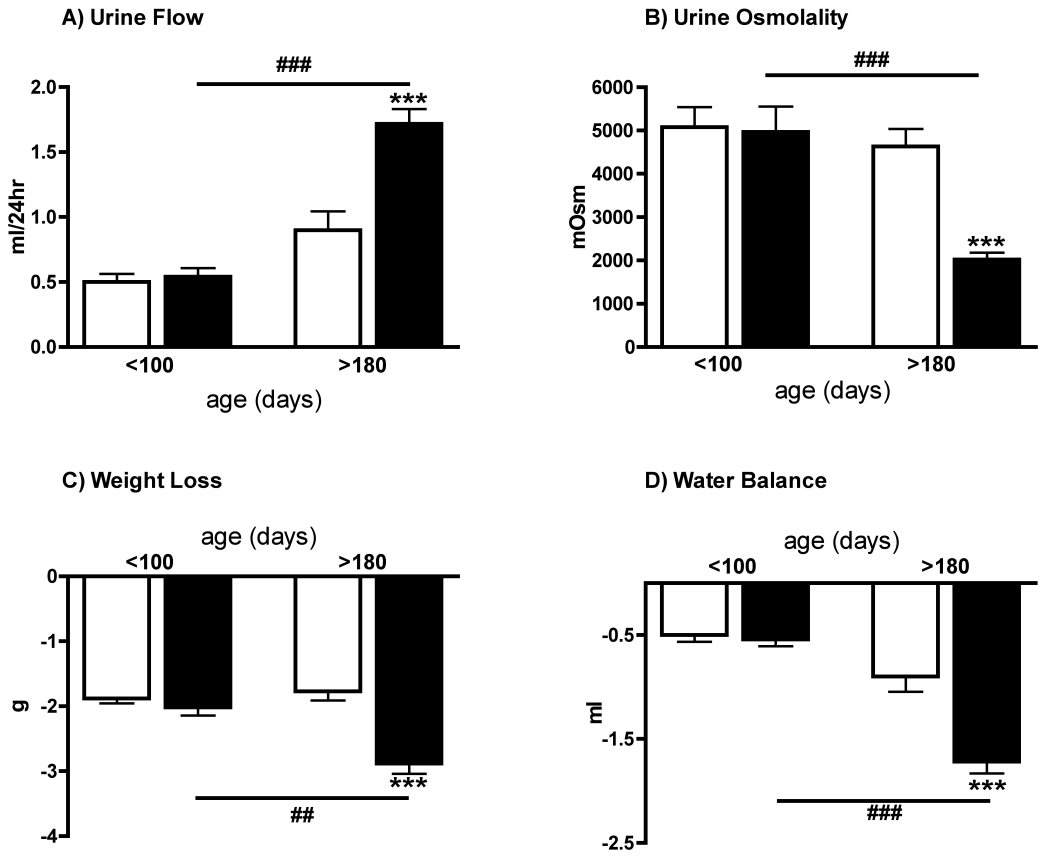

Figure 2.3: Response to water deprivation in C57Bl/6 (white) and 11βHSD2$^{-/-}$ (black) mice at <100 and >180 days (A) Urine Flow. (B) Urine Osmolality. (C) Weight Loss. (D) Water Balance. Data are means ± S.E.M. Statistical analysis was performed using a one-way ANOVA with Tukey post-test. ***P< 0.001 compared to age matched controls. ###P<0.001, ##P<0.01, compared to younger mice within the same genotype.

To establish the mechanisms of the impaired urine concentrating ability in 11βHSD2$^{-/-}$ mice, the response to a water deprivation challenge following the administration of ddAVP, a V_2R specific AVP analogue, was evaluated. ddAVP failed to rescue the phenotype; >180 day old 11βHSD2$^{-/-}$ mice continued to produce significantly higher volumes of more dilute urine during water deprivation challenge. Again, a substantially greater weight loss and an attenuated water balance reflected an augmented loss of body fluid in the >180 day 11βHSD2$^{-/-}$ mice (Table 2.1).

	<100 Days		**>180 Days**	
	C57Bl/6	**11βHSD2$^{-/-}$**	**C57Bl/6**	**11βHSD2$^{-/-}$**
UV (ml/24hr)	0.4 ± 0.1	0.6 ± 0.1	0.8 ± 0.1	1.5 ± 0.2^{ab}
UOsm (mOsm)	6928 ± 1327	2923 ± 388.7^{a}	4505 ± 262.6	2292 ± 203.7
Δ Weight (g)	-1.7 ± 0.1	-1.8 ± 0.1	-1.6 ± 0.2	-2.4 ± 0.4
Water Balance (ml/24hr)	-0.4 ± 0.1	-0.6 ± 0.1	-0.8 ± 0.1	-1.5 ± 0.2^{ab}

Table 2.1: Response to water deprivation following s.c. ddAVP administration. UV, urine flow. UOsm, urine osmolality. Δ Weight, change in body weight. Water Balance, calculated as the difference between water intake and urine flow over 24hrs. Data are means ± S.E.M. Statistical analysis was performed using one-way ANOVA and a Tukey post-test. a=P<0.01 compared to age matched controls, b=P<0.001 compared to younger mice of the same genotype.

2.3.1.2. The response to acute V_2R stimulation

Chronic stimulation of V_2R, as occurs during a 24-hour water deprivation challenge, is thought to facilitate water reabsorption by stimulating *de novo* synthesis of AQP2 in the collecting duct. In contrast, acute V_2R stimulation is associated with increased translocation of pre-existing AQP2 from intracellular vesicles to the apical membrane (Nielsen *et al*., 1993a, Nielsen *et al*., 1995a). Therefore, to evaluate specifically the response to acute V_2R stimulation, the urine concentration response to ddAVP administration during free access to water was assessed in >180 day C57Bl/6 and 11βHSD2$^{-/-}$ mice. Prior to the administration of ddAVP 11βHSD2$^{-/-}$ mice produced significantly higher volumes of urine (Figure 2.4.A) and drank significantly more water (Figure 2.4.B) than the C57Bl/6 controls. ddAVP administration resulted in anuria for up to 6 hours in the C57Bl/6 control mice (Figure 2.4.A). In contrast ddAVP had no effect on water intake during the 0-6 hour period (Figure 2.4.B). ddAVP significantly reduced urine flow in the 11βHSD2$^{-/-}$ mice between hours 0-6. However, the concentration response was impaired relative to the C57Bl/6 mice, and anuria was not observed (Figure 2.4.A). As with the C57Bl/6 controls, water intake was not significantly altered by treatment with ddAVP (Figure 2.4.B). By 24 hours urine flow had restored to basal levels in both groups of mice (Figure 2.4.A). In saline control experiments s.c. administration of saline had no effect on urine flow or water intake in either group of mice (Table 2.2).

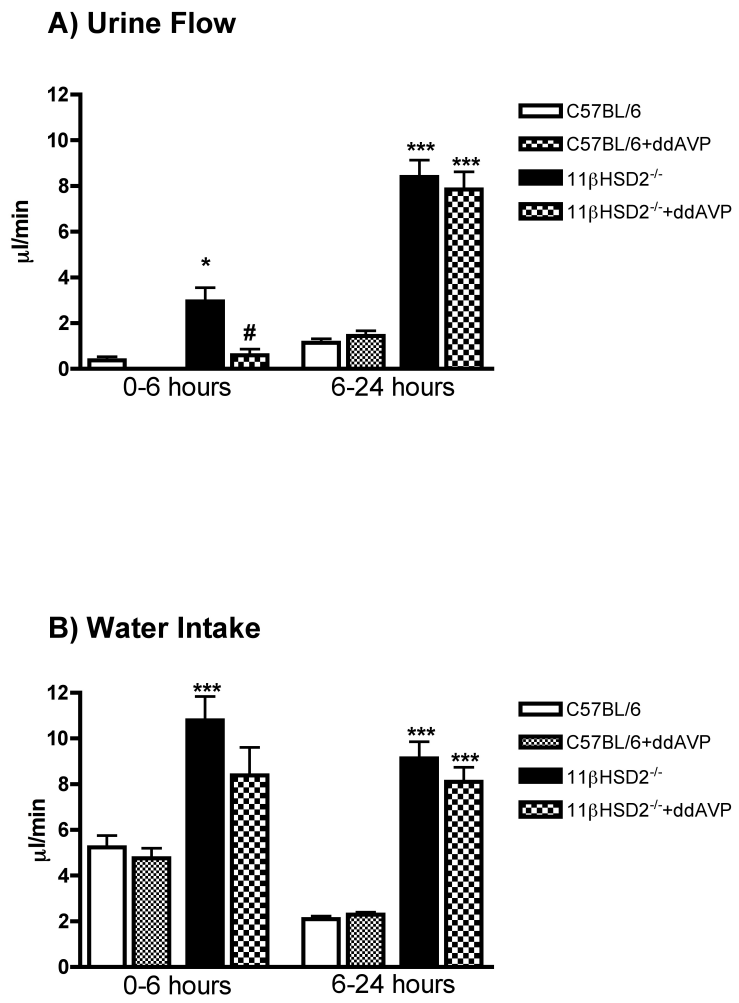

Figure 2.4: The effect of ddAVP on (A) Urine Flow and (B) Water Intake in 11βHSD2$^{-/-}$ (black) and C57Bl/6 (white) mice. Measurements were made during a baseline period (filled bars) and following ddAVP administration (1µg/kg s.c.) (hashed bars). 0-6 are rates recorded between hours 0-6. 6-24 are rates recorded between hours 6-24. Data are means ± S.E.M. Statistical analysis was performed using a one-way ANOVA and Tukey post-test. ***P<0.001, *P<0.5 compared to C57Bl/6 controls in same period. #P<0.5 compared to pre ddAVP values in the same mice in the same time period.

	0-6 hours				6-24 hours			
	C57Bl/6		11βHSD2$^{-/-}$		C57Bl/6		11βHSD2$^{-/-}$	
	Basal	**ddAVP**	**Basal**	**ddAVP**	**Basal**	**ddAVP**	**Basal**	**ddAVP**
UV (µl/min)	0.3±0.04	0.1±0.1	4.2±0.7	3.5±0.6	0.9±0.1	1.3±0.2	7.5±0.9	8.3±1.0
Water In (µl/min)	4.8±0.4	5.9±0.5	11.6±0.9	11.7±1.1	1.7±0.2	2.0±0.2	8.7±1.2	8.3±1.3

Table 2.2: The effect of saline on urine flow (UV) and water intake (Water In) in 11βHSD2$^{-/-}$ and C57Bl/6 mice. Measurements were made during a baseline period and following saline administration (30µl s.c.). 0-6 are rates recorded between hours 0-6. 6-24 are rates recorded between hours 6-24. Data are means ± S.E.M. Statistical analysis was performed using a one-way ANOVA.

2.3.1.3. The response to water restriction

Next the contribution of polydipsia to polyuria was evaluated in 11βHSD2$^{-/-}$ mice by the restriction of water intake to control levels. During the baseline period 11βHSD2$^{-/-}$ mice produced significantly higher volumes (Figure 2.5.A) of more dilute (Figure 2.5.B) urine than age-matched controls. Restriction of water intake caused a reduction in urine flow rate to a level that was not significantly different from that of the C57Bl/6 mice (Figure 2.5.A). Urine osmolality increased significantly during water restriction, however it remained significantly lower than that of the C57Bl/6 controls (Figure 2.5.B).

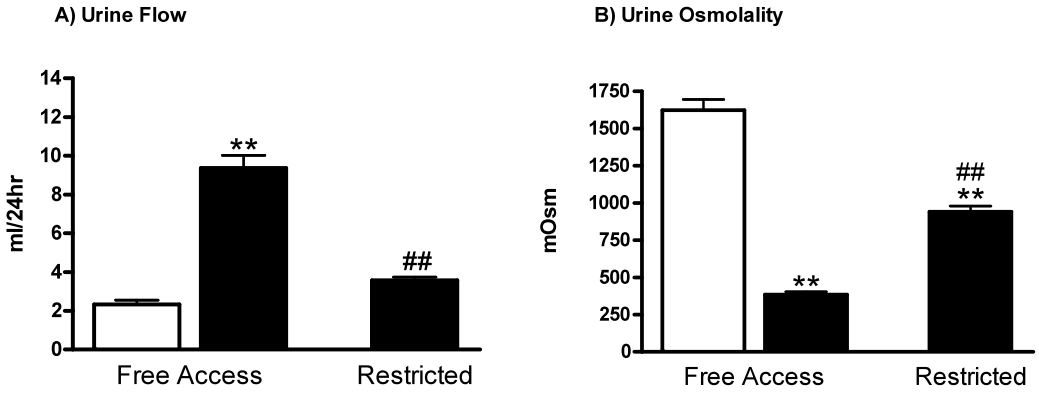

Figure 2.5: The effect of water restriction on (A) Urine Flow and (B) Urine Osmolality in C57Bl/6 (white) and 11βHSD2$^{-/-}$ (black) mice. Data are means ± S.E.M. Statistical analysis was performed using a one-way ANOVA and Tukey post-test. **P<0.001 compared to C57Bl/6 mice during the baseline period. ##P<0.001 compared to 11βHSD2$^{-/-}$ mice during the baseline period.

2.3.2. Electrolyte homeostasis in 11βHSD2-/- mice

In view of the postulated role of increased sodium retention and potassium excretion in AME, the urinary excretion of the electrolytes was assessed in conscious 11βHSD2$^{-/-}$ and C57Bl/6 control mice. Surprisingly, sodium excretion was significantly higher in the null mice than aged-matched C57Bl/6 mice at both <100 and >180 days (Figure 2.6.A). Since there was no significant difference in sodium intake (<100 day C57Bl6 0.54±0.009 versus <100 day 11βHSD2$^{-/-}$ 0.53±0.02 mmol/24hrs P>0.05, >180 day C57Bl6 0.55±0.01 versus >180 day 11βHSD2$^{-/-}$ 0.56±0.02 mmol/24hrs P>0.05) cumulative sodium balance was more negative in 11βHSD2$^{-/-}$ mice than the C57Bl/6 controls at both ages (Figure 2.6.B). Within genotypes sodium excretion increased in an age dependent manner: a higher natriuresis was observed in >180 day mice than the <100 day mice in both the control and null groups (Figure 2.6.A). This progressive increase in excretion was reflected in the sodium balance data: cumulative balance was more negative in the >180 day mice than the <100 day mice of the same genotype (Figure 2.6.B). Potassium excretion rates were not significantly different in the 11βHSD2$^{-/-}$ and C57Bl/6 mice (Figure 2.6.C). As a result, urinary sodium/potassium concentration ratios were significantly higher in the null mice than the C57Bl/6 controls at <100 and >180 days (Figure 2.6.D). Crucially, urinary aldosterone excretion rates were suppressed in the 11βHSD2$^{-/-}$ mice at <100 (C57Bl/6 4.0±0.2 versus 11βHSD2$^{-/-}$ 0.8±0.05 pmol/24hr, P<0.0001 using an unpaired t-test) and >180 days (C57Bl/6 6.2±0.9 versus 11βHSD2$^{-/-}$ 0.7±0.1 pmol/24hr, P<0.0001 using an unpaired t-test). These data suggested that loss of 11βHSD2 function resulted in hypoaldosteronism, in line with previous clinical and experimental observations.

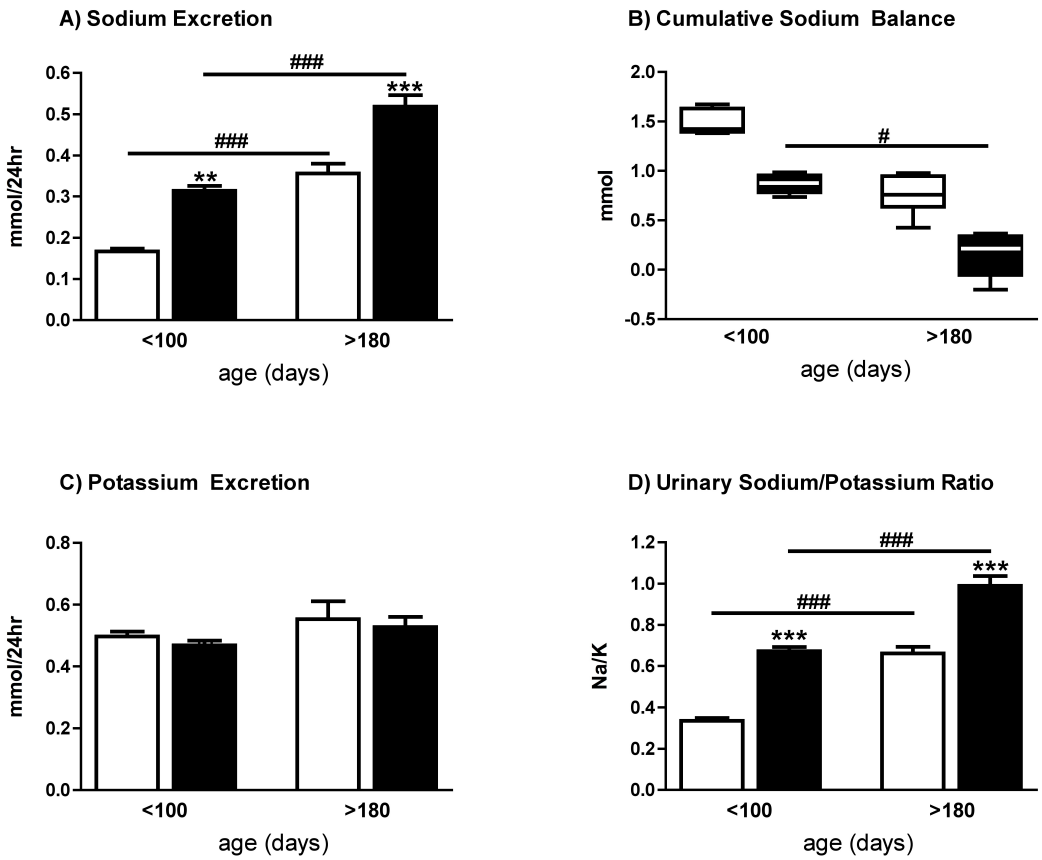

Figure 2.6: Sodium and potassium handling in C57Bl/6 (white) and 11βHSD2$^{-/-}$ (black) mice at <100 and >180 days. (A) Sodium Excretion. (B) Cumulative Sodium Balance over the four-day baseline period. (C) Potassium excretion. (D) Urinary Sodium/Potassium Concenrtration ratio. Data are means ± S.E.M., except for (B) which are medians ± range. Statistical analysis was performed using a one-way ANOVA and Tukey post-test (A, C, D) or Kruskal-Wallis test with Dunn's post-test (B) as appropriate. ***P<0.001, **P<0.01, compared to age matched controls. ###P<0.001, #P<0.05 compared to younger mice of the same genotype.

Previous evaluation of renal function in 11βHSD2$^{-/-}$ mice was performed in anesthetized mice, in which the administration of pharmacological agents was used to assess tubular function (Bailey *et al*., 2008). Since the current studies were performed in conscious mice, the evaluation of the acute response to exogenous markers of tubular function was not possible. Therefore, in an attempt to localize the natriuresis in the 11βHSD2$^{-/-}$ mice to a specific region of the nephron, the urinary excretion of phosphate, calcium and magnesium was evaluated. This provided an insight into the function of proximal tubule and loop of Henle respectively. Phosphate excretion was significantly higher in the 11βHSD2$^{-/-}$ mice than the C57Bl/6 controls at <100 days. By 180 days the excretion rate had decreased significantly to a level that was not significantly different from the age matched C57Bl/6 mice. The urinary excretion rates of calcium and magnesium were not significantly different between the 11βHSD2$^{-/-}$ and age-matched control C57Bl/6 mice at either <100 and >180 days (Table 2.3).

	<100 Days		>180 Days	
	C57Bl/6	**11βHSD2$^{-/-}$**	**C57Bl/6**	**11βHSD2$^{-/-}$**
Phosphate Excretion (μmol/24hr)	16.1±3.4	96.9±21.0[a]	26.4±8.1	38.7±8.4[b]
Calcium Excretion (μmol/24hr)	3.1±0.2	1.6±0.3	3.4±0.3	3.5±1.0
Magnesium Excretion (μmol/24hr)	40.3±2.2	25.4±0.9	32.8±5.2	44.5±4.5

Table 2.3: Urinary excretion rates of phosphate, calcium and magnesium in C57Bl/6 and 11βHSD2$^{-/-}$ mice aged <100 and >180 days. Data are means ± S.E.M. Statistical analysis was performed using one-way ANOVA and a Tukey post-test. Urine collections were made over a 4-day baseline period. a=P<0.01 when compared to age matched controls. b=P<0.05 when compared to younger mice of the same genotype.

2.4. Discussion

The syndrome of apparent mineralocorticoid excess is characterized by glucocorticoid-mediated activation of MR, the result of impaired 11βHSD2 function (Ferrari and Krozowski, 2000). Previous evaluation of 11βHSD2$^{-/-}$ mice found them to hypertensive but paradoxically volume contracted from an early age (Bailey *et al*., 2008). In accord with the Guytonian view of hypertension, it is likely that a transient volume expansion was involved in the initiation of hypertension, at time points prior to those evaluated (Guyton *et al*., 1984, Guyton and Hall, 2000). However, by 35 days compensatory mechanisms seem to have resulted in the resetting of fluid status to a volume depleted state. Consequently, alternative mechanism may be involved in the maintenance of hypertension. Hypertension in the absence of volume expansion was also found in the mouse of model of Cushing's syndrome, a condition driven by hypercortisolism. In this model of chronic exposure to excess glucocorticoids, hypertension developed despite severe polyuria and volume contraction (Dunbar *et al*., 2010). To evaluate the consequence of deranged glucocorticoid metabolism on water and sodium homeostasis, water and sodium turnover and urine concentrating ability were assessed in 11βHSD2$^{-/-}$ mice. The mice were evaluated at two ages, <100 days and >180 days, to determine whether the phenotype described was progressive. Through the evaluation of urinary divalent cation and phosphate excretion an indication of tubular function was obtained.

2.4.1. Basal water turnover is elevated in 11βHSD2$^{-/-}$ mice

11βHSD2$^{-/-}$ mice displayed a significant and progressive polyuria, producing large volumes of low osmolality urine. Urine flow was closely paralleled by water intake; consequently at >180 days 11βHSD2$^{-/-}$ mice were able to maintain a cumulative water balance not significantly different from the C57Bl/6 control mice. Despite being polyuric during free access to water, at <100 days the null mice had a functional concentration response to water deprivation. In contrast, at >180 days the 11βHSD2$^{-/-}$ mice continued to produce significantly larger volumes of more dilute urine following water removal, illustrative of a urine-concentrating defect. Therefore, the severity of the phenotype increased in a temporal manner. Water turnover was exacerbated at >180 days, and at this age polyuria was associated with an impaired response to water deprivation, indicative of a nephrogenic diabetes insipidus (D.I.) like phenotype.

2.4.2. Renal components to the polyuria in >180 day 11βHSD2$^{-/-}$ mice

Clinically, D.I., a disease characterized by severe polyuria and polydipsia, can be central or renal in origin depending on whether it is associated with an impaired central release of AVP, or an impaired renal response to AVP (Ball, 2007). To determine the origin of the condition ddAVP is administered in conjunction with a water deprivation challenge. If ddAVP normalizes urine-concentrating ability an impaired synthesis and release of AVP is assumed. In contrast, if ddAVP does not restore urine-concentrating ability an impaired renal response to V_2R activation is assumed (Lavin, 2009). The failure of ddAVP to normalize urine-concentrating

ability in >180 day 11βHSD2$^{-/-}$ mice suggested a nephrogenic component to the phenotype.

The evaluation of urine concentrating ability during a 24-hour water deprivation challenge provided an insight into the renal response to chronic AVP stimulation. In an attempt to resolve the acute response to V_2R stimulation, the response to ddAVP administration was evaluated in polyuric 11βHSD2$^{-/-}$ mice during free access to water. In contrast to the C57Bl/6 control mice, 11βHSD2$^{-/-}$ mice were unable fully to concentrate their urine following ddAVP administration; anuria was not observed. These data support the hypothesis that an impaired response to V_2R stimulation contributes to the polyuria in 11βHSD2$^{-/-}$ mice.

In an attempt to confirm a nephrogenic origin to the polyuria, the role of polydispia was assessed. Water restriction studies were performed in >180 day 11βHSD2$^{-/-}$ mice. Although water restriction normalized urine flow, urine osmolality remained significantly lower in the >180 day 11βHSD2$^{-/-}$ mice than the C57Bl/6 controls. These data suggest that the polyuria was not entirely driven by augmented water intake. Similar results were obtained in UTA1/3$^{-/-}$ mice, in which polyuria is driven by impaired renal handling of urea. Water restriction in UTA1/3$^{-/-}$ mice did not normalize water turnover (Fenton *et al*., 2004). In contrast, in mice with constitutively active Gαq, in which polyuria occurs as a consequence of primary polydipsia, restriction of water intake did normalize urine concentrating ability (Wang *et al*., 2006).

2.4.3. Basal sodium excretion is augmented in 11βHSD2$^{-/-}$ mice

An unexpected finding in this chapter is that urinary sodium excretion was significantly higher in 11βHSD2$^{-/-}$ mice than the age-matched controls at both <100 and >180 days. Since there was no significant difference in sodium intake between the two groups, these data reflect the impaired tubular reabsorption of sodium. This is in contrast to the tradition view of AME, in which the impaired renal natriuretic capacity of sodium is causative in hypertension, following which a steady state of balance and therefore normal excretion would be assumed.

Previously, a transient, age-dependent impairment of the intrinsic renal natriuretic capacity of 11βHSD2$^{-/-}$ mice has been demonstrated. Using renal clearance techniques it was established that the fractional excretion of sodium was lower in 11βHSD2$^{-/-}$ mice than C57Bl/6 controls at <60 days. However, at 80 days natriuresis was observed in the null mice, and by 120 days the fraction excretion of sodium had normalized (Bailey *et al*., 2008). Notably, the 11βHSD2$^{-/-}$ mice displayed significant hypertension at all ages. These data demonstrated that, although sodium retention may have been involved in the initiation of hypertension, at older ages elevated blood pressure persisted despite normal, and indeed elevated, sodium excretion. In combination with the data discussed in section 2.4.1, in which elevated basal water excretion was documented in the null mice, and in view of the previously described volume contraction (Bailey *et al*., 2008), these data suggest that alternative mechanisms for the increased blood pressure must be considered. Although paradoxical, several lines of evidence support the notion that, in models of

glucocorticoid excess, hypertension occurs independently of sodium and water retention.

Mineralocorticoid induced hypertension is dependent on the retention of sodium, therefore the elevation of blood pressure can be prevented by sodium restriction: the same is not true for glucocorticoid induced hypertension. In rats, cortisone induced hypertension was equivalent regardless of whether the animals were maintained on a high or low sodium diet. This was in contrast to mineralocorticoid induced hypertension, which was prevented by the administration of a low sodium diet (Knowlton and Loeb, 1957). Moreover, several studies in rats have demonstrated that chronic glucocorticoid induced hypertension persisted despite the induction of polyuria, natriuresis and a negative sodium balance (Okuno *et al*., 1981, Haack *et al*., 1977, Li *et al*., 2008). Studies in adrenalectomized rats demonstrated that although corticosterone reduced the urinary sodium/potassium ratio, the effect was entirely due to increased potassium excretion: sodium excretion was not altered. This was in contrast to aldosterone, which induced kaliuresis and antinatriuresis. Moreover, corticosterone was shown to modulate the response to aldosterone, reducing the steroids antinatriuretic capacity. These studies highlighted the complexity of the steroids' actions on renal electrolyte handling (Kenyon *et al*., 1984b). Similarly, in a comparable mouse model of glucocorticoid excess, chronic ACTH treatment resulted in hypertension despite the development of polyuria and natriuresis (Dunbar *et al*., 2010). Together, these data support the hypothesis that glucocorticoid induced hypertension is not dependent on renal sodium retention.

In an attempt to delineate the cause of natriuresis in 11βHSD2$^{-/-}$ mice, phosphate, calcium and magnesium excretion were assessed. Phosphate reabsorption primarily occurs in the proximal tubule (Strickler *et al*., 1964) mediated by Na/P_i cotransporters expressed on the apical membrane (Biber *et al*., 1996). Consequently, changes in phosphate excretion can be used as an assessment of proximal tubule sodium reabsorption, with increased excretion reflective of impaired reabsorption (Schneider *et al*., 1973). Therefore, the demonstration of phosphaturia in the 11βHSD2$^{-/-}$ mice is suggestive of impaired sodium reabsorption in the proximal tubule. These data are cohesive with those obtained from mice chronically treated with ACTH. Moreover, chronic ACTH administration was also shown to reduce NHE8 expression, further supporting the hypothesis that glucocorticoid excess results in reduced sodium reabsorption in the proximal tubule (Dunbar *et al*., 2010).

The thick ascending limb of the loop of Henle is a major site of divalent cation reabsorption, as discussed in section 1.2.2.1. In this region of the nephron cation reabsorption occurs paracellularly, driven by the transepithelial voltage gradient generated by NKCC2 (Bourdeau and Burg, 1979, Shareghi and Agus, 1982, Quamme, 1981). Therefore, calcium and magnesium excretion rates are indicative of NKCC2 mediated sodium reabsorption. The demonstration that calcium and magnesium excretion rates were not significantly different in the 11βHSD2$^{-/-}$ and C57Bl/6 mice suggests that sodium reabsorption in the loop of Henle was not altered in the null mice.

It is possible that impaired sodium reabsorption in the proximal tubule is a compensatory response to functional changes in the distal nephron. Previously, deranged ENaC function was documented in anesthetized 11βHSD2$^{-/-}$ mice. Notably, at early time points increased ENaC activity was associated with sodium retention (Bailey *et al*., 2008). It is postulated that in the 11βHSD2$^{-/-}$ mice adaptive changes occur in the proximal tubule in an attempt to normalize sodium excretion. Support for this hypothesis came from the evaluation of genetically modified mice in which the human GR was overexpressed in the collecting duct. Although overexpression of GR resulted in increased ENaC expression in the collecting duct, urinary sodium excretion was not altered in the mice. The maintenance of sodium balance was enabled by the compensatory downregulation of proteins involved in sodium reabsorption in proximal regions of the nephron (Nguyen Dinh Cat *et al*., 2009). These data suggest that the overactivation of GR in one region of the nephron can induce adaptive changes in other regions. Since the localization of 11βHSD2 is restricted to the distal nephron, it is conceivable that the discrete overactivation of GR in this region results in a transient increase in ENaC function, which is subsequently compensated for by reductions in sodium reabsorption in more proximal regions of the tubule.

Crucially, these data highlight the importance of comparing functional data obtained in anesthetized mice with that from conscious mice. The evaluation of the response to pharmacological agents in anesthetized mice enables the dissection of nephron function in specific regions of the tubule. However, as highlighted in the current and previously published studies (Bailey *et al*., 2009, Dunbar *et al*., 2010), these acute

experiments, in which renal function is challenged by the infusion of saline solutions and pharmacological manipulations, are not entirely reflective of chronic renal function. Therefore, the combined of evaluation of data obtained from anesthetized and conscious mice is required to gain a thorough understanding of renal function.

Paradoxically, despite the increased natriuresis, previous evaluation demonstrated hypernatremia in the 11βHSD2$^{-/-}$ mice (Bailey *et al*., 2008). The reason for this apparent discrepancy is uncertain; however it was also observed in the ACTH treated mice (Bailey *et al*., 2009, Dunbar *et al*., 2010). The demonstration of osmotically inactive sodium storage in the skin generates interesting hypotheses. Predominantly, the observation that the chronic sodium deprivation resulted in the mobilization of sodium from osmotically inactive skin reservoirs suggests that extra-renal mechanisms may be involved in the modulation of plasma sodium concentrations (Schafflhuber *et al*., 2007). In this context the evaluation of total body sodium content in the 11βHSD2$^{-/-}$ mice is of interest.

2.4.4. Basal potassium excretion is normal in 11βHSD2$^{-/-}$ mice

Despite the differences in sodium handling, a striking consistency in models of mineralocorticoid and glucocorticoid induced hypertension is hypokalemia (Knowlton and Loeb, 1957). Indeed, hypokalemia is a key characteristic of AME (New *et al*., 1977) and has previously been reported in the 11βHSD2$^{-/-}$ mice (Bailey *et al*., 2008, Kotelevtsev *et al*., 1999). In normal situations the fine-tuning of potassium balance occurs in the distal nephron, specifically in the connecting tubule

and collecting duct. Within the principal cells of the collecting duct potassium secretion is directly coupled to sodium reabsorption through ENaC, and is therefore under the influence of aldosterone. Through the increased expression of ENaC at the apical membrane and Na/K-ATPase at the basolateral membrane, aldosterone increases potassium excretion (Reviewed in (Unwin et al., 2011). However, despite these effects, potassium excretion was not significantly different in the 11βHSD2$^{-/-}$ and C57Bl/6 mice.

Aldosterone induced hypokalemia, in the absence of increased potassium secretion, has been documented in several experimental models. In dogs chronically infused with aldosterone, hypokalemia but not increased urinary excretion of potassium was documented (Pan and Young, 1982). Comparable observations were made in DOCA treated pigs (Grekin *et al*., 1980) and aldosterone treated rabbits (Dawborn and Ross, 1967). In these studies fecal potassium levels were also measured, thus excluding it as a route of potassium loss. An explanation for these paradoxical findings was proposed by Young (Young, 1988). In addition to increasing potassium secretion, aldosterone can induce its movement from extracellular to intracellular compartments (Young and Jackson, 1982). Moreover, there was a positive correlation between plasma aldosterone levels and the redistribution of potassium. Since low plasma potassium has an antikaliuretic effect, this model can be used to explain hypokalemia in the absence of kaliuresis (Young, 1988). Although less thoroughly studied, glucocorticoid excess may induce similar effects. Glucocorticoids excess was associated with increased Na/K-ATPase activity in the kidneys of adrenalectomized rats (Hendler *et al*., 1972) and in the erythrocytes from

patients with Cushing's syndrome (Gall *et al*., 1971). In human erythrocytes, glucocorticoid induced Na/K-ATPase activity resulted in increased intracellular concentrations of potassium (Kaji *et al*., 1981). These data suggest that like mineralocorticoids, glucocorticoids may induce the redistribution of potassium. The analysis of potassium distribution in 11βHSD2$^{-/-}$ mice would provide information on whether the previously observed hypokalemia (Bailey *et al*., 2008, Kotelevtsev *et al*., 1999) arose as a consequence of increased intracellular potassium.

In view of the fact that potassium excretion was not different between the 11βHSD2$^{-/-}$ and C57Bl/6 mice at either age, the urinary ratio of sodium/potassium paralleled that of sodium excretion. Consequently, the ratio was augmented in the 11βHSD2$^{-/-}$ mice at both <100 and >180 days. The reason for the disparity between these data, and those obtained in the 11βHSD2$^{-/-}$ mice on an MF1 background, is not clear (Kotelevtsev *et al*., 1999). However, since the age of the conscious mice evaluated in the original study was not specified, it is possible that the urinary excretion data was obtained prior to the postulated compensatory changes in tubular sodium handling, discussed in section 2.4.3. Moreover, urinary potassium excretion rates were not detailed, raising the possibility that the attenuated sodium/potassium ratio was entirely attributable to decreased sodium excretion. Whether the attenuated ratio persisted in older mice is of interest. Without the thorough temporal evaluation of patients with AME, it cannot be determined whether similar changes in renal sodium and potassium handling occur clinically. Given the rarity and severity of the disease these studies are unlikely.

Chapter 3: Evaluation of Renal Function and Structure in 11βHSD2-/- mice

3.1. Introduction

The studies described in this chapter were designed to evaluate the cause of the deranged water handling observed in the 11βHSD2$^{-/-}$ mice. The investigations detailed in section 2.3 suggested a nephrogenic origin to the increased water turnover. To assess this in more detail, renal function, with a focus on the collecting duct, was evaluated in the 11βHSD2$^{-/-}$ mice. In addition, the effect of increased urine flow on renal structure was also assessed.

3.1.1. AVP-AQP2 cascade in 11βHSD2-/- mice

The association between impaired glucocorticoid homeostasis and altered water turnover is well established. In both clinical and experimental studies, glucocorticoid deficiency is associated with an attenuated ability to dilute urine. Mechanistically, fluid retention is the result of increased AQP2 expression, secondary to non-suppressible AVP release (Boykin *et al*., 1978, Saito *et al*., 2000, Agus and Goldberg, 1971). Conversely, in conditions of chronic glucocorticoid excess, such as Cushing's syndrome, polyuria and polydipsia occur (Tierney, 2004). Although the phenotype persists in experimental models of glucocorticoid overexposure, little work has been done to determine the molecular mechanisms underlying the increased urine flow. Notably, studies in rats chronically treated with dexamethasone found no difference in AQP2 expression (Li *et al*., 2008), suggesting that glucocorticoid excess may not merely be the antithesis of glucocorticoid deficiency. However, the studies detailed in section 2.3 demonstrated that in addition to being polyuric, the 11βHSD2$^{-/-}$ mice had an impaired concentration response following ddAVP

administration, during both water deprivation and *ad libitum* water intake. These data were suggestive of deranged AQP2 function in the null mice. In view of the results in 2.3, and the role of the collecting duct in the fine-tuning of water balance, the studies detailed were designed to provide an insight into the function of the collecting duct in 11βHSD2$^{-/-}$ mice.

3.1.2. Renal Structure in 11βHSD2-/- mice

Medullary atrophy is commonly observed in mouse models of polyuria, documented in V_2R and AQP2 deficient mice amongst others (Yun *et al*., 2000, Yang *et al*., 2006). The murine kidney may be particularly susceptible to polyuria-induced injury since extensive medullary atrophy is infrequently reported in sufferers of congenital D.I. (van Lieburg *et al*., 1999). In rare instances non-obstructed hydronephrosis, occurring secondarily to the increased urine flow has been described (van Lieburg *et al*., 1999, Yoo *et al*., 2006). In humans nephrogenesis continues throughout gestation, consequently the kidneys tend to be mature at birth. In contrast, rodent kidneys are not fully developed at birth, with changes in tubular structure occurring postnatally (Speller and Moffat, 1977). Subsequently, postnatal insults can impair renal development, which may explain the increased propensity to polyuria-induced injury in mice. In accord with these hypothesizes, our MRI analysis has demonstrated extensive medullary atrophy in 11βHSD2$^{-/-}$ mice at >180 days (Figure 3.1). To evaluate whether the medullary injury was the cause or consequence of increased water turnover, gross and fine renal structure were evaluated in the 11βHSD2$^{-/-}$ mice at <100 and >180 days.

A) MRI

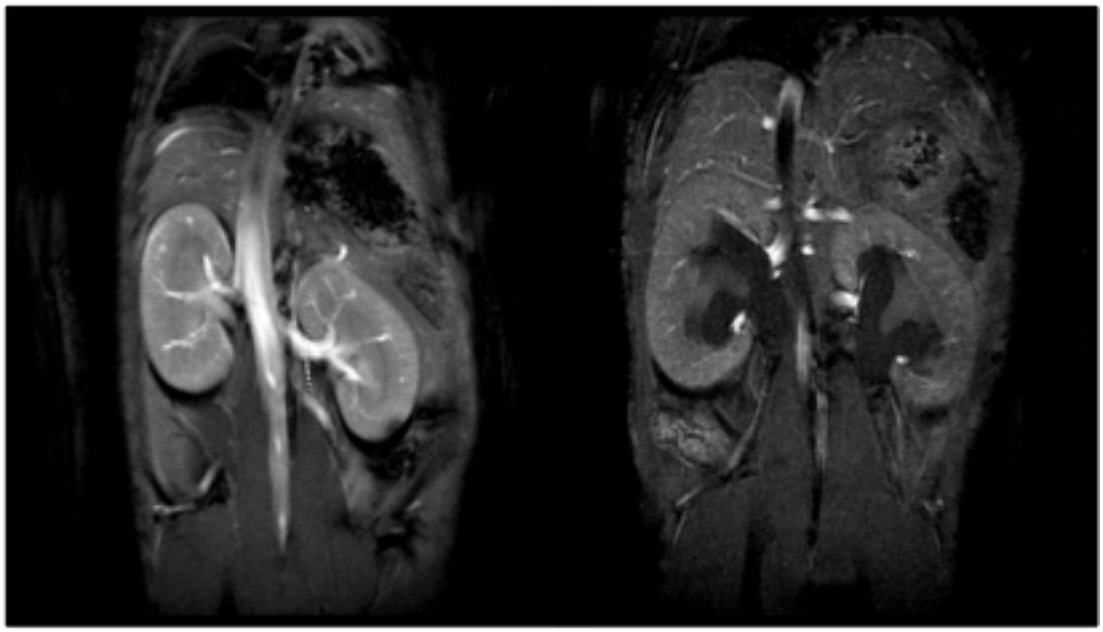

Figure 3.1.A: MRI analysis of renal structure in a C57Bl/6 (left) and 11βHSD2$^{-/-}$ mouse aged >180 days.

Hypothesis

1. Polyuria in 11βHSD2$^{-/-}$ mice is nephrogenic in origin
2. Increased urine flow is primarily the result of impaired collecting duct function, specifically an impaired AQP2 response to V_2R stimulation
3. As in other murine models of polyuria, the increased urine flow at >180 days causes renal injury, which exacerbates the phenotype further

3.2. Methods

3.2.1. q-PCR analysis

3.2.1.1. Isolation of RNA

Following decapitation kidneys were resected from mice, cut in half through the papilla and snap frozen on dry ice. Kidney sections were stored at -80°C until analysis. Initially kidney halves were cut into smaller sections, on dry ice using a scalpel. RNA extraction was then performed using an RNeasy mini kit (Qiagen, UK) following the manufacturers protocol. Kidney halves were homogenized using a hand held homogenizer (Bio-Gen PRO200, Pro Scientific, USA) in 800µl RLT Buffer. Following homogenization a further 800µl RLT Buffer was added. Samples were centrifuged at 13000rpm for 3 minutes and a 600µl aliquot of supernatant mixed with 600µl of 70% ethanol by inversion. 700µl of this solution was then loaded into RNeasy mini columns, which were centrifuged at 13000rpm for 15 seconds. The flow-through was discarded and the step repeated with the remaining 700µl of solution. 350µl RW1 buffer was added to the RNeasy column, which was centrifuged at 13000rpm for 15 seconds and the flow through discarded. 10µl DNase 1 stock solution was then added to 70µl RDD buffer and the 80µl solution added to the RNeasy column. Following a 15-minute incubation at room temperature, an additional 350µl of RW1 buffer was added to the column, which was span at 13000rpm for 15 seconds, the flow-through was discarded. 500µl RPE buffer was then added to the column, which was centrifuged at 13000rpm for 2 minutes. The RNeasy column was then transferred into a fresh collection tube and an additional minute centrifugation undertaken to remove any residual solution. To elute the RNA from the column 50µl RNase-free water was added, the column places in a sterile

1.5ml eppendorf tubes (Eppendorf, UK) and centrifuged at 13000rpm for 1 minute. A microvolume spectrophotometer (Nanodrop, ThermoScientific, UK) was used to determine the concentration of the isolated RNA. RNA quality was assessed by electrophoresis on 1% agarose gels made with 0.5% TBE buffer. High quality extractions were determined by the presence of a band at 2kb and 5kb representing 18s and 28s ribosomal RNA respectively. An intensity ratio of 1:2 was used as confirmation that the RNA was intact.

3.2.1.2. Generation of cDNA

Reverse transcription of the RNA was performed using a High Capacity cDNA Reverse Transcription Kit (Applied Biosystems, UK) following the manufacturers protocol. 500ng of RNA was used per reaction. Amplification was performed using thermal cycler (Vertiti 96-Well Thermal Cycler, Applied Biosystems, UK) using the following protocol, 10 minutes at 25°C, 120 minutes at 37°C, 5 minutes at 85°C. cDNA quality was confirmed by an end-point pcr using primers directed against 11βHSD1.

3.2.1.3. q-PCR analysis of mRNA abundance

q-PCR assays were generated using the universal probe library kit (Roche, UK) following the manufacturers protocol. All reactions contained 200nM primer, 100nM Probe, 5µl Roche probe mastermix, 2.8µl Roche water and 2µl cDNA. cDNA was diluted 1 in 40 in Roche water prior to analysis. Standard curves were generated using a stock cDNA, consisting of equal aliquots of all the cDNA samples

that were to be compared to the curve. Seven point curves (1 in 10, 1 in 20, 1 in 40, 1 in 80, 1 in 160, 1 in 320 and 1 in 640 dilutions) were used for quantification. All samples and standards were evaluated in triplicate. q-PCR reactions were performed using a light cycler (LightCycler 480 Real-Time PCR system, Roche, UK). Quantification was performed using the second derivative maximum method.

3.2.1.4. Primers and analysis

Primers were designed using ProbeFinder version 2.45 for Mouse, (Roche Diagnostics, UK). Primer sequences were as detailed in Table 3.1. For analysis all values were normalized to the abundance of house-keeping genes. At <100 days values were normalized to an average of three house-keeping genes (18s, TBP and PPIA) since there was no significant difference in their average abundance between the two cohorts at this age (C57Bl/6 155.9±7.9 versus 11βHSD2$^{-/-}$ 156.4±2.5 $P>0.05$, unpaired t-test). In contrast, at >180 days the abundance of TBP and PPIA were substantially different between the C57Bl/6 and 11βHSD2$^{-/-}$ mice, therefore the values were normalized to 18s, the abundance of which was not significantly different between the two cohorts (C57Bl/6 174.2±7.5 versus 11βHSD2$^{-/-}$ 145.0±17.4 $P>0.05$, unpaired t-test). All data are presented as a percentage of the mean value recorded in C57Bl/6 mice (n=8).

	Left Primer	Right Primer
18S	ctcaacacgggaaacctcac	cgctccaccaactaagaacg
TBP	gggagaatcatggaccagaa	gatgggaattccaggagtca
PPIA	acgccactgtcgcttttc	gcaaacagctcgaaggagac
AQP2	tagccctgctctctccattg	gagcagccggtgaaatagat
AQP3	ctggggaccctcatcctt	tggtgaggaagccaccat
AQP4	tggaggattgggagtcacc	tgaacaccaactggaaagtga
NKCC2	tgggttgtcaacttctgcaa	gctccgggaaatcaggtagt
UT-A	gaaatgccggaagaaaagg	tcattgggtttttcaatcttca
Caspase-3	tgaagacattttggaattaatgga	tcaccatggcttagaatcaca
HIF-1α	gcactagacaaagttcacctgaga	cgctatccacatcaaagcaa
TonEBP	tcagacaagcggtggtga	agggagctgaagaagcatca

Table 3.1: RT-PCR primers. Designed using ProbeFinder version 2.45 for Mouse, Roche Diagnostics, UK.

3.2.2. Western blot analysis of AQP2

3.2.2.1. Protein extraction and quantification

An isolation solution was made composed of 250mM sucrose (BDH Laboratory supplies, VWR, USA) and 10mM triethanolamine (Sigma-Aldrich, UK). On the day of protein extraction five Complete Protease Inhibitor Cocktail Tablets (Roche Applied Science, UK) and 2.5ml phenylmethanesulfonyl fluoride (pmsf, Sigma-Aldrich, UK) solution (50mg pmsf in 25ml isopropyl ethanol) were added to 50ml isolation solution. 1.5ml of the solution was then added, on ice, to each kidney. Due to the limited number of 11βHSD2$^{-/-}$ mice available, in the free access to water groups kidney halves were evaluated. Kidneys were cut in half through the papilla to ensure proportional representation of medulla and cortex. The kidneys were homogenized in 2ml ependorf tubes containing metal beads using a mixer mill (MM301 Ball Mill, Retsch, UK). The resultant solution was centrifuged at 2000rpm for 1 minute. Final protein concentration was assessed using a BCA Protein Assay kit (Pierce Biotechnology, USA) following the manufacturer's protocol. In brief, 25µl of sample, standard, or blank were added to a clear 96 well plate (IWAKI, R&L Slaughter Ltd, UK) in duplicate. Mixing BCA reagents A and B in a ratio of 50:1 made a working reagent, 200µl of which was added to each sample. Following a 30 minute incubation at 37°C the plate was allowed to cool to room temperature and then absorbance measured at 562nm (OPTI Max Tunable Microplate Reader, Molecular Devices, UK).

3.2.2.2. Electrophoresis

For western blot analysis 1μg/μl protein stock solutions were made in 5x laemmli buffer. Samples were heated at 95°C for 5min prior to electrophoresis, which was performed at 150mV for 1 hr, on 10% SDS-PAGE gel. 8-16μg of protein was loaded per lane. Following a 20 minute incubation of the gel in transfer buffer, proteins were electrotransferred to a hydrophobic polyvinylidene difluoride (PVDF) membrane (Amersham Hybond-P, GE Healthcare, UK) using a semi-dry method (10mV for 30 minutes). Subsequently, the blot was incubated in PBST-0.1% containing 5% nonfat dry milk at room temperature for 1 hour. Membranes were incubated over night with a primary antibody against AQP2 (Cell Signaling Technology, USA) at 1/1000 dilution at 4°C overnight. The membranes were washed 3x 5 minutes in PBST-0.1%, and then incubated with a secondary antibody (goat anti-rabbit, Santa Cruz, USA) for 2 hours at room temperature. Membranes were again washed 3x 5 minutes in PBST-0.1% and developed using ECL (Thermo Scientific, UK). For quantification membranes were stripped and re-probed with a primary antibody against GAPDH (Santa Cruz, USA). Membranes were washed 1x 5 minutes in PBST-0.1% and then incubated for 1 hour at 40°C in stripping buffer. Following this, membranes were washed 3x 5 minutes in PBST-0.1% and re-probed with anti-GAPDH, following the same method as detailed above.

3.2.2.3. Buffers and Gels

Laemelli loading buffer:	2% sodium dodecyl sulphate (SDS), 80% glycerol, 1M Tris-Base, bromophenol blue, 0.1M dithiothreitol (DTT)
Tank buffer:	0.025M Tris-Base, 0.192M Glycine, 0.1% SDS, pH 8.3
Transfer Buffer:	0.25M Tris-Base, 0.192M Glycine, 0.1% SDS, 20% methanol
Striping Buffer:	0.1% SDS, 1% Tween, 0.2M Glycine
Running Gel:	1.5M Tris-Cl pH 8.8, 0.1% SDS, 10% acrylamide, 0.05% tetramethylethylenediamine (TEMED), 0.067% ammonium peroxodisulphate (APS)
Stacking Gel:	0.12M Tris-Cl pH 6.8, 0.1% SDS, 4% acrylamide, 0.05% TEMED, 0.067% APS,

3.2.2.4. Analysis

Densitometric analysis was performed using the gel analyzer tool within the Image-J software analysis program. All AQP2 densitometries were normalized to the corresponding densitometries of GAPDH. The ratio of AQP2/GAPDH was then used for statistical analysis. The individual dehydrated blot values were expressed as a percentage of the average value measured in the hydrated blots from the corresponding group (n=4-6).

3.2.3. Plasma AVP radioimmunoassay

Trunk blood was collected from decapitated mice and centrifuged at 10000rpm for 5 minutes at 4°C in order to isolate the plasma from the hematocrit. Plasma samples were acidified with 2M hydrochloric acid (HCl), 0.25ml per 1ml of plasma. AVP was then extracted from the plasma samples using Sep-Pak C_{18} cartridges (Water Associates, USA). Initially the cartridges were conditioned using 5ml methanol. 5ml of distilled water was then used to equilibrate the cartridge. Subsequently, the plasma samples were added to the cartridges, all samples were diluted with distilled water so that the final volume added to the cartridges was 1ml. The cartridges were then washed with 5ml 1% acetic acid, in order to remove any retained interferences. Finally, the AVP was eluted into glass test tubes using 2ml methanol. The samples were then dried under nitrogen gas and reconstituted in 200µl assay buffer (50mM Tris pH 7.4 (12.14g Tris in 1l deionised water, 10ml 5M HCl, 3.5g neomycin sulphate, 1.75g human serum albumin, pH was adjusted to 7.4 and then made up to 2l with deionised water)). For the assay 50µl AVP standard or plasma extract was mixed with 25µl antibody (1:20000 dilution so final dilution in each assay tube was 1:80000) and 25µl 125I-AVP ($[^{125}I]Tyr^{2},Arg^{8}$] Perkin Elmer, UK) in radioimmunoassay cups (Sarstedt, UK) in duplicate at 0°C. For the standard curve a stock of AVP (4pg/50ml) serially diluted 1:2 to give concentrations of 2, 1, 0.5, 0.25, 0.125 pg/50µl. The radioimmunoassay tubes were then centrifuged at 2000rpm for 1 minute and incubated at 4°C for 48 hours. Following the incubation 300µl of charcoal suspension (6.07g Tris in 500ml deionised water, 5ml 5M HCl, 2g neomycin sulphate, 1.85g EDTA, 5g BSA. The pH was adjusted to 7.4 and then the solution made up to a final volume of 1l using deionised water. For the charcoal

solution 0.062g dextran T70 (Amersham Biosciences, Sweden) was dissolved in 5ml buffer, this was then mixed with 95ml buffer and 0.6g Norit charcoal (Norit N.V, The Netherlands)) was added to each tube. The tubes were then centrifuged at 3000rpm for 15 minutes following which the supernatant was aspirated off. The charcoal free pellet was then counted using a scintillation-gamma counter (1470 Wallac Wizard Gamma Counter, GMI, USA) (n=2-5).

3.2.4. Gross renal structural analysis

Following resection, kidneys were fixed in 10% formalin (Sigma-Aldrich, UK) for up to 48-hours and then transferred to 70% ethanol for long term storage. Both poles of the kidneys were removed using a scalpel, leaving mid transverse sections approximately 2mm wide. The central sections were imaged using a microscope (Lecia DFC320, Lecia Micorsystems, Germany) at magnification 1.25. A ruler with mm graduations was included on each image as a scale reference (n=5-6).

3.2.5. Fine renal structural analysis

Mid transverse sections were embedded in paraffin. 4μm sections were cut and stained with hematoxylin and eosin (H+E, Histology Core Service, University of Edinburgh). Images were captured using a microscope (Zeiss Axioscope, Zeiss, USA) at magnification 40. The amount of glomeruli in ten H-E stained sections per mouse (n=5 per group) were counted to evaluate nephron loss. Post-acquisition morphometric analysis was performed to quantify total tubule, luminal and basement membrane areas in >180 day old mice. The number of nuclei per tubule was also

assessed. Since there was no qualitative difference in the tubules from <100 day C57Bl/6 and 11βHSD2$^{-/-}$ mice they were not quantified. Quantification was performed in a blinded fashion using the Image-J software analysis program. Areas were measured using the free hand tool and nuclei counted using the multi-point selection tool. Up to 10 sections from 3 mice per group were evaluated, totaling >600 tubules per group.

3.2.6. Analysis of urinary urea and albumin

Urinary urea was measured using a commercially available colourmetric assay kit (QuantiChrom, BioAssay Systems, USA). In brief, urine samples were diluted 50 fold in deionised water. A working reagent consisting of equal volumes of reagent A and B was mixed no more than 20min prior to performing the assay. 5µl of diluted urine and 200µl of working reagent were added to each well of a clear 96 well plate (IWAKI, R&L Slaughter Ltd, UK). A standard (5mg urea/dL) and blank (deionised water) were also included on each plate. All samples were assessed in duplicate. Following 20 minutes incubation at room temperature a plate reader (OPTI max tunable microplate reader, Molecular Devices, UK) was used to measure colour intensity using an optical density of 430 nm. Urinary urea concentrations were converted to excretion rates using the appropriate urine flow rate, and then expressed in mg/24hr (n=4). Urinary albumin was measured by the Clinical Analysis Core Service at the University of Edinburgh, using commercially available colourmetric assays.

3.2.7. Analysis of renal cell death

As above, mid transverse-paraffin embedded renal sections were cut into 4μm slices using a microtome. The sections were transferred to micro slides (SuperFrost Plus Microslides, VWR, USA) and dried overnight at 37°C. Terminal deoxynucleotidyl transferase dUTP nick end labeling (TUNEL) staining was used to assess DNA fragmentation, and therefore cell death. In this technique dUTPs are incorporated into the fragmented DNA by the enzyme terminal deoxynucleotidyl transferase. Since the dUTPs are labeled with fluorescence (fluorescein-12-dUTP), fragmented DNA can be imaged using a fluorescence microscope. TUNEL staining was performed using DeadEnd Fluorometric TUNEL System kit (Promega, UK), following the manufacturers protocol. Initially, slides were immersed in xylene to deparaffinize the sections (2x 5 minutes). A 5-minute wash in 100% ethanol was then performed. Sections were then rehydrated by immersion in decreasing concentrations of ethanol (100, 95, 85, 70 and 50%) for 3 minutes each. The sections were then washed in 0.85% NaCl for 5 minutes followed by 5 minutes in phosphate buffered saline (PBS). Sections were fixed by 15-minute immersion in 4% methanol-free formaldehyde solution in PBS and then washed in twice PBS for 5 minutes. The sections were then permeabilized by incubation for 10 minutes with 20μg/ml. Following permeabilization the sections were washed in PBS for 5 minutes, fixed by immersion in 4% methanol-free formaldehyde solution in PBS for 5 minutes, and again washed in PBS for 5 minutes. Sections were then incubated for 10 minutes with 100μl of equilibration buffer. 50μl of terminal deoxynucleotidyl transferase, recombinant (rTdT) incubation buffer was then added to the sections.

The slides were covered with plastic coverslips to ensure even distribution of the buffer and the slides incubated in a humidified chamber at 37°C for 60 minutes. The coverslips were then removed and the reaction terminated by immersing the slides in 2x saline-sodium citrate (SSC) for 15 minutes. Finally the slides were washed 3 times in PBS (5 minutes each) and counterstained with propidium iodide. Following the second fixation step one section was incubated with DNase I to cause DNA fragmentation, this slide acted as the positive control. For the negative control addition of rTdT was omitted from one section.

TUNEL stained sections were imaged using a laser scanning microscope with a moving stage (Zeiss, USA) at 40x magnification. A 3x3 square scan-area at the base of the papilla was selected for analysis since this was region was excluded from the region of medullary damage. Quantification of positive nuclei was performed using the Image-J software analysis program. Positive (green) nuclei were counted using the multipoint selection tool, and then expressed as a percentage of total nuclei (red and green).

3.3. Results

The mRNA abundance of AQP2 was compared in kidneys from hydrated C57Bl/6 and 11βHSD2$^{-/-}$ mice. AQP2 mRNA abundance was significantly lower in the 11βHSD2$^{-/-}$ mice than aged-matched C57Bl/6 mice at both <100 and >180 days (Figure 3.2.A and Figure 3.2.B respectively).

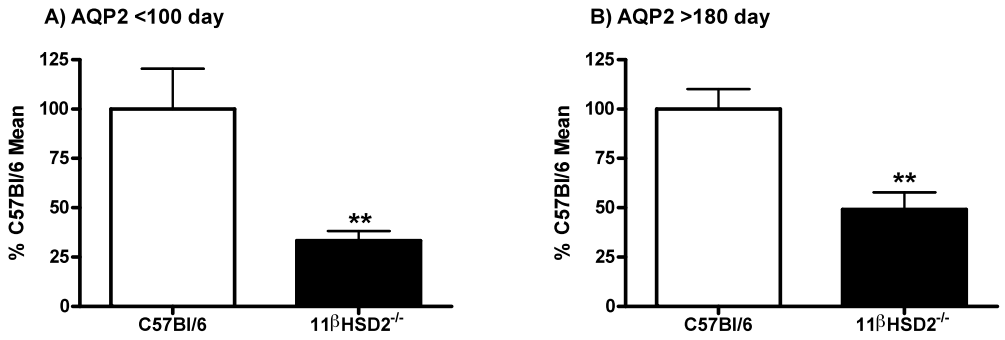

Figure 3.2: AQP2 abundance in hydrated C57Bl/6 (white) and 11βHSD2$^{-/-}$ (black) mice at (A) <100 and (B) >180 days. Data are means ±S.E.M. Statistical analysis was performed using an unpaired t-test, **P<0.01.

To evaluate whether attenuated AVP contributed to the decreased abundance of AQP2 in the null mice, plasma AVP levels were assessed. Measuring plasma AVP in mice is challenging and data were not obtained from each mouse; consequently the data presented must be interpreted as preliminary only. Nevertheless, plasma AVP tended to be higher in the 11βHSD2$^{-/-}$ mice than the C57Bl/6 at both <100 and >180 days (Figure 3.3.A), supporting the concept that there was a nephrogenic origin to the polyuria

.

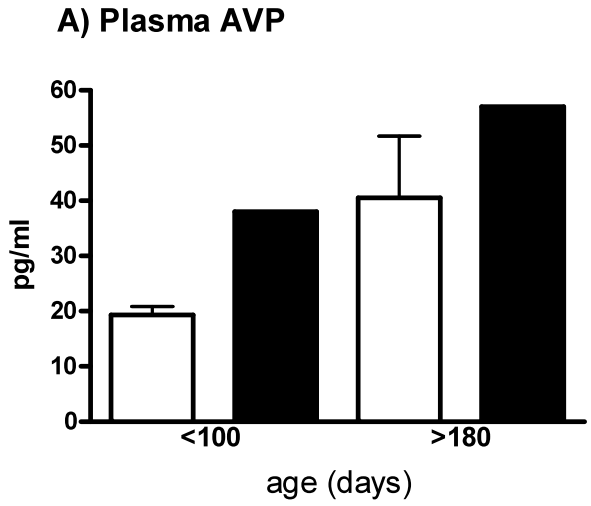

Figure 3.3.A: Basal plasma AVP concentrations in C57Bl/6 (white) and 11βHSD2$^{-/-}$ (black) mice at <100 and >180 days.

AQP3 and AQP4 mRNA abundance were evaluated to examine the involvement of the basolateral collecting duct water channels in the polyuria observed in 11βHSD2$^{-/-}$ mice. AQP3 abundance was significantly lower in the 11βHSD2$^{-/-}$ mice than the C57Bl/6 controls at both <100 (Figure 3.4.A) and >180 (Figure 3.4.B) days. In contrast AQP4 abundance was normal in the null mice at <100 days (Figure 3.4.C) but significantly lower than in the C57Bl/6 controls >180 days (Figure 3.4.D).

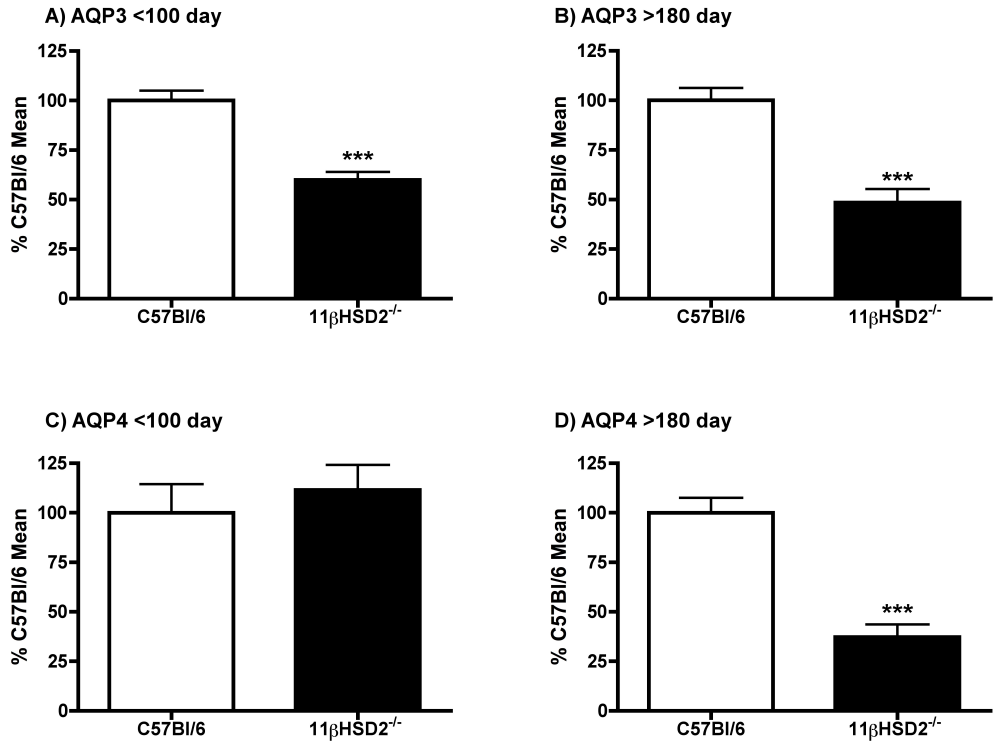

Figure 3.4: Abundance of basaolateral collecting duct AQPs in C57Bl/6 (white) and 11βHSD2$^{-/-}$ (black) mice. (A) AQP3 at <100 days. (B) AQP3 at >180 days. (C) AQP4 at <100 days. (D) AQP4 at >180 days. Data are means ± S.E.M. Statistical analysis was performed using an unpaired t-test, ***P<0.001.

The reabsorption water from the collecting duct is dependent on the corticomedullary osmotic gradient generated by the loop of Henle. In view of the central role of NKCC2 in this process, its abundance was evaluated in the C57Bl/6 and 11βHSD2$^{-/-}$ mice. Renal abundance of NKCC2 was not different in the C57Bl/6 and 11βHSD2$^{-/-}$ mice at <100 days (Figure 3.5.A). In contrast, at >180 days renal NKCC2 abundance was significantly lower in the 11βHSD2$^{-/-}$ mice than the aged match C57Bl/6 mice (Figure 3.5.B).

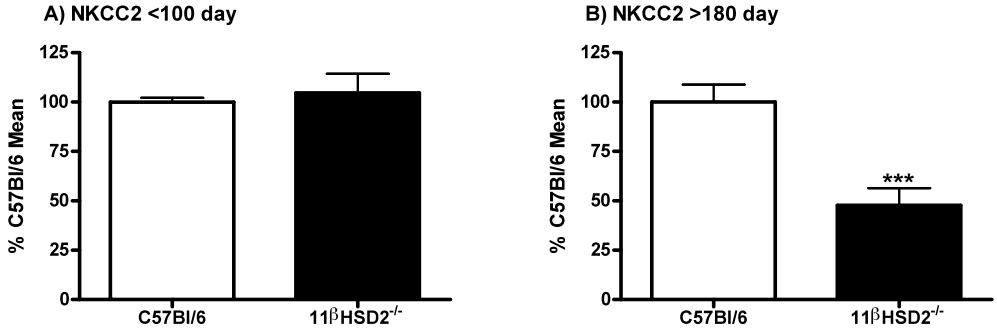

Figure 3.5: Abundance of NKCC2 in C57Bl/6 (white) and 11βHSD2$^{-/-}$ (black) mice at (A) <100 day and (B) >180 days. Data are means ± S.E.M. Statistical analysis was performed using an unpaired t-test, ***P<0.001.

Given that impaired renal handling of urea has been implicated in glucocorticoid induced polyuria (Li *et al*., 2008) the renal mRNA abundance of UT-A was assessed in the 11βHSD2$^{-/-}$ and C57Bl/6 mice. Since the UT-A gene encodes UT-A1 and UT-A3 its evaluation gave an indication of the abundance of the urea transporters (Fenton *et al*., 2002). UT-A abundance was substantially reduced in 11βHSD2$^{-/-}$ mice at <100 days. Abundance was ~50% lower in the null mice than the aged matched controls (Figure 3.6.A), but this did not reach statistical significance (P=0.16). At >180 days UT-A abundance was significantly lower in the null mice, a ~70% reduction was observed in the 11βHSD2$^{-/-}$ mice compared to the aged matched controls (Figure 3.6.B). The physiological relevance of these data was determined by the evaluation of urinary urea. Urinary excretion of urea was significantly higher in the 11βHSD2$^{-/-}$ mice than C57Bl/6 controls at both <100 and >180 days (Figure 3.6.C). Since food intake was not significantly different between the two cohorts at either <100 or >180 days (<100 days C57Bl/6 4.1±0.1 versus 11βHSD2$^{-/-}$ 4.1±0.1 and >180 days C57Bl/6 4.2±0.1 versus 11βHSD2$^{-/-}$ 4.3±0.2 g/24hr), increased protein intake did not contribute to the increased urinary excretion of urea.

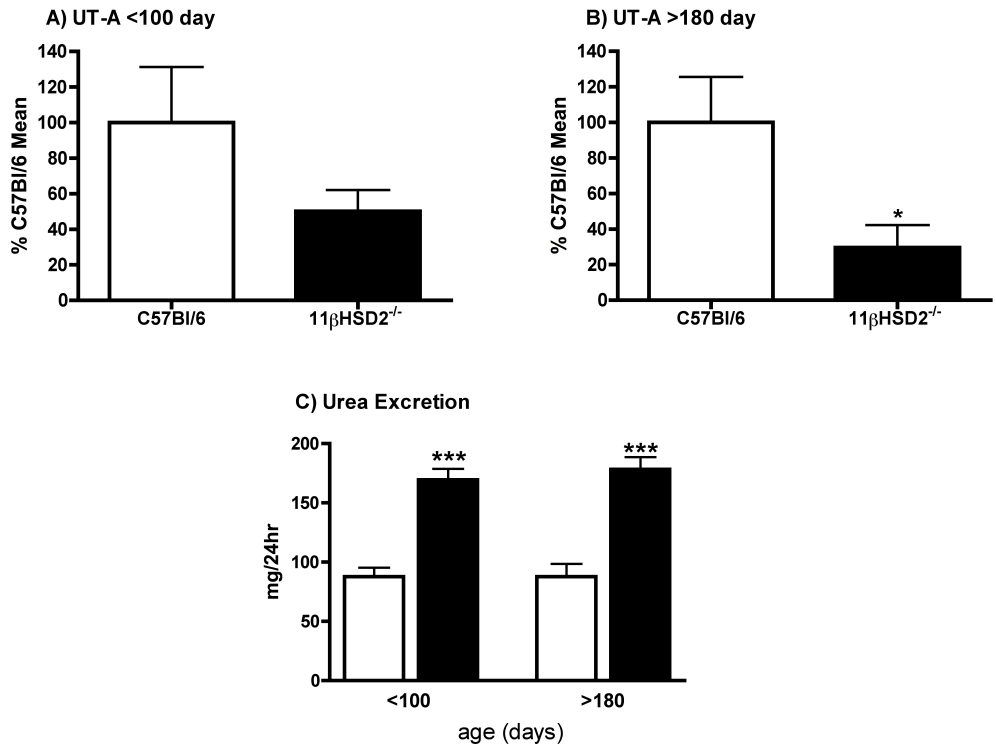

Figure 3.6: Abundance of UT-A and urea excretion in C57Bl/6 (white) and 11βHSD2$^{-/-}$ (black) mice. (A) UT-A at <100 days. (B) UT-A at >180 days. (C) Urinary urea excretion. Data are means ± S.E.M. Statistical analysis was performed using an unpaired t-test or one-way ANOVA with Tukey post-test as appropriate, ***P<0.001, *P<0.05 compared to age matched C57Bl/6 controls.

In view of the attenuated AQP2 mRNA abundance in hydrated 11βHSD2$^{-/-}$ mice, semi-quantitive immunoblotting was used to assess the role AQP2 in the impaired response to water deprivation in >180 day 11βHSD2$^{-/-}$ mice. As previously described (Frokiaer *et al*., 1999), AQP2 presented as 29kDa and 35-50kDA bands, representing non-glycosylated and glycosylated forms of the channel respectively. Consistent with a functional concentration response, water deprivation resulted in an increase in AQP2 protein abundance in C57Bl/6 mice (Figure 3.7.A and Figure 3.7.C). This was ~2 fold in both groups (Figure 3.8.A).

In <100 day 11βHSD2$^{-/-}$ mice, the water deprivation challenge caused a ~3 fold increase in renal AQP2 abundance (Figures 3.7.A and 3.8.A). In contrast the AQP2 response to water deprivation was blunted in the >180 day 11βHSD2$^{-/-}$ mice (Figure 3.7.D), abundance was ~1.2x higher in the kidneys from dehydrated mice (Figure 3.8.A).

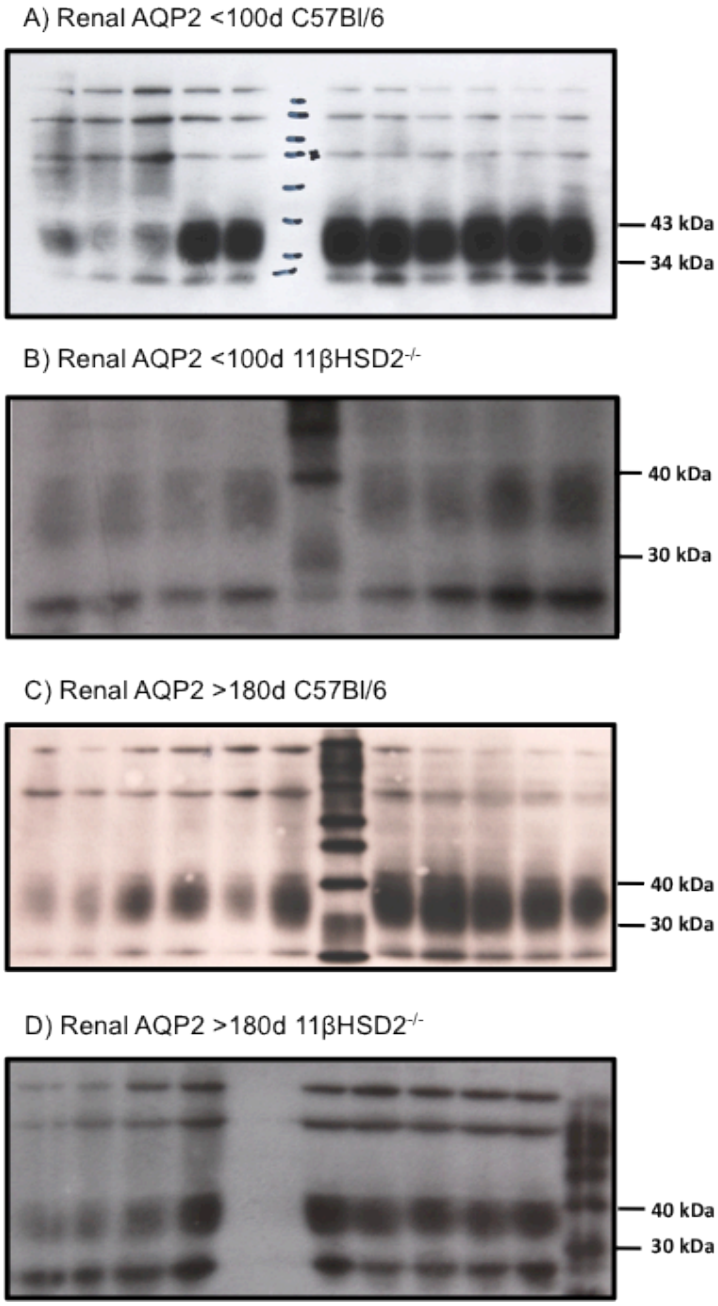

Figure 3.7: Semiquantitive immunoblots showing the effect of water deprivation on AQP2 protein abundance in kidneys from C57Bl/6 and 11βHSD2$^{-/-}$ mice at <100 (A+B) and >180 (C+D) days. Hydrated kidney blots on the left; dehydrated kidney blots on the right.

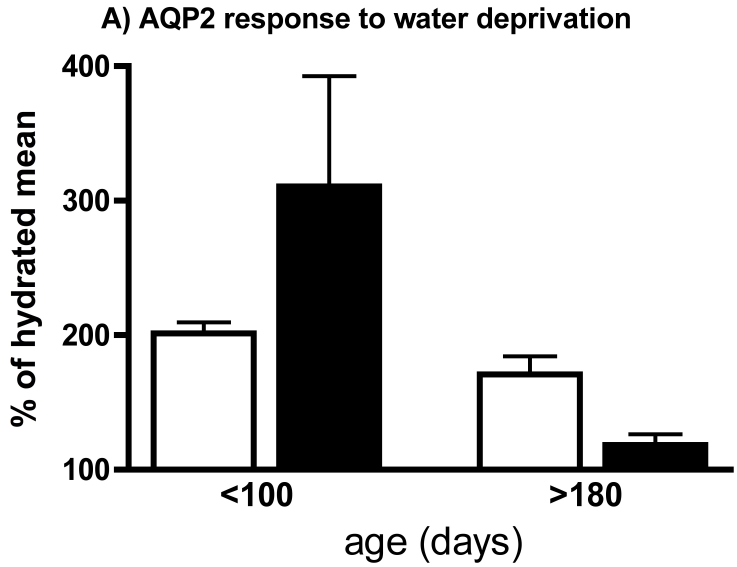

Figure 3.8: The effect of water deprivation on AQP2 protein abundance in kidneys from C57Bl/6 (white) and 11βHSD2$^{-/-}$ (black) mice aged <100 and >180 days. All data were normalized to GAPDH. Data are the individual densitometry values of the water-deprived kidney bands expressed as a percentage of the mean value for the hydrated kidney bands in the corresponding group. 100% is therefore no difference in abundance, whereas 200% is a 2-fold increase. Data are means ± S.E.M. Statistical analysis was performed using a one-way ANOVA.

3.2.2. Renal structure in 11βHSD2$^{-/-}$ mice

Kidney morphology was evaluated to assess whether renal injury correlated with increased water turnover in 11βHSD2$^{-/-}$ mice. Despite being polyuric, the kidneys of 11βHSD2$^{-/-}$ appeared normal at <100 days. At the gross level there was no obvious structural difference between the kidneys from C57Bl/6 and 11βHSD2$^{-/-}$ mice (Figure 3.9.A and Figure 3.9.B respectively). Similarly, at the fine level, tubular structure was normal in <100 day C57Bl/6 and 11βHSD2$^{-/-}$ mice (Figure 3.10.A and Figure 3.10.B respectively). The tubules were densely packed and the lumens narrow in both cohorts. By >180 days severe renal injury was evident in all of the kidneys evaluated from 11βHSD2$^{-/-}$ mice. At this age the kidneys displayed severe medullary atrophy, exposed papilla and dilated renal pelvises (Figure 3.9.D). Given that kidneys from >180 day C57Bl/6 mice were structurally normal (Figure 3.9.C), this was not merely an effect of aging. At the fine level, tubular structure was damaged in >180 day 11βHSD2$^{-/-}$ mice (Figure 3.10.D). Varying degrees of tubular dilation were observed, with membrane blebbing and debris within the lumen evident in the most severely dilated tubules (Figure 3.10.D).

Glomeruli number was assessed to evaluate whether the renal injury was associated with nephron loss. Glomeruli number was not significantly different between the C57Bl/6 and 11βHSD2$^{-/-}$ mice at either <100 and >180 days (Figure 3.11.A). Since glomeruli number was not reduced in the 11βHSD2$^{-/-}$ mice, urinary albumin excretion was evaluated as an assessment of glomeruli function. Urinary albumin excretion was substantially higher in <100 day 11βHSD2$^{-/-}$ mice than the age-matched C57Bl/6 controls. By >180 days the excretion rate had increased further, to

levels that were significantly higher than both aged matched C57Bl/6 mice and the <100 day 11βHSD2$^{-/-}$ mice. In contrast, there was no difference in albumin excretion between the C57Bl/6 mice at <100 and >180 days. (Figure 3.11.B)

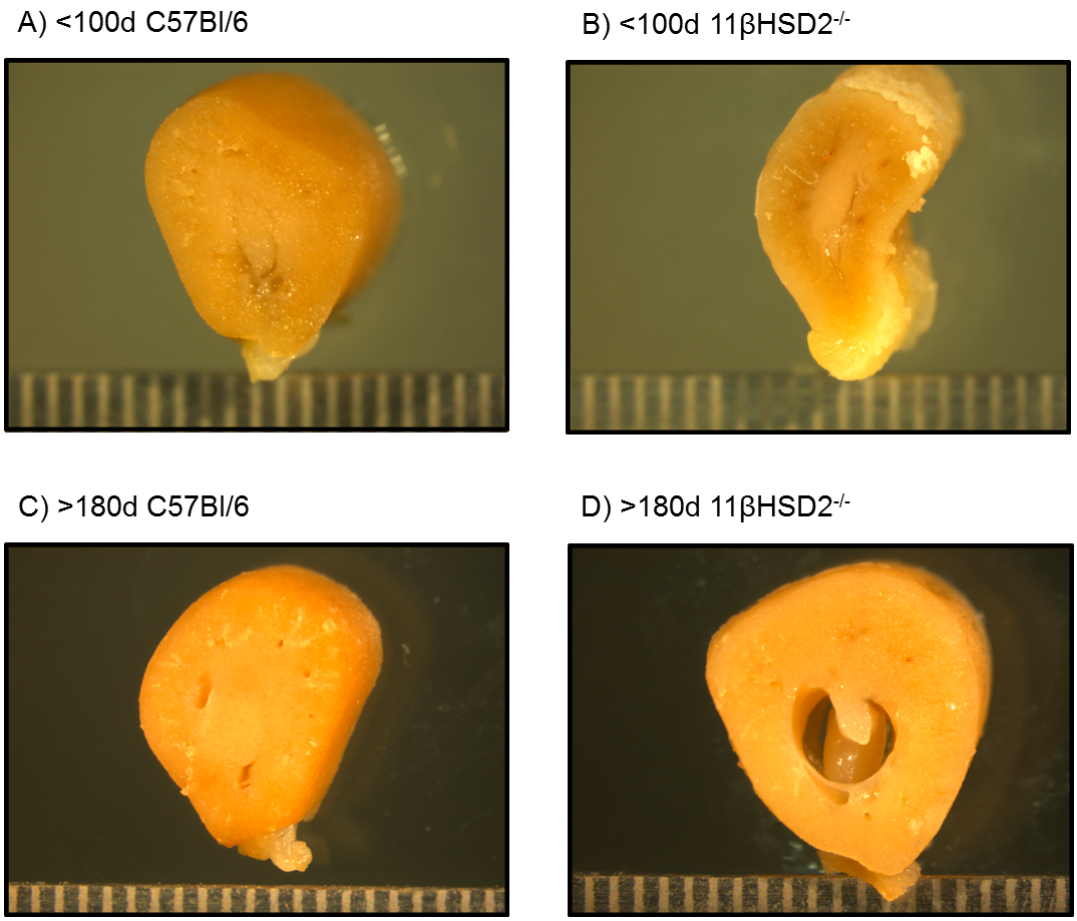

Figure 3.9: Histological evaluation of gross renal structure. Mid transverse sections approximately 2mm thick from <100 day C57Bl/6 (A), <100 day 11βHSD2$^{-/-}$ (B), >180 day C57Bl/6 (C) and >180 day 11βHSD2$^{-/-}$ (D) mice were evaluated.

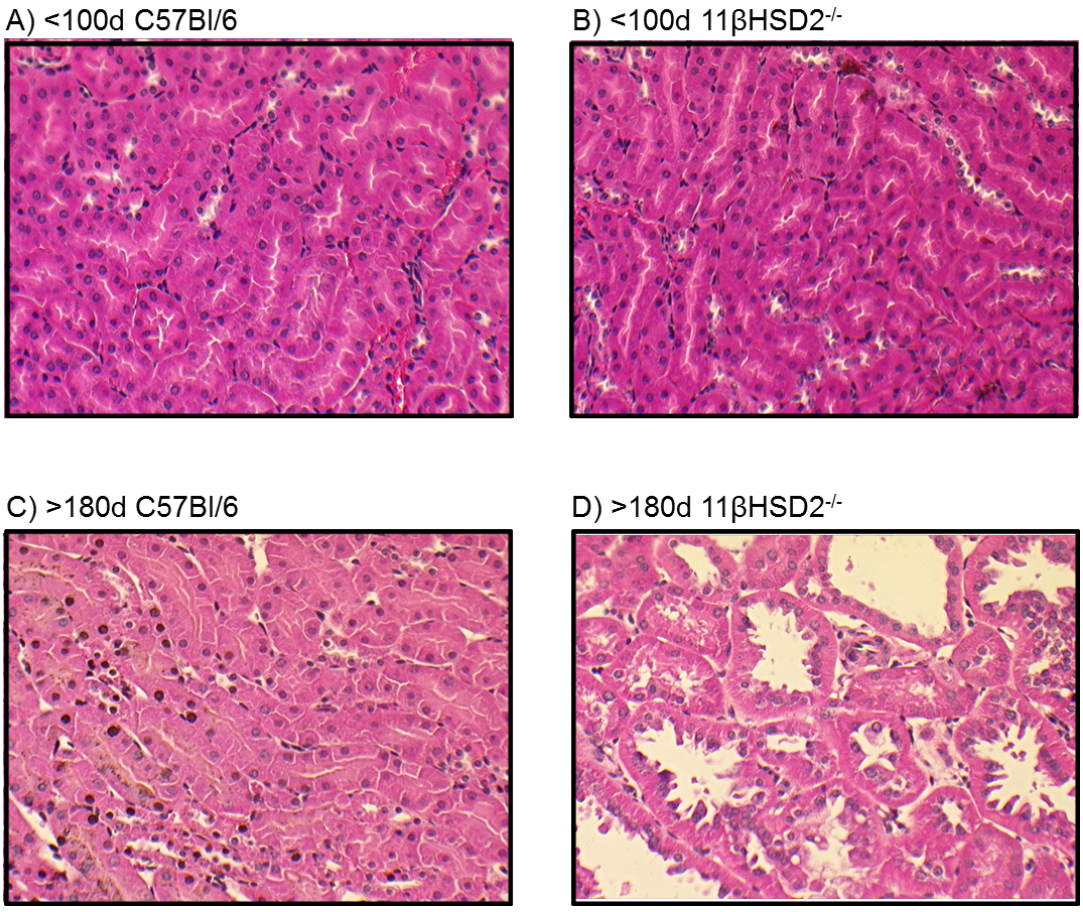

Figure 3.10: Histological evaluation of tubular structure. H+E stained sections were evaluated from <100 day C57Bl/6 (A), <100 day 11βHSD2$^{-/-}$ (B), >180 day C57Bl/6 (C) and >180 day 11βHSD2$^{-/-}$ (D) mice.

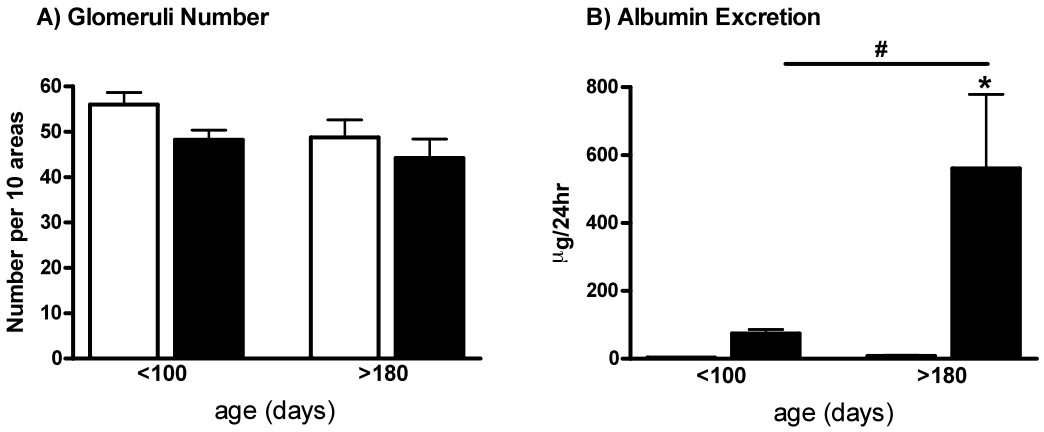

Figure 3.11: Evaluation of glomeruli number and function in C57Bl/6 (white) and 11βHSD2$^{-/-}$ (black) mice aged <100 and >180 days. (A) Glomeruli Number. (B) Urinary Albumin Excretion. Data are means ± S.E.M. Statistical analysis was performed using a one-way ANOVA and Tukey post-test. *P<0.05 compared to age matched controls. #P<0.05 compared to younger mice within the same genotype.

To quantify the qualitative observations, morphometric analysis was performed on tubules from >180 day C57Bl/6 and 11βHSD2$^{-/-}$ mice. Consistent with the qualitative observations, luminal area was significantly larger in the 11βHSD2$^{-/-}$ mice than the C57Bl/6 controls (Figure 3.12.A). As a result of this, total tubule area was also significantly higher in the 11βHSD2$^{-/-}$ mice (Figure 3.12.B). Basement membrane width was not significantly different between the C57Bl/6 and 11βHSD2$^{-/-}$ mice (Figure 3.12.C), indicative of an absence of hypertrophy. However, hyperplasia was evident, the number of nuclei per tubule was significantly higher in the 11βHSD2$^{-/-}$ mice than the control C57Bl/6 mice (Figure 3.12.D).

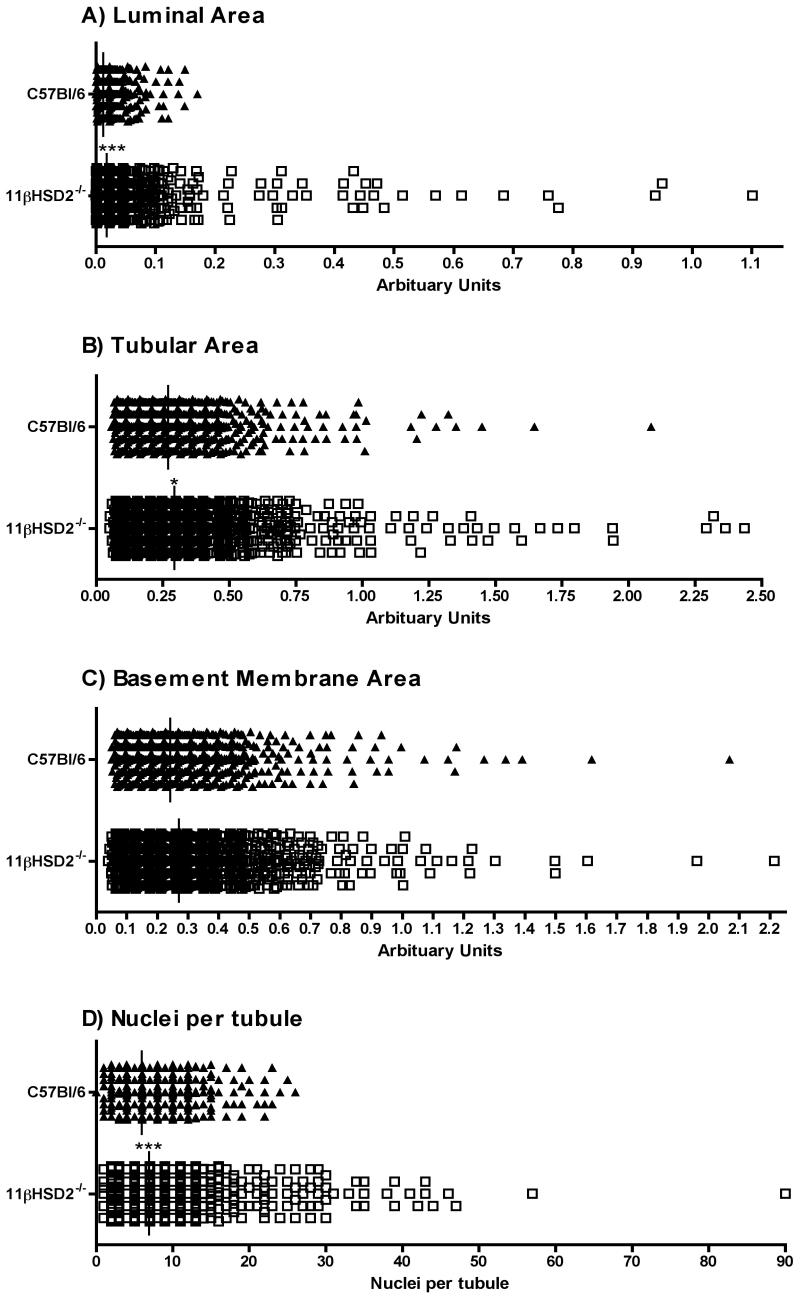

Figure 3.12: Morphometric evaluation of tubules from >180 day old C57Bl/6 (filled triangles) and 11βHSD2$^{-/-}$ (open squares) mice. (A) Luminal Area. (B) Tubular Area. (C) Basement Membrane Width. (D) Nuclei per Tubule. Data are individual measurements with the median value indicated by the vertical line. Statistical analysis was performed using a Mann-Whitney test *P<0.05, ***P<0.001.

In an attempt to identify the cause of medullary atrophy observed in > 180 day old 11βHSD2$^{-/-}$ mice, TUNEL staining was used to evaluate apoptotic cell death. As shown in Figure 3.13.A, there was no significant difference in the amount of TUNEL positive nuclei in C57Bl/6 and 11βHSD2$^{-/-}$ mice at either <100 or >180 days. There was, however, a significant increase in the amount of TUNEL positive nuclei observed in each group at >180 days compared to the younger mice of the same genotype. The amount of TUNEL positive nuclei at >180 days was uncharacteristically high in both groups of mice (C57Bl/6 61±16 versus 11βHSD2$^{-/-}$ 46±11 %), indicative of false positive staining, as previously characterized in murine kidneys (Pulkkanen *et al*., 2000). An additional assessment of cell death was therefore utilized. q-PCR analysis of Caspase-3 mRNA abundance demonstrated that there was no significant difference in the amount of renal apoptotic cells in 11βHSD2$^{-/-}$ and C57Bl/6 mice at <100 (Figure 3.13.B) and >180 days (Figure 3.13.C).

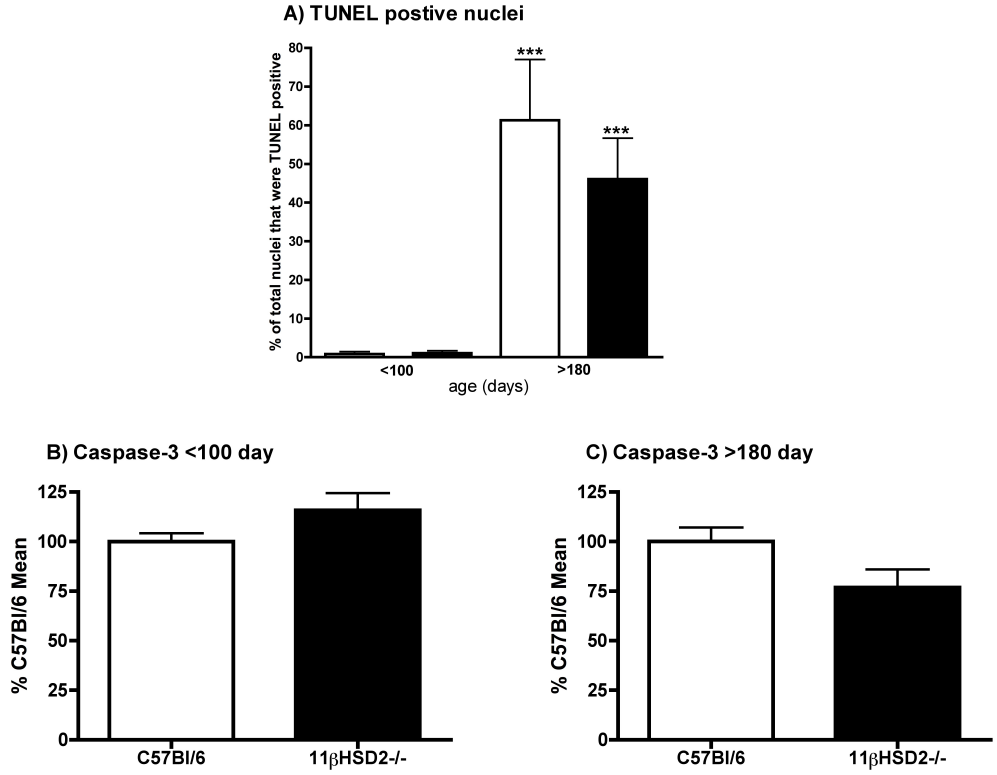

Figure 3.13: Evaluation of apoptotic cell death in C57Bl/6 (white) and 11βHSD2$^{-/-}$ (black) mice. (A) TUNEL staining. Caspase-3 mRNA abundance in (B) <100 and (C) >180 day mice. Data are means ± S.E.M. Statistical analysis was performed using a one-way ANOVA and tukey post-test or an unpaired t-test as appropriate. ***P<0.001 when compared to <100 day mice of the same genotype.

It has been postulated that in mice, polyuria and the resultant tubular dilation can cause reductions in local blood flow (Oppermann *et al*., 2007). To evaluate whether the medullary atrophy in >180 day 11βHSD2$^{-/-}$ mice was the result of local hypoxia, hypoxia inducible factor 1, alpha subunit (HIF-1α) mRNA abundance was assessed. Abundance of HIF-1α was not significantly different between 11βHSD2$^{-/-}$ and C57Bl/6 mice at either <100 (Figure 3.14.A) or >180 days (Figure 3.14.B).

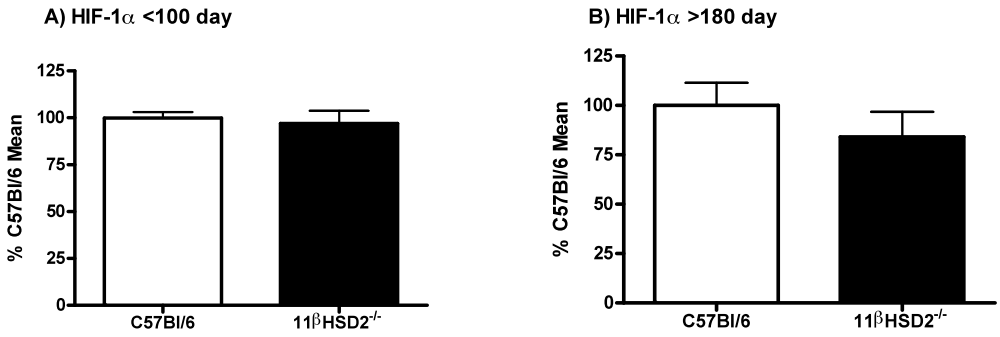

Figure 3.14: Abundance of HIF-1α in C57Bl/6 (white) and 11βHSD2$^{-/-}$ (black) mice at (A) <100 day and (B) >180 days. Data are means ± S.E.M. Statistical analysis was performed using an unpaired t-test.

In view of the role of TonEBP in the maintenance of medullary cellular integrity its abundance was evaluated in C57Bl/6 and 11βHSD2$^{-/-}$ mice at <100 (Figure 3.15.A) and >180 (Figure 3.15.B) days. There was no significant difference in the abundance of TonEBP in C57Bl/6 and 11βHSD2$^{-/-}$ mice at either age.

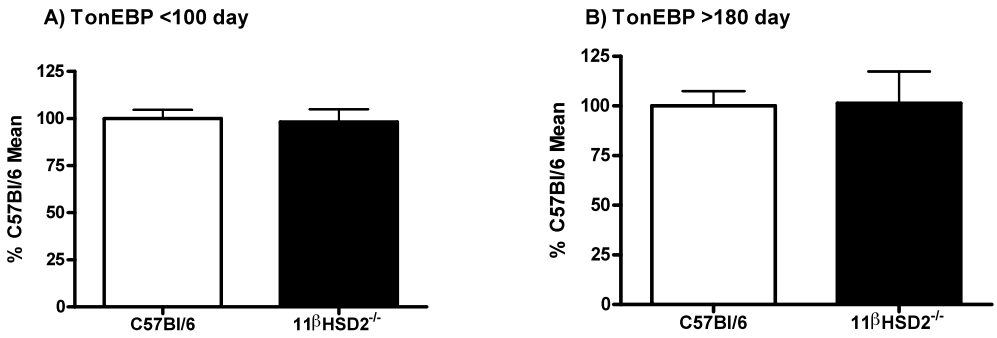

Figure 3.15: Abundance of TonEBP in C57Bl/6 (white) and 11βHSD2$^{-/-}$ (black) mice at (A) <100 day and (B) >180 days. Data are means ± S.E.M. Statistical analysis was performed using an unpaired t-test.

3.4. Discussion

3.4.1. Evaluation of basal renal function in 11βHSD2$^{-/-}$ mice

3.4.1.1. Basal collecting duct function

In accordance with other models of glucocorticoid excess, 11βHSD2$^{-/-}$ mice have an increased water turnover, displaying both polyuria and polydipsia. Notably water restriction and ddAVP administration failed to normalise urine concentrating ability, suggestive of a nephrogenic D.I. like phenotype. Clinically, nephrogenic D.I. is caused by mutations in the genes encoding AQP2 and V_2R. ~95% of cases arise from X-linked mutations in the gene encoding V_2R, which render the kidney insensitive to the actions of AVP. The remaining ~5% of cases are caused by autosomal recessive mutations in the gene encoding AQP2, with the mutations causing the retention of the channel in the ER and subsequently its degradation (Nielsen *et al*., 2007, Bichet, 1996). The demonstration that AQP2 mRNA abundance was lower in hydrated 11βHSD2$^{-/-}$ mice than the aged matched controls, at both <100 and >180 days, suggests that attenuated levels of the channel contribute to the increased urine flow.

The importance of AQP2 in basal water handling has been demonstrated through the evaluation of genetically modified mice. In humans point mutation T126M within the AQP2 gene causes the retention of the channel in the ER and consequently nephrogenic D.I. The generation of "knock-in" mice expressing this form of the channel illustrated the importance of the AQP2 in urine-concentrating ability. Although the mice appeared normal at birth they rapidly became dehydrated, failed

to thrive, and consequently died within a week (Yang *et al*., 2001). Since neonatal mortality was not observed in the polyuric AQP3 (Ma *et al*., 2000) and AQP4 (Ma *et al*., 1997) knockout mice, these studies highlighted the importance of apical AQP2 as the rate-limiting barrier in the modulation of basal urine concentration.

The reabsorption of water through AQP2 is dependent on its translocation from intracellular vesicles to the apical membrane. Although conclusions about the localisation of AQP2 cannot be drawn from the current studies, the demonstration that basal levels of AQP2 were reduced in the 11βHSD2$^{-/-}$ mice may explain the attenuated response to acute ddAVP stimulation during free access to water, discussed in section 2.3. In the acute setting, administration of ddAVP failed to induce anuria in the null mice. It is postulated that the intracellular AQP2 reservoir in the 11βHSD2$^{-/-}$ mice was not sufficient to induce a full concentration response following acute V_2R stimulation.

Since the AQP2 gene does not contain a GRE (Tchapyjnikov *et al*.), it is unlikely that the decreased mRNA abundance of the channel in the 11βHSD2$^{-/-}$ mice is the direct result of decreased glucocorticoid inactivation. As discussed in section 1.2.4.1 AQP2 expression and localisation are regulated by AVP. Acutely, AVP induces the trafficking of intracellular AQP2 to the apical membrane, whereas chronic stimulation results in the increased abundance of the channel (Nielsen *et al*., 1993a, Nielsen *et al*., 1995a). To evaluate the role of AVP in the regulation of AQP2 in the 11βHSD2$^{-/-}$ mice, plasma AVP concentrations were assessed during hydration. The

data presented suggest that there was a trend towards increased plasma AVP in the null mice. These data are in contrast to the known inhibitory effect of glucocorticoids on AVP transcription (Kim *et al*., 2001, Jard, 1991) and the demonstration of non-suppressible AVP release in glucocorticoid deficient models (Boykin *et al*., 1978, Saito *et al*., 2000). However, the evaluation of patients with Cushing's syndrome found that basal plasma AVP levels were not significantly different from the control subjects. Moreover, the AVP response to a water deprivation test was augmented in the Cushing's patients. Despite this, basal polyuria and an impaired response to ddAVP administration were also documented (Knoepfelmacher *et al*., 1997). These data suggest that chronic glucocorticoid excess is associated with a renal insensitivity to AVP.

Further support for this hypothesis came from the demonstration that AQP3, but not AQP4, abundance was decreased in the 11βHSD2$^{-/-}$ mice at <100 days. Chronic stimulation of V_2R, as occurs during a water deprivation challenge, increases renal AQP3 abundance. In contrast AQP4 is not regulated by V_2R stimulation (Terris *et al*., 1996). Therefore, the observation that AQP3, but not AQP4, abundance was decreased in the 11βHSD2$^{-/-}$ mice is cohesive with a renal escape from AVP stimulation. Despite this, in an experimental model of AVP escape AQP3 abundance was increased, despite attenuated levels of AQP2 (Ecelbarger *et al*., 1997, Ecelbarger *et al*., 2001b). The reason for the separation of AQP2 and AQP3 regulation was not determined. However, since the studies were performed over a relatively short period of time, the increase in AQP3 may have been an initial compensatory response to decreased apical AQP2. In line with this hypothesis is the demonstration

that in inducible AQP2$^{-/-}$ mice, increased abundance of AQP3 was reported six weeks following the induction of AQP2 deletion (Yang *et al*., 2006). Whether the increase in expression was a transient effect was not determined.

Crucially, the normal expression of AQP4 in the null mice at <100 days suggests that the difference in the abundances of AQP2 and AQP3 were not merely reflective of medullary atrophy, as might be assumed at >180 days.

The mechanism underlying AVP escape has not been fully determined. However, prolonged AVP stimulation has been shown to decrease V_2R mRNA abundance, binding capacity and cAMP production (Tian *et al*., 2000, Saito *et al*., 2001) implicating impaired receptor function in the phenomenon. Additionally, proteomic evaluation of the vasopressin escape model demonstrated the increased expression of several proteins involved in V_2R internalisation, adding support to the hypothesis that altered V_2R signalling contributes to the insensitivity to AVP (Hoorn *et al*., 2005). Within the time frame of this thesis it was not possible to assess V_2R receptor abundance and function, evaluation of which would provide an insight into whether the apparent renal insensitivity to AVP stimulation in the 11βHSD2$^{-/-}$ mice was the result of decreased receptor function.

Although the data presented suggest that plasma AVP was increased in the null mice, the low number of mice available for analysis means that caution should be taken

when drawing conclusions from these experiments. Evaluation of plasma AVP in mice is hampered by both the low volume of plasma available for analysis and the difficultly of obtaining non-stressed samples. Acute stress was shown to increase the activity of AVP positive neurons in the hypothalamus (Zhao and Ai, 2011), implicating the release of the neurohormone in the stress response. In the current studies plasma samples were obtained from decapitated mice. Since carbon dioxide has been shown to have profound affects on plasma AVP concentrations (Reed *et al*., 2009) the mice were not anesthetised prior to decapitation, consequently, minimal stress was unavoidable. In an attempt to reduce the effect of stress on the data, values more than two standard deviations from the mean were excluded from analysis, thus limiting the number of useable mice per cohort. Ideally, the data would be verified using plasma samples obtained from conscious, unrestrained mice. However, this technique is not without problems; hypovolemia is a powerful stimulus for AVP release. Since the plasma volume of mice is particularly low, plasma AVP concentrations directly correlate to the amount of blood withdrawn. Therefore, effort must be taken to simultaneously replace any blood removed (Professor Peter Bie, personal communication).

Although the cause of the deranged water handling in 11βHSD2$^{-/-}$ was not determined, it is likely that the severe hypokalemia documented in the model contributes to the phenotype (Bailey *et al*., 2008, Kotelevtsev *et al*., 1999). The effect of hypokalemia on renal water handling has been extensively studied. In rats chronic hypokalemia is associated with polydipsia, polyuria and decreased renal AQP2 abundance (Berl *et al*., 1977, Marples *et al*., 1996, Amlal *et al*., 2000), in line

with the phenotype observed in the 11βHSD2$^{-/-}$ mice. Similarly, in rats chronically treated with aldosterone, decreased apical AQP2 and polyuria were documented. It is likely that the altered water handling in this model occurred secondarily to the resultant hypokalemia, however this was not confirmed (de Seigneux *et al*., 2007). In hypokalemic rats, urine-concentrating defects were reversed by the administration of a normal potassium diet (Marples *et al*., 1996). Whether the normalisation of plasma potassium would have the same effect in 11βHSD2$^{-/-}$ mice is of interest.

3.4.1.2. Generation of the osmotic gradient

As discussed in section 1.2.2 the loop of Henle is responsible for the generation of the corticomedullary osmotic gradient. The dissipation of this gradient would impair the reabsorption of water from the collecting duct regardless of the function of the AVP-AQP2 cascade. The demonstration that NKCC2 mRNA abundance was not significantly different between the 11βHSD2$^{-/-}$ mice and C57Bl/6 controls at <100 days suggests that the polyuria observed at this age is not the result of an impaired osmotic gradient. In contrast the mRNA abundance of NKCC2 was significantly lower in the null mice at <180 days. Therefore, the impairment of the cortico-medullary gradient may contribute to the exacerbated urine flow in >180 day 11βHSD2$^{-/-}$ mice. Indeed, the attenuation of the osmotic gradient may explain the reduced sensitivity to AVP in the null mice at this age. However, as with AQP3 and AQP4, the contribution of the extensive medullary atrophy, observed at >180 days in 11βHSD2$^{-/-}$ null mice, should taken into consideration when interpreting these data.

In the inner medulla, the longitudinal osmotic gradient is partly attributable to the accumulation of urea. The demonstration that urea excretion was elevated, and UT-A mRNA abundance decreased, in the null mice at both <100 and >180 days implies an impaired medullary concentration of urea.

Chronic glucocorticoid excess is associated with altered renal handling of urea. Studies in rats on a low protein diet demonstrated that 7-day dexamethasone administration resulted in the increased fractional excretion of urea. In contrast, the same effect was not observed following acute (2-day) glucocorticoid administration, suggesting that prolonged elevations of glucocorticoids are required to alter tubular urea transport (Knepper *et al*., 1975). The augmented excretion of urea, induced by glucocorticoid excess, has been implicated in the development of the polyuria frequently observed in the models. In rats, chronic dexamethasone treatment resulted in polyuria and an impaired concentration response to water deprivation, a similar phenotype to that observed in the 11βHSD2$^{-/-}$ mice. Evaluation of renal transporter abundance demonstrated the decreased expression of UT-A1 and UT-A3. Since the abundance of AQP2 was not altered, the polyuria was attributed to the impaired medullary concentration of urea (Li *et al*., 2008). Detailed evaluation of urea transporter expression following glucocorticoid treatment provided a causative mechanism for the increased urea excretion. Protein expression of UT-A1 was found to be significantly higher in adrenalectomized rats than sham-operated controls. Glucocorticoid replacement resulted in the attenuation of UT-A1 expression to control levels, thus supporting the hypothesis that glucocorticoids are involved in the suppression of UT-A1 (Naruse *et al*., 1997). Subsequent studies showed that

dexamethasone treatment resulted in inhibition of UT-A promoter 1 activity in cell culture (Peng *et al*., 2002). Investigations in mice in which β-galactosidase (β-gal) was placed under the control of the UT-A promoter illustrated the physiological reference of these *in vitro* findings. Administration of dexamethasone to the mice resulted in a reduction in β-gal activity in the inner medulla, and contemporaneously a decrease in UT-A1 and UT-A3 mRNA (Fenton *et al*., 2006). The demonstration that UT-A mRNA abundance was lower in 11βHSD2$^{-/-}$ mice than aged matched C57Bl/6 controls is in line with these observations, and suggests that decreased expression of UT-A1 and UT-A3 may contribute to the polyuria.

Given that the deletion of 11βHSD2 provides glucocorticoids with unrestricted access to MR, it could be postulated that glucocorticoid activation of MR is causative in the augmented urea excretion observed in null mice. However, in adrenalectomized rats, dexamethasone induced reductions in UT-A1 protein abundance were not attenuated by spironolactone (Gertner *et al*., 2004). These data suggested that the effects of glucocorticoids were not mediated by the mineralocorticoid receptor, and were more likely the result of glucocorticoid receptor activation. This hypothesis was supported by the observation that the glucocorticoid receptor antagonist, RU-486, prevented dexamethasone-induced inhibition of the UT-A1 promoter *in vitro* (Peng *et al*., 2002).

3.4.1.3. The AQP2 response to water deprivation

In view of the apparent role of AQP2 in the increased urine flow in 11βHSD2$^{-/-}$ mice, its involvement in the response to water deprivation was assessed. Protein levels of AQP2 were ~2 fold higher in dehydrated C57Bl/6 mice than their hydrated counterparts at both <100 and >180 days. In line with a functional response to water deprivation, the abundance of AQP2 was also higher in dehydrated than hydrated 11βHSD2$^{-/-}$ mice at <100 days. In contrast, at >180 days the abundance of AQP2 following water removal was only marginally higher than that measured during free access to water, implicating the channel in the impaired response to water deprivation at this age. It is a limitation of these studies that comparable AQP2 mRNA abundance data was not obtained from dehydrated mice. Consequently, the cause for the reduced protein expression during dehydration cannot be determined. However, assuming a close correlation between mRNA and protein expression, it is postulated that the augmented AQP2 response to water deprivation in the <100 day 11βHSD2$^{-/-}$ mice is the result of attenuated basal expression.

As discussed in 1.2.4.2 phosphorylation of Ser-256 induces the translocation of intracellular AQP2 to the apical membrane. Ser-256 is one of four AVP-regulated phosphorylation sites on the AQP2 gene, all of which reside in the carboxyl terminal tail. Although less thoroughly characterised, Ser-261, Ser-264 and Ser-269 are also involved in determining the localisation of AQP2. Clathrin-coated pits mediate endocytosis of AQP2, a process that is dependent on membrane scission by the GTPase dynamin (Sun *et al*., 2002). Co-immunoprecipitation studies demonstrated that 256D and 269D (D representing aspartic acid, which mimics phosphorylation)

had an attenuated interaction with dynamin compared to wildtype AQP2. Moreover, internalisation of the constitutively phosphorylated forms of the channel was slower than that of the wildtype, suggesting that apical membrane accumulation of AQP2 when phopshorylated at Ser-256 and Ser-269 is in part due to impaired endocytosis (Moeller *et al*., 2010). The use of phospho-specific antibodies to evaluate the phosphorylation state of AQP2 would provide an insight into whether impaired shuttling of AQP2 to the apical membrane contributed to the attenuated response to water removal in the >180 day 11βHSD2$^{-/-}$ mice.

3.4.2. Evaluation of renal structure in 11βHSD2$^{-/-}$ mice

The kidneys from <100 day 11βHSD2$^{-/-}$ mice were structurally normal at both the gross and tubular level despite significant polyuria. In contrast at >180 days extensive renal damage was observed in the null mice. At the gross level severe medullary atrophy was documented, to the extent that the papilla was exposed. Similarly, tubular structure was damaged in the >180 day 11βHSD2$^{-/-}$ mice. The tubules displayed varying degrees of dilation, as a result of which the total tubular area was increased in the 11βHSD2$^{-/-}$ mice. Basement membrane width was not significantly different between the C57Bl/6 and 11βHSD2$^{-/-}$, suggesting that there was no hypertrophy, however, hyperplasia was evident, with increased nuclei per tubule.

Glomeruli number was not significantly different between the 11βHSD2$^{-/-}$ and C57Bl/6 mice at either <100 or >180 days. However, despite this increased urinary

excretion of albumin was documented in the null mice at both ages, indicative of glomeruli damage. Albumin, which is synthesized by the liver, accounts for approximately 60% of total plasma protein in humans. The kidneys filter roughly 0.99% of plasma albumin, the majority of which is taken up by proximal tubule cells, such that in healthy individuals the final urinary concentration is <100mg/24hr. The glomerular barrier is both size and charge selective. Since albumin has a relatively large radius and negative charge it is predominantly restricted from the filtrate (Lund *et al*., 2003). The demonstration that albumin excretion was augmented in 11βHSD2$^{-/-}$ mice at <100 days, and had increased substantially by >180 days is suggestive of glomeruli injury in the null mice.

Hypertension, as documented in 11βHSD2$^{-/-}$ mice (Bailey *et al*., 2008, Kotelevtsev *et al*., 1999) is associated with endothelial dysfunction and glomerular hyperfiltration. Therefore the augmented albumin in the urine of 11βHSD2$^{-/-}$ mice may be the result of hypertension induced glomeruli damage. Alternatively, the albuminuria could be the result of over exposure to glucocorticoids during development. Although acute glucocorticoid administration has been shown to reduce glomerular disease and proteinuria, through a reduction in local inflammation (Leech *et al*., 2000), prenatal glucocorticoid exposure has been frequently documented to result in postnatal renal injury. Within the placenta 11βHSD2 acts to protect the foetus from over exposure to maternal glucocorticoids (Reviewed in (Yang, 1997). Since the 11βHSD2$^{-/-}$ mice in the current investigations were generated from null-null crosses, the effects of over exposure to glucocorticoids *in utero* must be considered when interpreting the results.

Maternal glucocorticoid administration during gestation has been demonstrated to cause renal injury in mice (Dickinson *et al*., 2007) and rats (Ortiz *et al*., 2003, Singh *et al*., 2007). In these studies renal injury was classified as a reduction in glomeruli number. Moreover, increased glomerulosclerosis was observed (Ortiz *et al*., 2003). Although glomeruli number was not different between the two cohorts in the current studies, it is possible that damage to glomerular barrier, occurring as a consequence of *in utero* glucocorticoid exposure, may have contributed to the albuminuria in 11βHSD2$^{-/-}$ mice.

To evaluate whether apoptotic cell death contributed to the medullary injury TUNEL staining was performed. Although there was no significant difference in the amount of TUNEL positive nuclei counted in the C57Bl/6 and 11βHSD2$^{-/-}$ mice at either <100 or >180 days, the amount of positive nuclei recorded in both cohorts at >180 day was surprisingly high. It has previously been documented that false positive staining is particularly prevalent in the murine kidney (Pulkkanen *et al*., 2000). Therefore, a second assessment of apoptosis was utilised. Caspase-3 is a key protein in the execution of apoptosis, involved in the many of the proteolytic events central to programmed cell death. Moreover, its mRNA expression has been used to evaluate apoptosis in murine renal injury models (Zhang *et al*., 2006). Evaluation of the renal caspase-3 mRNA demonstrated that there was no difference in abundance between the 11βHSD2$^{-/-}$ and C57Bl/6 control mice at either <100 or >180 days. These data suggested that increased apoptosis may not have been the cause of medullary atrophy.

To evaluate whether hypoxia contributed to the loss of tissue, renal HIF-1α abundance was assessed. HIF-1α expression increases during hypoxia, and through the induction of protective genes, aids cellular survival when oxygen levels are low. The involvement of HIF-1α in murine renal hypoxia has been illustrated using genetically modified mice. Mice heterozygous for HIF-1α had an exacerbated response to ischemia-reperfusion injury, assumedly because the protective effects of the gene were reduced (Hill *et al*., 2008). Since HIF-1α abundance was not different in the 11βHSD2$^{-/-}$ and C57Bl/6 mice it is unlikely that hypoxia contributed to the renal injury. Similarly, TonEBP abundance was not different between the two cohorts, suggesting that an impaired response to medullary hypertonicity was not causative in the renal injury. Notably, these studies are limited by the evaluation of mRNA abundance at only two time points: one prior to, and one after, the development of extensive renal injury. The evaluation of mRNA abundance at intermittent time points would provide a more thorough understanding of the mechanisms involved in initiation the medullary atrophy.

Extensive renal injury has been documented in several polyuric mouse models, suggesting that increased urine flow may contribute to the medullary damage. Support for this hypothesis came from the evaluation of inducible AQP2$^{-/-}$ mice. Within six weeks of AQP2 gene excision, extensive medullary atrophy was observed. At this time urine flow was ~25ml/24hrs, ~2 fold greater than that observed in the 11βHSD2$^{-/-}$ mice at >180 days (Yang *et al*., 2006). These data support the notion that increased urine flow is involved in the development of medullary atrophy, perhaps with the extent of the polyuria determining the time

course of damage. This may explain the absence of injury in the <100 day 11βHSD2$^{-/-}$ mice, in which the polyuria was less severe. The more detailed analysis of the temporal correlation between renal structure and urine flow rate in the 11βHSD2$^{-/-}$ mice would provide an insight into whether there is threshold for polyuria induced renal injury.

The reason that the murine kidney is particularly susceptible to flow induced injury has not been determined, however an interesting hypothesis has been proposed by Schnermann's laboratory (Oppermann *et al*., 2007). Following furosemide administration it was demonstrated that renal blood flow was reduced (assessed using doppler probes). Since furosemide induced the vasodilation of isolated perfused arterioles it was postulated that the reductions in blood flow were secondary to diuresis. It was proposed that increased urine flow resulted in increased intratubular pressure, tubular dilation, compression of peritubule capillaries and consequently reductions in local blood flow. The demonstration that furosemide induced reductions in blood flow were attenuated by renal decapsulation supported the hypothesis. Since the amount of nephrons per kidney weight is substantially higher in mice than humans, this theory could explain why medullary injury is less commonly observed clinically in nephrogenic D.I. The use of doppler probes to measure total and medullary perfusion in the 11βHSD2$^{-/-}$ mice would provide confirmation of this hypothesis in the model.

Chapter 4: Separation of the role of 11βHSD2 in the kidney and brain

4.1. Introduction

The studies detailed in this chapter were designed to evaluate and separate the role of 11βHSD2 in the kidney and brain in the regulation of salt and water homeostasis. To specifically assess the contribution of the enzyme in these organs to the phenotype observed in the global 11βHSD2$^{-/-}$ mice, two strains of transgenic mice already established in the Centre for Cardiovascular Science were utilized. Firstly, to assess the role of renal 11βHSD2, global null mice in which *hsd11b2* had been selectively reintroduced into the kidney were evaluated (referred to as 'KRDKO mice'). Secondly, selective targeting of *hsd11b2* in the brain was achieved by cre-lox recombination (referred to as 'brain 11βHSD2$^{-/-}$ mice').

4.1.1. 11βHSD2$^{-/-}$/ApoE$^{-/-}$ kidney rescue mice

The studies detailed were conducted to evaluate the role of 11βHSD2 in the kidney. Ideally, the experiments would have been performed in mice in which *hsd11b2* had been selectively targeted in the ASDN: using AQP2 driven cre-recombinase to selectively delete floxed *hsd11b2* in this region of the nephron. However, given the availability of the KRDKO mice, the opportunity to gain an insight into the role of renal 11βHSD2 was capitalised. Within the Centre for Cardiovascular Science an 11βHSD2$^{-/-}$/ApoE$^{-/-}$ double-knockout mouse (DKO) has been generated (Deuchar *et al*., 2011). This model was created primarily to evaluate the contribution of 11βHSD2 to lesion development in atherosclerosis.

Deletion of 11βHSD2 with apolipoprotein-E (ApoE) resulted in exacerbated atherosclerosis, with accelerated lesion formation that was not dependent on the administration of a high fat diet. In an attempt to separate the effects of 11βHSD2 deletion from the resultant hypertension, amiloride and eplerenone were administered to the mice. Since amiloride blocks ENaC it was used to target the hypertension, whereas the MR antagonist eplerenone was used to evaluate the consequences of receptor over-activation. Amiloride but not eplerenone caused a significant reduction in blood pressure; however eplerenone was more effective at reducing lesion formation. These data therefore suggested that the effects of 11βHSD2 deletion on atherosclerosis were independent of hypertension in the double knockout mice (Deuchar *et al*., 2011). To substantiate further this conclusion, double knockout mice in which 11βHSD2 had been selectively introduced back into the kidney were generated. In view of the postulated renal origin to the altered salt and water homeostasis in the global 11βHSD2$^{-/-}$ mice, the KRDKO mice made available to study the role of 11βHSD2 in renal function. The model was used to assess the role of renal 11βHSD2, in the absence of 11βHSD2 in the brain.

Homologous recombination was used to "knock-in" 11βHSD2 in the kidney. In this model the *hsd11b2* transgene was placed under the control of the AQP2 promoter. Consequently 11βHSD2 was selectively expressed in cells that express AQP2. Within the kidney AQP2 is localised to the collecting duct (Fushimi *et al*., 1993). Since the DCT is devoid of AQP2, 11βHSD2 expression was not reinstated in this region of the nephron. As previously stated, in the mouse nephron 11βHSD2 may also be expressed in the DCT (Campean *et al*., 2001). Extra renal expression of

AQP2 has also been characterised in humans (Mobasheri *et al*., 2005) and mice (Yang *et al*., 2006). In mice AQP2 transcript and protein expression have been demonstrated in the testis, vas deferens and inner ear (Yang *et al*., 2006). This is in contrast to humans in which expression has also been described in discrete regions of the central nervous system (Mobasheri *et al*., 2005). Therefore, in the KRDKO mice any alterations in water and sodium homeostasis are likely the result of renal, rather than extra-renal, 11βHSD2.

$ApoE^{-/-}$ mice are not hypertensive (Hartley *et al*., 2000, Nogueira *et al*., 2007) and have a normal water intake at <12 months (Raber *et al*., 2000). Therefore it was postulated that the targeting of ApoE would not contribute in a major way to any renal phenotype in the double knockout mice. Nevertheless, to control for the loss of ApoE, $ApoE^{-/-}$ mice were evaluated along with DKO and KRDKO mice in the studies detailed.

4.1.2. Nestin.Cre.HSD2Flx mice

To assess specifically the contribution to the phenotype observed in the global $11\beta HSD2^{-/-}$, of 11βHSD2 in the brain, cre-lox recombination was used. Selective targeting of *hsd11b2* in the brain was achieved by a conventional breeding strategy in which nestin.cre mice (mice in which the enzyme cre-recombinase is under the control of the nestin promoter) were crossed with *hsd11b2*.floxed mice (mice in which loxP sites were inserted in the intronic regions prior to exon 2 and after exon 5 of the *hsd11b2* gene).

Cre-recombinase, a 38kDa enzyme isolated from bacteriophage p1, catalyzes the recombination of DNA between two identical 34 base-pair loxP sites (referred to as 'floxed' regions). Although such loxP sites frequently occur in the bacteriphage genome, their endogenous expression is statistically unlikely in the mouse, therefore favouring specific recombination of the targeted floxed gene. When inserted in the same orientation, cre-recombinase excises the sequence of DNA flanked by the loxP sites (Figure 4.1).

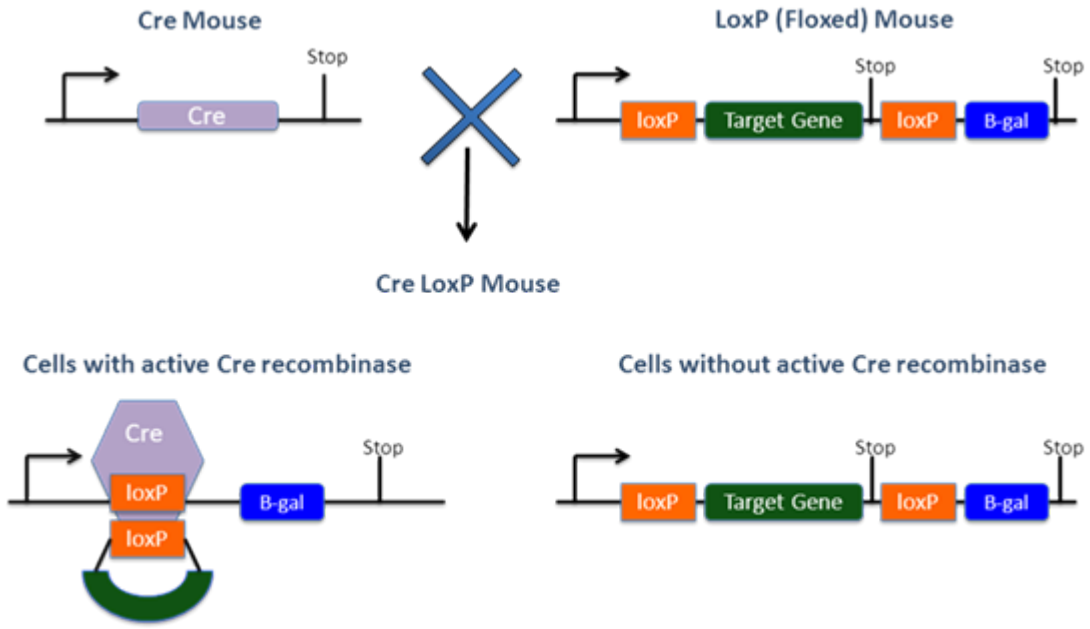

Figure 4.1: The use of Cre-Lox technology to create tissue specific knockout mice. LoxP sites flank a region of the target gene. This region will be excised in cells that express the enzyme cre-recombinase. In cells without cre-recombinase the target gene remains functional. Here, β-galactosidase is included as an internal control. Cells in which the target gene has been deleted will stain positive for X-gal. In contrast an absence of X-gal staining represents the absence of gene targeting.

Since cre-recombinase is not endogenously expressed in mammals, spatial regulation of its activity and therefore gene deletion can be achieved through the use of tissue-specific promoters (Kos, 2004). In the studies detailed, cre-recombinase expression was driven by the nestin promoter. Nestin, originally identified in neuroepithelial stem cells, is a class 6 intermediate filament protein (Lendahl *et al*., 1990). Within the central nervous system nestin is expressed in both glial cells and neurons (Shi *et al*., 2008). In mice nestin is highly expressed in the central nervous system throughout embryogenesis. Expression is evident from the seventh day of gestation, mainly in proliferative zones and becoming more wide spread throughout embryogenesis. Postnatal nestin expression decreases in correlation with decreased neuronal proliferation (Dahlstrand *et al*., 1995). The relevance of this for the current study is that nestin-cre driven recombination, occurs throughout neuronal development, and will delete 11βHSD2 expression wherever nestin is expressed. In embryogenesis, this will target 11βHSD2 in the cerebellum, thalamus and hypothalamus (Brown *et al*., 1996, Holmes *et al*., 2006b). However, in adult mice the expression of 11βHSD2 in the brain is exquisitely localised to the NTS (Holmes *et al*., 2006b). This is in contrast to rats in which a more widespread localization has been described (Geerling *et al*., 2006b, Roland *et al*., 1995, Robson *et al*., 1998). Consequently the selective targeting of 11βHSD2 in the mouse brain provides the unique opportunity to evaluate, in the adult, the role of the enzyme in the NTS. Since the NTS has been implicated in salt appetite (Geerling *et al*., 2006a), this was evaluated along with sodium and water homeostasis in the model.

Hypothesis

1. Rescue of renal 11βHSD2 function in KRDKO mice will normalize water turnover and blood pressure
2. Mice in which 11βHSD2 has been selectively targeted in the brain, specifically the NTS, will have normal renal function
3. Specific targeting of 11βHSD2 in the NTS will result in an increased salt appetite

4.2. Methods

4.2.1. Animals

All experiments were performed on male mice aged ~180 days since this was the age at which the phenotype was most severe in the global 11βHSD2$^{-/-}$ mice.

4.2.1.1. KRDKO mice

DKO mice were generated as described previously (Deuchar *et al*., 2011). Targeting of 11βHSD2 in the kidney was performed using homologous recombination, with expression of human 11βHSD2 placed under the control of the AQP2 promoter. The crossing of these mice, with DKO mice resulted in the generation of the KRDKO mice (Armour, 2010). Renal enzyme activity assays were performed to assess how effective the 11βHSD2 transgene induction was in the kidneys of KRDKO (Danielle Armour, personal communication). It was demonstrated that 11βHSD2 activity was partially restored in the KRDKO mice. Renal enzyme activity in the KRDKO mice was ~30% that of the ApoE$^{-/-}$ mice. In the experiments detailed n=3-9 throughout.

4.2.1.2. Brain 11βHSD2$^{-/-}$ mice

Mice in which the *hsd11b2* gene has been flanked with loxP sites (referred to as 'floxed 11βHSD2') were used as controls. Floxed mice were generated by Taconic, UK. Nestin.Cre mice were obtained from the Jackson Laboratory, USA (Tronche *et al*., 1999). In the experiments detailed n=3-9 throughout.

4.2.2. Evaluation of blood pressure in conscious KRDKO mice

Tail cuff plethysmography was used to measure systolic blood pressure in conscious restrained mice. Initially, the mice underwent a training regime to allow acclimatization to the restraint tube and the warming chamber. Training was performed over five consecutive days prior to the experimental recordings. Vasodilation of the tail vein was induced by warming the mice to 37˚C in the warming chamber. Mice were then restrained in a Perspex tube and tail cuff plethysmography performed. On each training day eight consecutive blood pressure measurements were taken per mouse, being completed over a ten-minute period. Throughout the experimental protocol blood pressure recordings were made over five consecutive days. Eight measurements were made per mouse per day, again over ten minutes; these values were then averaged to give one reading per mouse per day. Since there was no difference between the pressures obtained on the inflate or deflate cycle the blood pressures presented represent combined recordings. For analysis daily measurements were combined to give a five-day average per mouse. Experiments were performed in a blinded fashion to prevent experimental bias.

4.2.3. Evaluation of renal function

Mice were anesthetized using thiobutabarbital sodium salt hydrate (100mg/kg i.p. Inactin hydrate, Sigma-Aldrich, UK) and prepared surgically for renal clearance. A tracheotomy was performed using polyethylene tubing (P90, Smiths-Medical, UK). A saline-filled polyethene cannula (P10 polyethene tubing, Smiths-Medical, UK) was inserted into the right jugular vein for the infusion of a saline solution. The carotid artery was cannulated with heparinised-saline filled polyethene tubing (P10

polyethylene tubing, Smiths-Medical, UK), which was connected to a pressure transducer (disposable blood pressure-transducer, AD Instruments, UK). Mean arterial blood pressure was measured throughout the experiment (PowerLab, AD Instruments, UK). Finally, a supra-pubic incision was made and the bladder cannulated (P10 into P50 polyethylene tubing, Smiths-Medical, UK) for urine collection. Following surgery animals were infused i.v. (0.2ml/hr per 10g AL2000 model, World Precision Instruments, USA) with a solution containing 120mM NaCl, 15mM $NaHCO_3$ 5mM KCl, 0.5% FITC-Inulin (Fluorescence Isothiocyanate, Sigma-Aldrich, UK). Following a 60-minute equilibrium period, a 20µl arterial blood sample was taken for haematocrit analysis. Following a further 40-minute period, a second blood sample was taken for haematocrit analysis. The haematocrit values presented represent the average of both measurements. Terminal blood was collected at the end of the experiment for the measurement of plasma sodium and potassium concentration (AVI 9180 Electrolyte Analyzer, Roche, UK). Values outside the range of the analyzer were assigned maximum or minimum range values as appropriate. In the experiments detailed in KRDKO mice, following the second haematocrit sample amiloride (2mg/kg i.v. Sigma-Aldrich, U.K) was administered. After a 10 minute acclimatization period a second 40 minute urine collection was made, after which terminal blood was collected.

4.2.4. Evaluation of water and sodium turnover in brain 11βHSD2$^{-/-}$ mice

Metabolic cage studies were performed to evaluate basal sodium and water handling as detailed in 2.2.2.1. In brief, following four days acclimatization, baseline measurements were made over four days. Subsequently water was removed from the

mice for 24-hours to assess urine concentrating ability. Throughout the study water and food intake and urine output were measured. Mouse body weight was monitored daily.

4.2.5. Evaluation of salt appetite in brain 11βHSD2$^{-/-}$ mice

Metabolic cage studies were performed to evaluate salt appetite. In these investigations mice had *ad libitum* access to two drinking bottles, one of which contained water, the other 1.5% NaCl. Bottle position was rotated every 24 hours to ensure that side preference did not influence the results. Following four days acclimatization, baseline measurements were made over seven days. During this period water, NaCl and food intake, urine output and body weight were measured daily.

4.2.6. Evaluation of the role of MR in salt appetite in brain 11βHSD2$^{-/-}$ mice

The role of mineralocorticoid receptor activation in salt appetite was evaluated in a separate cohort of mice using the antagonist spironolactone. Spironolactone was distributed (0.5g, Sigma-Aldrich., UK) in an elastomer matrix (2g, Silastic MDX4-4210 medical grade elastomer, Dow Corning, UK). The pellets were cured overnight at 37˚C. After confirming salt preference, as detailed above, spironolactone pellets were implanted subcutaneously under isoflurane anaesthetic. A small incision was made in the neck and the pellet inserted. The wound was closed using auto-wound clips (Clay Adams, USA). Our previous work shows that the pellets release

spironolactone over a two week period and achieve a plasma concentration that would completely block MR (Bailey *et al*., 2009).

4.2.7. Enzyme Activity Assay

These assays were independently performed by Dr Caitlin Wyrwoll and Dr Danielle Armour. In brief, tissues were homogenised in Krebs Buffer and centrifuged at 4°C for 5 minutes at 2000 rpm. The supernatant was collected and protein concentration determined using a Bradford-base protein assay (Bio-Rad Protein Assay, Bio-Rad Laboratories, USA). 0.1 mg/ml homogenate was used per assay. Assay reactions contained 100μM co-factor (NAD^+, Sigma-Aldrich, UK), 100nM substrate (1,2,6,7-^{3}H-corticosterone, GE Heathcare Life Sciences, Anachem, UK) and 18μg tissue homogenate. Following 3 minutes incubation the reactions were terminated by the addition of HPLC grade ethyl acetate. Once settled, the aqueous phase of the reaction mix was isolated, dried down under oxygen-free nitrogen and resuspended in absolute ethanol. Thin layer chromatography assays were performed to determine the conversion of ^{3}H-corticosterone to dehydrocorticosterone, illustrative of 11βHSD2 activity. For the foetal assays, to increase the levels of enzyme activity, assays were performed on pooled samples from a litter, with 5-7 litters evaluated per group per tissue.

4.2.8. Analysis

Analysis was performed as detailed (section 2.2.3). In the salt appetite studies sodium preference was calculated by expressing the amount of 1.5% NaCl consumed

during a 24-hour period as a percentage of the total volume of fluid consumed. Sodium balance was evaluated by calculating the difference between combined sodium intake and urinary sodium excretion as detailed (section 2.2.3). Urinary protein, electrolyte and osmolar excretion were assessed as detailed (section 2.2.3).

FITC-Inulin clearance was used to calculate glomerular filtration rate (GFR) as detailed (Lorenz, 2002). All dilutions were made using HEPES buffer at pH7.4, since the fluorescence is pH sensitive. Urine samples were diluted 1:100, plasma samples were diluted 1:1000. A seven point standard curve was generated for analysis. All samples were assessed in duplicate. Once loaded into a black 96 well plate (Microfluor Solid Microplate, Thermo Scientific, UK) fluorescence was measured using a Wallac Multilabel HTC counter (model 1420, Perkin Elmer, USA) with excitation at 485nm and emission at 538nm. GFR was calculated using the standard equation below, in which UV represents urine flow and U_{Inu} and P_{Inu} inulin concentrations in urine and plasma respectively.

$$GFR = U_{Inu}UV/P_{Inu}$$

4.2.9. Statistics

Data are presented as mean ± S.E.M. except for cumulative data, which are medians ± range. Statistical analysis was performed using an un-paired t-test, one-way ANOVA or Mann-Whitney test with Tukey post-test to compare between groups as appropriate.

4.3. Results

4.3.1. Blood pressure and renal sodium handling in KRDKO mice

To assess the role of 11βHSD2 in the kidney in the regulation of blood pressure, tail cuff plesmography was performed on ApoE$^{-/-}$, DKO and KRDKO mice over a five-day period. Global deletion of 11βHSD2 in the ApoE$^{-/-}$ mice resulted in hypertension. Systolic blood pressure was significantly higher in the DKO mice than the control ApoE$^{-/-}$ mice. Blood pressure was partially rescued by 11βHSD2 transgene induction in the kidney. Blood pressure was significantly lower in the KRDKO mice than the DKO mice, but remained significantly higher than that of the ApoE$^{-/-}$ mice (Figure 4.2.A). ApoE$^{-/-}$ mice were normotensive: blood pressure was not significantly different that in C57Bl/6 mice (ApoE$^{-/-}$ 101±1.5 vs C57Bl/6 102±2.4 mmHg, P>0.05, unpaired t-test).

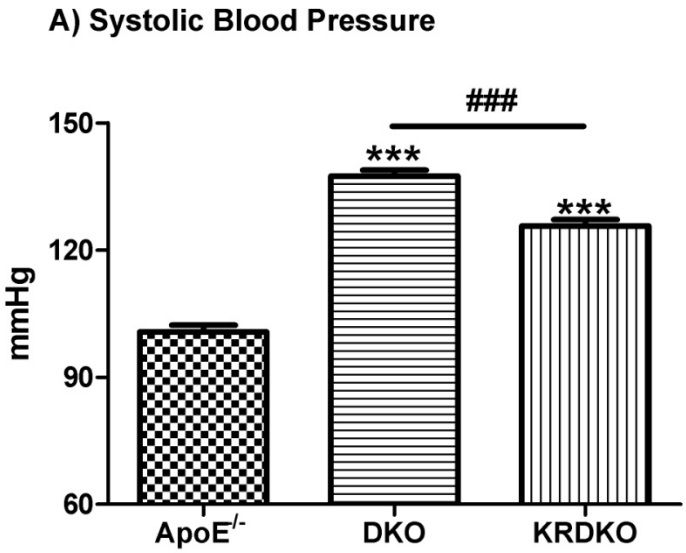

Figure 4.2: Systolic blood pressure in ApoE$^{-/-}$ mice (hashed), DKO mice (horizontal stripes) and KRDKO mice (vertical stripes). Data are means ±S.E.M. Statistical analysis was performed using a one-way ANOVA and Tukey post-test. ***P<0.001 compared to ApoE$^{-/-}$ mice, ###P<0.001 compared to DKO mice.

Renal sodium handling was evaluaed to assess its role in the hypertension observed in the DKO and KRDKO mice. Fractional sodium excretion was substantially higher in the DKO and KRDKO mice than the ApoE$^{-/-}$ controls (Figure 4.3.A). Since amiloride's natriuretic capacity was lost in the DKO and KRDKO mice (Figure 4.3.B), the increased sodium excretion may be partially attributable to impaired ENaC function. Haematocrit values recorded in the DKO and KRDKO mice were significantly higher than those of the ApoE$^{-/-}$ mice, suggestive of volume contraction (Figure 4.3.C). Hypokalemia, a cardinal feature of AME, was observed in both the DKO and KRDKO mice (Figure 4.3.D). Since fractional potassium excretion was substantially higher in the DKO and KRDKO mice than the ApoE$^{-/-}$ mice, this may have contributed to the hypokalemia. Urine osmolality was significantly lower in the DKO and KRDKO mice than the ApoE$^{-/-}$ mice indicative of a urine-concentrating defect, however urine flow rate was not significantly different between the three groups. GFR values were not significantly different between the ApoE$^{-/-}$, DKO and KRDKO mice (Table 4.1).

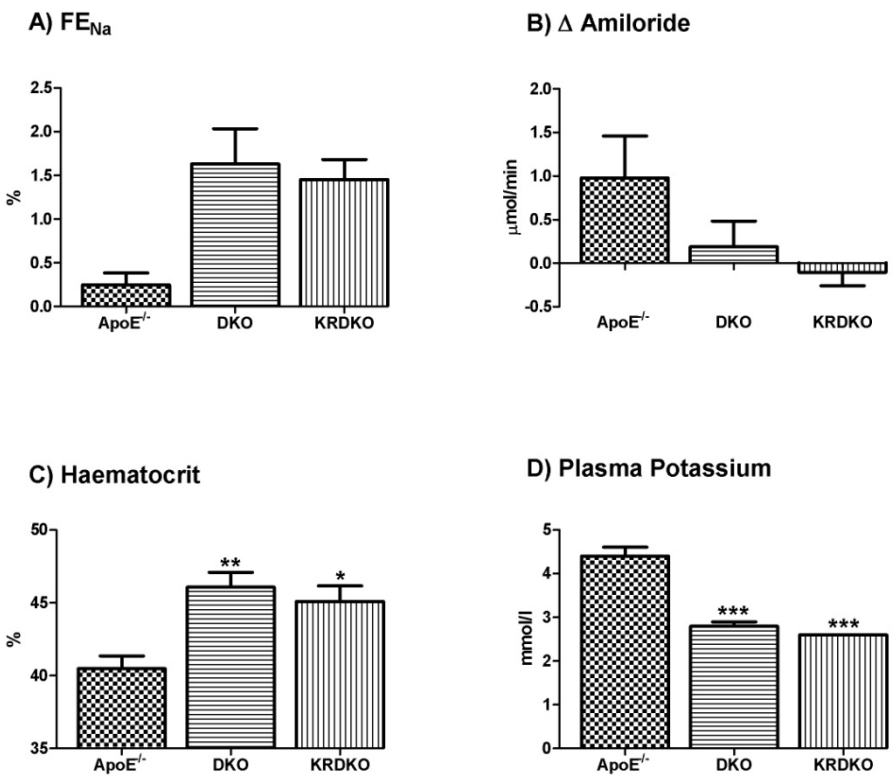

Figure 4.3: Renal function and plasma status in ApoE$^{-/-}$ mice (hashed), DKO mice (horizontal stripes) and KRDKO mice (vertical stripes). (A) Fractional excretion of sodium. (B) The effect of amiloride on sodium excretion. (C) Haematocrit. (D) Plasma potassium concentrations. Data are means ±S.E.M. Statistical analysis was performed using a one-way Anova and Tukey post-test. ***P<0.001, **P<0.01, *P<0.5 compared to ApoE$^{-/-}$ mice.

	ApoE$^{-/-}$	DKO	KRDKO
GFR (µl/min)	314±25	229±27	307±57
FE_K (%)	24±9	45±9	40±6
UV (µl/min)	3.1±0.3	4.6±0.8	5.4±1.0
UOsm (mOsm)	991±94	652±25***	661±10***

Table 4.1: Basal renal function in ApoE$^{-/-}$, DKO and KRDKO mice. GFR, glomerular filtration rate. FE_K, fractional excretion of potassium. UV, urine flow. UOsm, urine osmolality. Data are means ±S.E.M. Statistical analysis was performed using a one-way Anova and Tukey post-test. ***P<0.001 compared to ApoE$^{-/-}$ mice.

4.3.2. Water and sodium homeostasis in brain 11βHSD2$^{-/-}$ mice

Professor Megan Holmes and Dr Caitlin Wyrwoll performed the validation of the brain specific deletion of 11βHSD2 in the NestinCre.HSD2flx mice (personal communication). In this model the sequence encoding β-galactosidase was inserted in the construct after the region of the target gene that was flanked by loxP sites. Consequently, β-galactosidase was expressed in tissues in which 11βHSD2 had been deleted. As shown in Figure 4.4. X-gal staining occurred in the brain but not the kidney, confirming tissue specific targeting. Further confirmation was provided by tissue specific enzyme activity assays. The discrete location of 11βHSD2 in the NTS of adult mice meant that enzyme activity was too low to accurately measure in adult brains. Since expression of 11βHSD2 in the brain is wide spread throughout embryogenesis, activity was in measured in foetal brain extracts at day E13. Enzyme activity was significantly reduced (~75%) in the brain 11βHSD2$^{-/-}$ mice compared to the floxed controls (Figure 4.5.A). In contrast there was no significant difference in placental or whole body enzyme activity (Figure 4.5.A). These data substantiated the conclusion that 11βHSD2 deletion was specifically targeted to the brain. Notably, the activity of 11βHSD2 in the kidneys of adult mice was not significantly different in the brain 11βHSD2$^{-/-}$ mice and the floxed controls (Figure 4.5.B). Together, these data suggested that the nestin.cre was not leaky, and 11βHSD2 targeting was restricted to the brain in the brain 11βHSD2$^{-/-}$ mice.

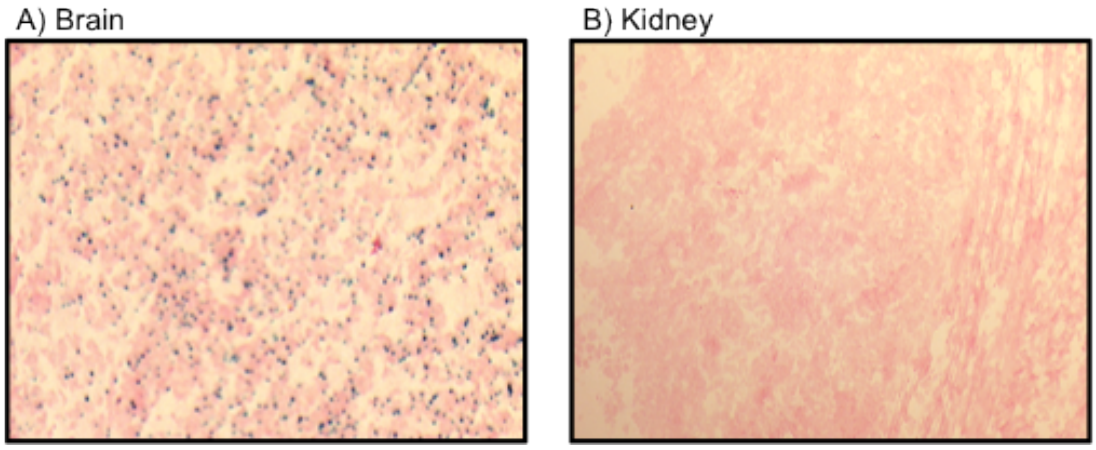

Figure 4.4: Confirmatory X-gal staining in brain 11βHSD2$^{-/-}$. Example staining showed from (A) The Brain and (B) The Kidney. Images courtesy of Holmes and Wyrwoll (personal communication).

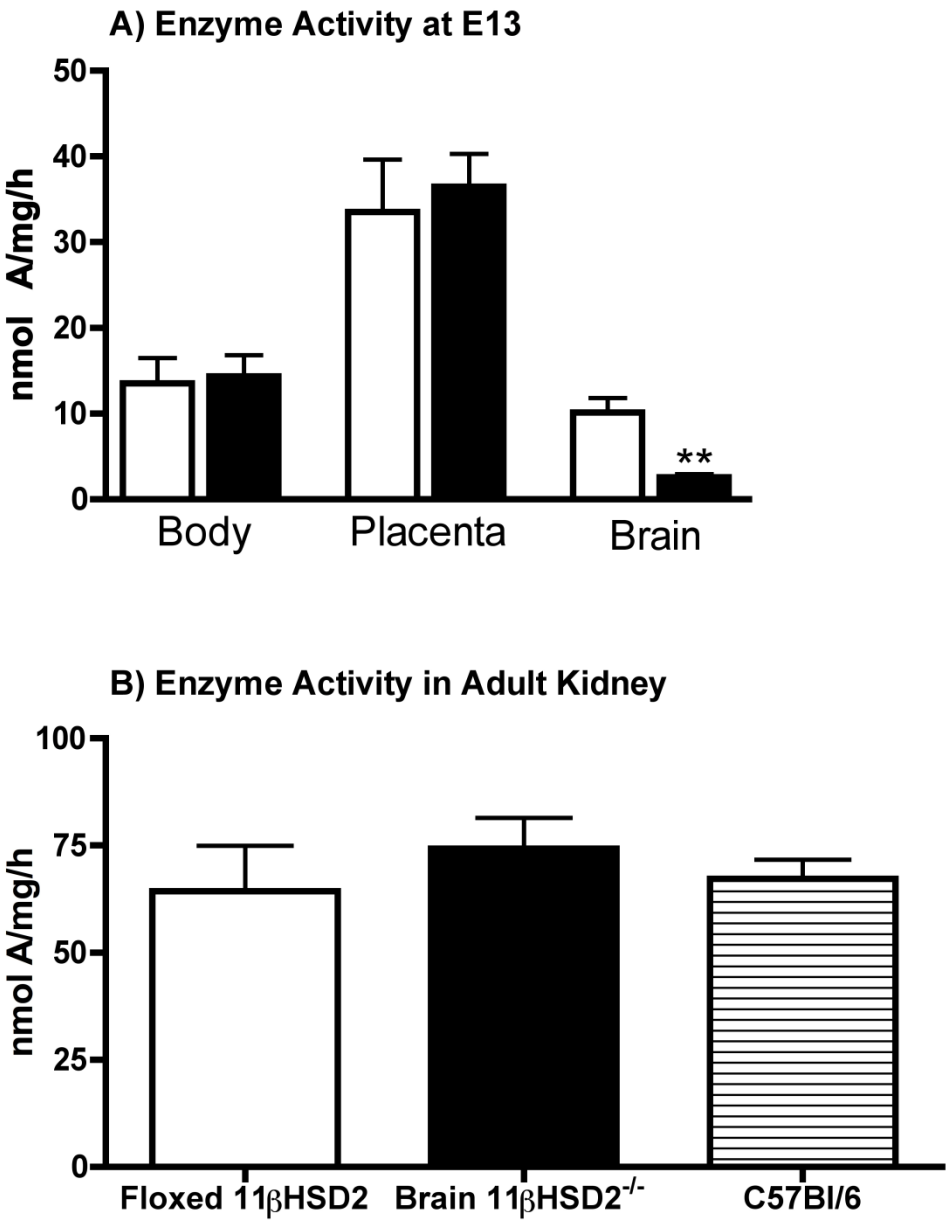

Figure 4.5: 11βHSD2 enzyme activity in Floxed 11βHSD2 control mice (white) Brain 11βHSD2$^{-/-}$ mice (black) and C57Bl/6 controls (horizontal stripes). (A) Enzyme activity in E13 foetus'. (B) Enzyme activity in adult kidneys (n=5). Data are means ± S.E.M. Statistical analysis was performed using an unpaired t-test and one-way ANOVA as appropriate. Data courtesy of Holmes and Wyrwoll (personal communication).

To evaluate the role of 11βHSD2 in the NTS in water homeostasis, urine flow and water intake were measured over a four-day baseline period in floxed control and brain 11βHSD2$^{-/-}$ mice. In contrast to the global 11βHSD2$^{-/-}$, deletion of 11βHSD2 in the NTS did not alter basal water turnover. Urine flow (Figure 4.6.B) and water intake (Figure 4.6.A) were not significantly different between the brain 11βHSD2$^{-/-}$ and the floxed 11βHSD2 control mice. Similarly, urine osmolality, an indicator of urine concentrating ability, was not significantly different between the two groups (Figure 4.6.C). Consequently, cumulative water balance over the four-day period was approximately 8ml in both groups of mice (Figure 4.6.D).

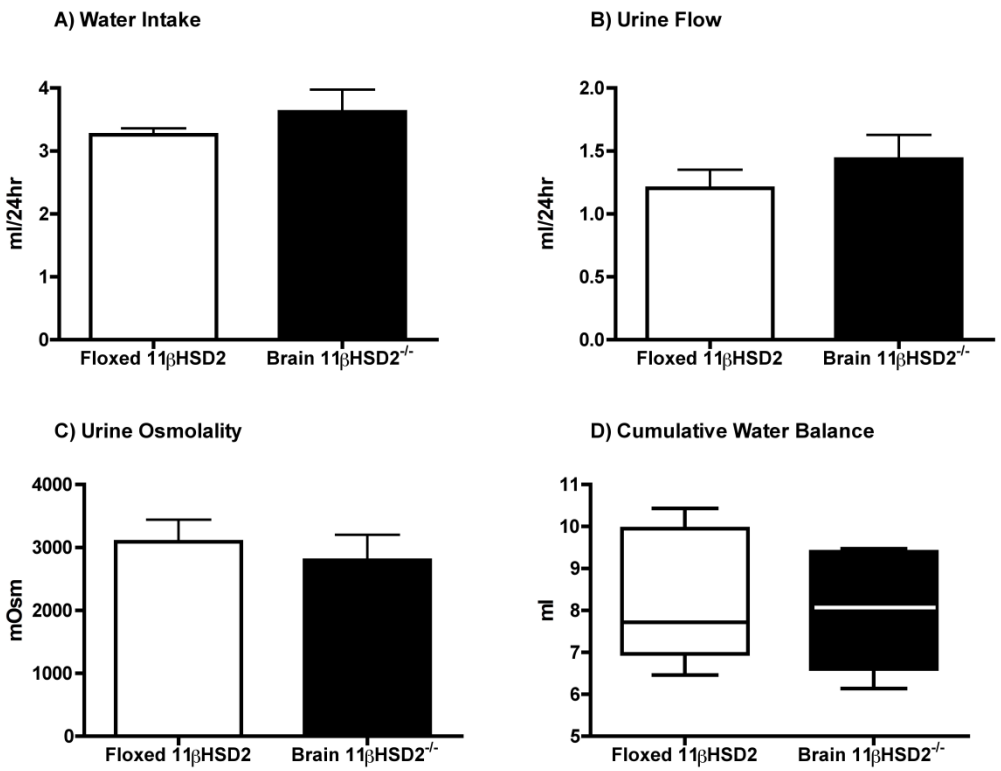

Figure 4.6: (A) Water Intake in floxed 11βHSD2 mice (white) and aged-matche brain 11βHSD2$^{-/-}$ mice (black). (B) Urine Flow. (C) Urine Osmolality. (D) Cumulative Water Balance calculated over the four-day baseline period. Data are means ±S.E.M. Statistical analysis was performed using an unpaired t-test or Mann-Whitney test as appropriate.

Since basal water turnover was not altered by the deletion of 11βHSD2 in the brain, it was postulated that the response to water deprivation would also be functional in the brain 11βHSD2$^{-/-}$ mice. Following water deprivation, urine flow reduced in both groups of mice, however the brain 11βHSD2$^{-/-}$ mice produced significantly lower volumes of urine than the floxed control mice during this period (Figure 4.7.A). These data were reflected in the water balance data, which was significantly more negative in the floxed 11βHSD2 mice than the brain 11βHSD2$^{-/-}$ mice (Figure 4.7.D). In response to water removal, urine osmolality increased to a similar extent in both groups of mice. Consequently, there was no significant difference between the osmolality values recorded in the floxed controls and the brain 11βHSD2$^{-/-}$ mice (Figure 4.7.B). Weight loss, used as an indicator of body fluid loss, was approximately equal in the floxed 11βHSD2 and brain 11βHSD2$^{-/-}$ mice. Both groups lost approximately 1.5g of weight following water removal (Figure 4.7.C). These data suggested that both groups of mice had a functional concentration response following water removal.

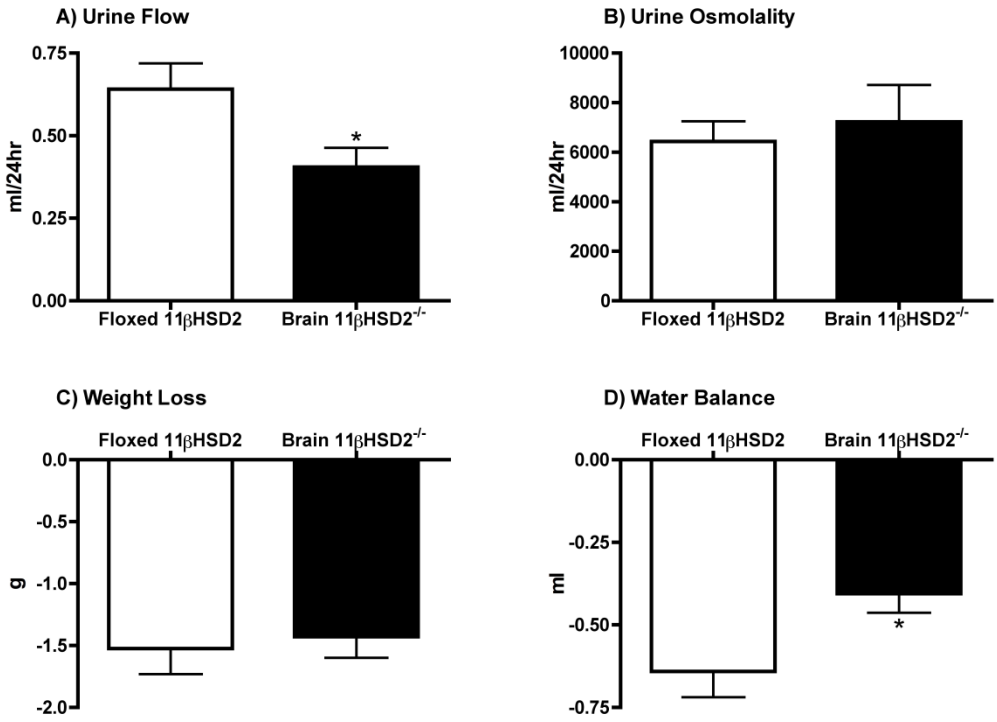

Figure 4.7: Response to water deprivation in floxed 11βHSD2 mice (white) and aged matched brain 11βHSD2$^{-/-}$ (black. (A) Urine Flow. (B) Urine Osmolality. (C) Weight Loss. (D) Water Balance calculated during the 24-hour water deprivation challenge. Data are means ±S.E.M. Statistical analysis was performed using an unpaired t-test. *P<0.05 compared to age matched controls.

Basal sodium turnover was evaluated in the control and brain 11βHSD2$^{-/-}$ mice. Urinary sodium excretion was not significantly different between the two groups of mice (Figure 4.8.A); both brain 11βHSD2$^{-/-}$ and floxed 11βHSD2 mice excreted approximately 0.3 mmol/24hrs. Similarly, sodium intake, was not different between the two groups (Figure 4.8.B). Cumulative sodium balance was therefore equivalent in the brain 11βHSD2$^{-/-}$ and floxed 11βHSD2 mice (Figure 4.8.C). Plasma sodium was in the normal physiological range in both groups (Figure 4.8.D).

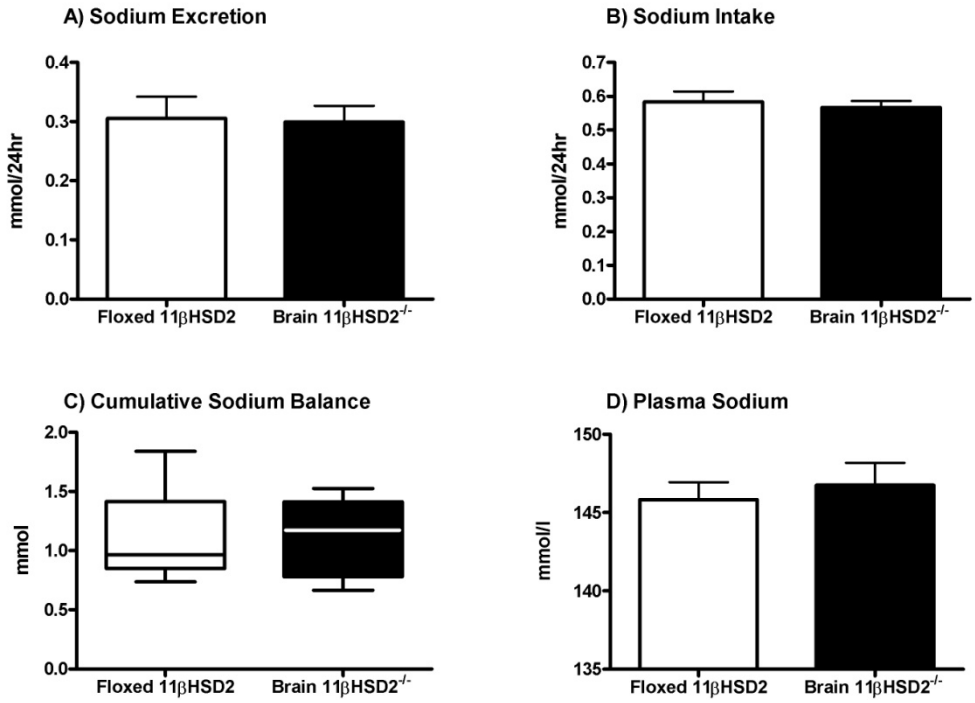

Figure 4.8: Sodium homeostasis in floxed 11βHSD2 mice (white) and aged matched brain 11βHSD2$^{-/-}$ mice (black). (A) Urinary Sodium Excretion. (B) Sodium Intake. (C) Cumulative Sodium Balance calculated over the four-day baseline period. (D) Plasma Sodium. Data are means ±S.E.M. Statistical analysis was performed using an unpaired t-test (A,B,D) or Mann-Whitney test (C) as appropriate.

Table (4.2) Renal function was not affected by the deletion of 11βHSD2 in the brain.

	Floxed 11βHSD2	**Brain 11βHSD2$^{-/-}$**
Food Intake (g/24hr)	4.5±0.2	4.3±0.2
CreatinineConcentration (μmol/ml)	3.4±0.2	3.2±0.5
Phosphate Excretion (μmol/24hr)	24.3±7.7	24.3±5.4
Calcium Excretion (μmol/24hr)	4.1±0.7	5.5±0.8
Magnesium Excretion (μmol/24hr)	41.2±2.9	37.7±4.0
Albumin Excretion (μg/24hr)	18.4±2.1	15.9±3.6
Urea Excretion (mg/24hr)	71.6±4.3	72.3±10.3
Osmolar Excretion (mOsm/24hr)	3471±211	3713±210

Table 4.2: Data are means ±S.E.M. Statistical analysis was performed using an unpaired t-test. Urine collections were made over a 4-day baseline period.

Mean arterial blood pressure was not altered by the deletion of 11βHSD2 in the brain. In contrast to the global deletion of 11βHSD2, specific targeting of 11βHSD2 in the brain did not result in volume contraction; haematocrit values were not significantly different between brain 11βHSD2$^{-/-}$ and floxed control mice (Table 4.3)

	Floxed 11βHSD2	**Brain 11βHSD2$^{-/-}$**
Mean Arterial Blood Pressure (mmHg)	81.2±4.4	72.2±4.2
Haematocrit (%)	43.5±1.3	42.8±0.1

Table 4.3: Data are means ±S.E.M. Statistical analysis was performed using an unpaired t-test.

11βHSD2-positive neurons in the NTS have been implicated in the behavioural drive to consume sodium, being activated in response to sodium deficiency (Geerling *et al*., 2006a). Sodium appetite therefore was evaluated in the brain 11βHSD2$^{-/-}$ mice. When given the option of drinking water or 1.5% NaCl, the brain 11βHSD2$^{-/-}$ drank significantly more NaCl than the floxed control mice (Figure 4.9.A). The increased consumption was specific for sodium since thirst was not altered by the deletion of 11βHSD2 in the brain. Brain 11βHSD2$^{-/-}$ mice did not drink significantly more water than the floxed control mice (Figure 4.9A).

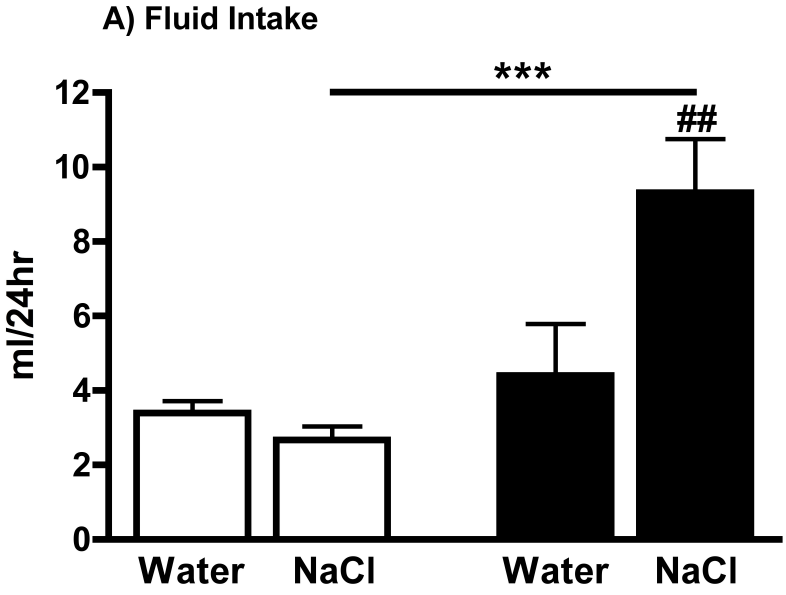

Figure 4.9.A: Salt appetite in floxed 11βHSD2 mice (white) and aged-matched brain 11βHSD2$^{-/-}$ mice (black). (A) Water and 1.5% NaCl intake. Data are means ±S.E.M. Statistical analysis was performed using a one-way ANOVA and Tukey post-test. ***P<0.001 compared to age matched controls. ##P<0.01 compared to water intake in the same mice.

During the sodium preference experiment urine flow was approximately four times greater in the brain 11βHSD2$^{-/-}$ mice than the floxed control mice (Figure 4.10.A). Cumulative water balance over the seven-day period however was not significantly different between the two groups of mice (Figure 4.10.B). Urinary sodium excretion was significantly higher in the brain 11βHSD2$^{-/-}$ mice than the floxed control mice (Figure 4.10.C), which suggested that the mice were not retaining sodium. Indeed, although sodium balance was positive in both groups of mice, it was significantly less positive in the brain 11βHSD2$^{-/-}$ than the floxed control mice despite the increased salt intake (Figure 4.10.D).

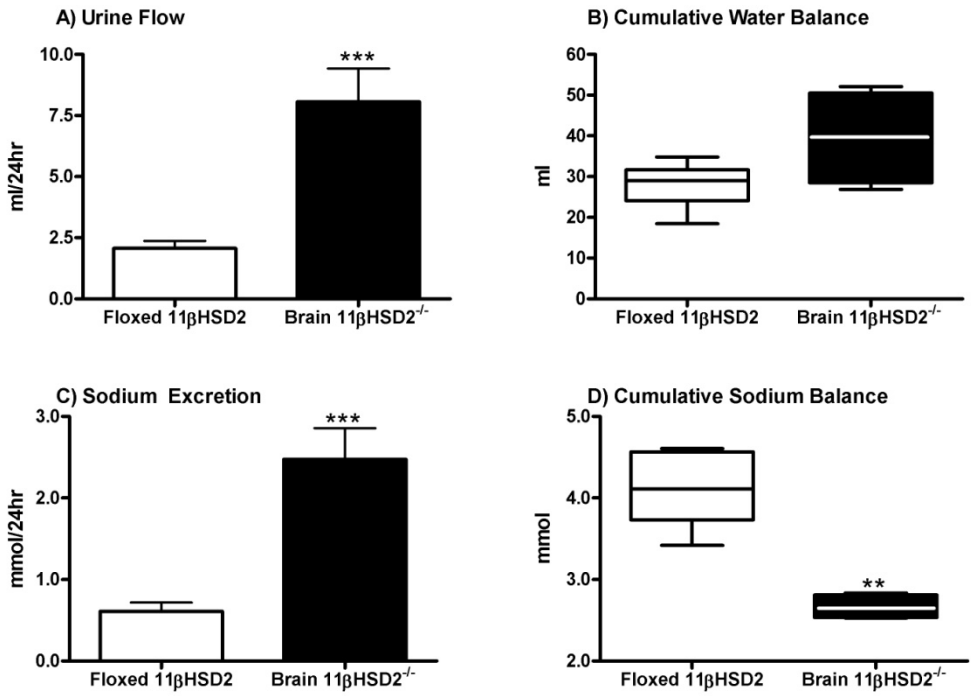

Figure 4.10: Water and sodium turnover during salt preference studies in floxed 11βHSD2 mice (white) and aged-matched brain 11βHSD2$^{-/-}$ mice (black). (A) Urine Flow. (B) Cumulative Water Balance. (C) Sodium Excretion. (D) Cumulative Sodium Balance. Data are means ±S.E.M. Statistical analysis was performed using an unpaired t-test (A, C) or Mann-Whitney test (B,D) as appropriate. ***P<0.001, **P<0.01 compared to age matched controls.

Spironolactone was used to evaluate the role of mineralocorticoid receptor activation in salt appetite in separate groups of mice. The innate salt appetite in brain 11βHSD2$^{-/-}$ mice was confirmed. During the basal period, 1.5% NaCl intake was higher in the brain 11βHSD2$^{-/-}$ mice than the floxed control mice. As previously demonstrated, NaCl consumption accounted for the majority of fluid intake in the brain 11βHSD2$^{-/-}$ mice. In contrast salt aversion was evident in the floxed 11βHSD2 control mice (Figure 4.11.A).

Spironolactone administration had no effect on water intake in either the floxed control, or brain 11βHSD2$^{-/-}$, mice. NaCl consumption was not altered by MR blockade in the floxed control mice. However, spironolactone substantially reduced NaCl intake in the brain 11βHSD2$^{-/-}$ mice; NaCl consumption was approximately 40% lower following spironolactone (Figure 4.11.B). As shown in Figure 4.12.A the effects of spironolactone on 1.5% NaCl intake in the brain 11βHSD$^{-/-}$ mice were rapid and sustained. Although sprionolactone was administered subcutaneously, it was unlikely that the reduction in NaCl intake was secondary to altered renal sodium handling. Blockade of MR increases natriuresis, which would be postulated to increase salt intake. Indeed following spironolactone administration cumulative sodium balance was not significantly different in the brain 11βHSD2$^{-/-}$ mice and the floxed controls (floxed 11βHSD2 8.3±0.8 vs brain 11βHSD2$^{-/-}$ 10.3±0.8 mmol, $P>0.05$, Mann-Whitney test). These data support the hypothesis that the reduced NaCl intake in the brain 11βHSD2$^{-/-}$ mice following spironolactone was not secondary to altered renal sodium handling.

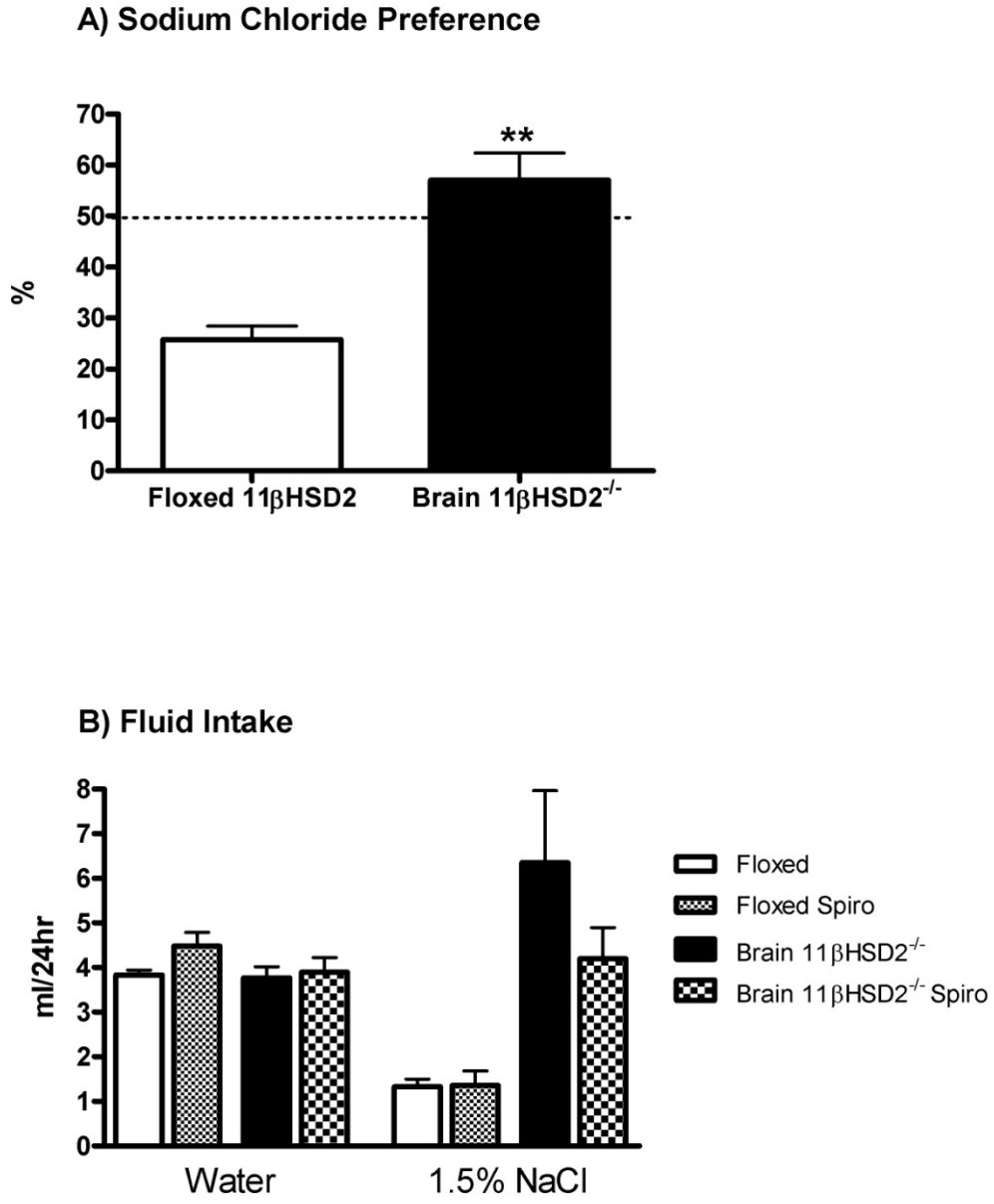

Figure 4.11: 1.5% NaCl Consumption Preference (A) and Fluid Intake (B) in floxed 11βHSD2 mice (white) and brain 11βHSD2$^{-/-}$ mice (black). Hashed bars are the consumption values following spironolactone. Data are means ± S.E.M. Statistical analysis was performed using an unpaired t-test (A) or one way ANOVA (B), **P<0.01.

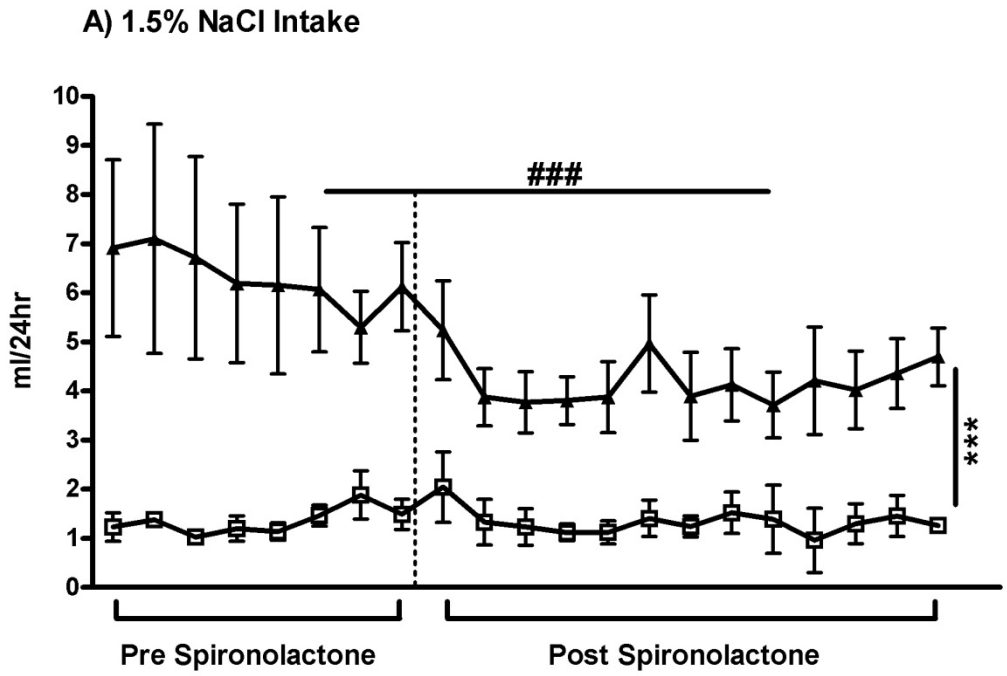

Figure 4.12: 1.5% NaCl consumption in brain 11βHSD2$^{-/-}$ (filled triangles) and floxed 11βHSD2 control mice (open squares). (Pre) values were recorded over 8 days prior to spironolactone and (Post) values over 14 days following spironolactone. The vertical dotted line represents spironolactone mini pellet implantation. Data are presented as means ± S.E.M. Statistical comparisons were made using a one-way ANOVA. ***P<0.001 compared to floxed mice. ###P<0.001 compared to pre-spironolactone.

4.4. Discussion

Global 11βHSD2$^{-/-}$ mice have impaired renal function, with a severe and progressive polyuria which, at older ages, resulted in an attenuated response to water deprivation. Moreover, progressive hypertension and hypokalemia have been described, in line with the clinical characteristics of AME (Kotelevtsev *et al*., 1999, Bailey *et al*., 2008). At >180 days the deranged renal function was associated with acute structural damage at both a gross and tubular level. It was postulated that the phenotype was renal in origin and that the polydipsia was a secondary response to increased urine flow. To resolve this genetically, selective targeting of 11βHSD2 in the kidney and brain was harnessed to permit tissue specific evaluation of 11βHSD2. Moreover, the restricted expression of 11βHSD2 to the NTS in the brains of adult mice (Holmes *et al*., 2006b) provided the unique opportunity to evaluate the role of the enzyme in salt appetite.

Given the distribution of 11βHSD2 in the brain and kidney, organs pivotal in the modulation of salt and water homeostasis, tissue specific targeting circumvents the complexity of dissecting the etiology of the phenotype observed in the global 11βHSD2$^{-/-}$ mice. Within the time frame of this thesis, only KRDKO and brain 11βHSD2$^{-/-}$ mice were available for physiological evaluation. The evaluation of renal specific 11βHSD2$^{-/-}$ mice would provide further validation of the conclusions drawn.

4.4.1. Evaluation of KRDKO mice

Clinically, full or partial loss of 11βHSD2 activity causes AME, a condition in which hypertension is thought to be driven by volume expansion, occurring secondarily to renal sodium retention (Ferrari and Krozowski, 2000). Moreover, AME has been characterised as a continuum disorder (Li *et al*., 1998), with the degree of enzyme impairment directly correlating with the severity of the phenotype. Clinically, blood pressure can be normalised by kidney transplantation (Palermo *et al*., 2000). The observation that blood pressure was reduced, but not normalised, by partial restoration of renal 11βHSD2 activity supports the hypothesis that blood pressure correlates with renal 11βHSD2 activity.

In line with previous observations (Bailey *et al*., 2008) renal sodium excretion was increased, and the natriuretic response to amiloride lost, in the DKO mice aged ~180 days. At this age attenuated trafficking of ENaC to the apical membrane of the collecting duct was proposed to underpin the increased natriuresis (Bailey *et al*., 2008). Partial rescue of 11βHSD2 activity in the kidney did not restore renal sodium handling and hypokalemia was observed in both the DKO and KRDKO mice. Since fraction excretion of potassium was substantially higher in the DKO and KRDKO mice than the ApoE$^{-/-}$ mice, renal potassium wasting likely contributed to the low plasma levels. In accordance with the global 11βHSD2$^{-/-}$ mice, DKO and KRDKO mice were volume contracted; suggesting that at this age hypertension is dissociated from volume expansion. In combination with the observed natriuresis, these data suggest that there may be extra-renal components to the hypertension at this time point. In combination with published data from the heterozygous and global

11βHSD2$^{-/-}$ mice (Kotelevtsev *et al*., 1999, Bailey *et al*., 2008, Bailey *et al*., 2011), these data provide an insight into the threshold of AME as a continuum disorder.

The phenotype observed in KRDKO mice, which have ~30% normal renal 11βHSD2 function, is markedly different to the phenotype previously described in the heterozygous 11βHSD2 mice, which have ~50% renal 11βHSD2 function. During basal conditions 11βHSD2 heterozygous mice were not hypertensive and had plasma potassium and haematocrit values within the normal physiological range (Bailey *et al*., 2011, Kotelevtsev *et al*., 1999). These data suggest that whereas ~50% enzyme activity is sufficient to maintain renal function and blood pressure during basal conditions, ~30% is not.

Although basal renal function is normal, the 11βHSD2 heterozygous mice have a salt sensitive phenotype. Administration of a high salt diet resulted in hypertension, transient volume contraction and hypokalemia, in line with the phenotype observed in the global 11βHSD2$^{-/-}$ mice. The phenotype induced by salt loading was not normalised by spironolactone (Bailey *et al*., 2011). Similarly, the MR antagonist eplerenone had no significant effect on blood pressure in the DKO mice (Deuchar *et al*., 2011). These data suggest the involvement of non-MR mediated mechanisms in the AME phenotype. Notably, the GR receptor antagonist, RU38486, prevented the development hypertension and hypokalemia in the heterozygous mice (Bailey *et al*., 2011), suggesting a role for GR overactivation in the AME phenotype.

The demonstration that the natriuretic capacity of amiloride was lost in the DKO and KRDKO mice at ~180 days suggests a decrease in functional ENaC at this age. This may explain the observation that, although amiloride caused a significant reduction in blood pressure in the DKO mice, it was unable to reduce it to control levels (Deuchar *et al*., 2011). Furthermore, that ENaC mediated sodium retention may not be entirely responsible for the hypertension at this age. Indeed clinically, administration of amiloride does not normalise blood pressure unless given in combination with other drugs (Stewart *et al*., 1988, Knops *et al*., 2011). Moreover the doses required are often high (Cooper and Stewart, 1998), and therefore may also block NHE3 in the proximal tubule (Yun *et al*., 1995, Orlowski, 1993) and thereby contribute to the depressor effects of amiloride. In the DKO mice amiloride was administered chronically, and at a relatively high dose (Deuchar *et al*., 2011). Consequently, off target effects may explain the hypotensive response at an age when the acute natriuretic capacity of amiloride was lost.

Although urine osmolality was significantly lower in the KRDKO and DKO mice than the ApoE$^{-/-}$ mice, urine flow was not different between the three groups when measured under anaesthesia. The absence of polyuria in the DKO and KRDKO mice is in contrast to the observations made in conscious global 11βHSD2$^{-/-}$ mice, in which significantly elevated urine flow was documented. This apparent disparity may be attributable to the effects of anaesthesia on renal function (Dudley *et al*., 1954, Maddox *et al*., 1977). In humans anaesthesia and surgery are associated with antidiuresis, moreover antidiuretic effects of inactin have been reported experimentally (Giri and Peoples, 1965). That the absence of polyuria was the result

of anaesthesia is corroborated by preliminary metabolic cage data from the DKO, KRDKO and ApoE-/- mice. These data demonstrated that the DKO mice were polyuric and polydipsic. Deranged water handling prevailed in KRDKO mice, although the absolute water turnover was reduced compared to the DKO mice (Table 4.4. Data courtesy of Dr Yuri Kotelevtsev). This suggests that partial restoration of renal 11βHSD2 activity is able to reduce, but not normalise, the increased water turnover in the DKO mice.

	ApoE$^{-/-}$	**DKO**	**KRDKO**
Urine Flow (ml/24hr)	2.6±0.2	16.5±2.1***	12.7±1.5***
Water Intake (ml/24hr)	4.6±0.4	20.8±2.0***	16.6±1.6***

Table 4.4:. Basal water handling in ApoE$^{-/-}$, DKO and KRDKO mice. Data are presented as means ± S.E.M. ***P<0.001 compared to ApoE$^{-/-}$ mice. (n=4-6)

A confounding factor when evaluating the DKO, and potentially KRDKO mice, is the extensive atherosclerosis observed at this age. Although renal artery stenosis has not been characterised in the model, the possibility that lesions within the renal artery impede blood flow and induce renal failure should be considered. Although, the close correlation with the phenotype observed in the global 11βHSD2$^{-/-}$ mice supports a pivotal role for renal enzyme function in blood pressure regulation and water homeostasis.

4.4.2. Evaluation of brain 11βHSD2$^{-/-}$ mice

4.4.2.1. Renal function was not impaired by the deletion of 11βHSD2 in the brain

Mean arterial blood pressure was not significantly different between brain 11βHSD2$^{-/-}$ mice and the floxed controls. Although in combination with the results from KRDKO mice these data support the hypothesis that hypertension is driven by the kidney, this conclusion must be treated with caution. It may be that loss of 11βHSD2 function in the NTS has a more predominant role when blood pressure is perturbed, or in situations of stress and/or physiological challenges. In agreement with this hypothesis, glucocorticoid administration to the dorsal hindbrain (the region containing the NTS) of Sprague-Dawley rats resulted in an augmented blood pressure response to a novel restraint stress test. The same effect was not observed following systemic glucocorticoid administration (Scheuer *et al*., 2007). Additionally, in borderline hypertensive rats, (which have an increased endogenous stress response), blockade of GR in the dorsal hindbrain reduced the hypertensive response to restraint. GR blockade had no effect on the blood pressure response on control rats (Bechtold et al., 2009). Therefore, it is postulated that although basal blood pressure was not altered by deletion of 11βHSD2 in the NTS, the response to blood pressure challenges may be impaired in the brain 11βHSD2$^{-/-}$ mice.

Baseline water and electrolyte handling were not altered by the selective deletion of 11βHSD in the brain; renal function and haematocrit values were all similar to the

floxed control mice. Similarly, the brain 11βHSD2$^{-/-}$ mice also had a functional response to water deprivation.

Previous attempts to resolve the respective roles of MR and 11βHSD2 in the brain and kidney have evaluated the effects of s.c. and i.c.v. drug delivery. Accordingly, whereas subcutaneous aldosterone induced polyuria in unilaterally nephrectomised rats; i.c.v. delivery had no effect (Gomez-Sanchez, 1986). Similar results have been obtained using carbenoxolone to inhibit 11βHSD2 (Gomez-Sanchez and Gomez-Sanchez, 1992). However, these studies are limited by the non-selective nature of carbenoxolone (Hult *et al*., 1998) and the spill over effects of i.c.v. and s.c. drug delivery. The use of cre-lox technology to selectively delete 11βHSD2 permits a more accurate evaluation of the role of the enzyme than enabled by the global 11βHSD2$^{-/-}$ mice, or the use of s.c. and i.c.v. inhibitor administration. The studies described, in combination with the preliminary data from KRDKO mice, support the hypothesis that the altered water turnover observed in the global 11βHSD2$^{-/-}$ mice is of renal origin.

4.4.2.2. Deletion of 11βHSD2 in the brain resulted in an increased salt appetite

Despite strong circumstantial evidence (Cooney and Fitzsimons, 1996, Geerling *et al*., 2006a), the role of 11βHSD2 in salt appetite is yet to be confirmed. The investigations described in this chapter demonstrated that salt appetite was augmented in the brain 11βHSD2$^{-/-}$ mice. Furthermore, the brain 11βHSD2$^{-/-}$ mice

preferred to drink 1.5% NaCl to water, with saline accounting for ~70% of their total fluid intake. Therefore, the loss of 11βHSD2 function in the brain, specifically the NTS, caused increased sodium intake. Typically salt appetite is driven by sodium depletion and the resultant volume contraction (Geerling and Loewy, 2008). However, since basal renal sodium handling and plasma sodium concentrations were normal in the brain 11βHSD2$^{-/-}$ mice there was no physiological drive for the increased salt intake and it was not retained chronically. These data are the first demonstration of salt appetite occurring in the absence of sodium depletion and with normal renal function.

Since the maintenance of extracellular fluid status is essential for survival the drive to consume sodium during deficiency is highly motivated. Recent data suggest that sodium intake can activate central reward pathways terminating in the nucleus accumbens (Voorhies and Bernstein, 2006), a region of the brain implicated in addictive behaviour. The activation of such reward pathways may underpin the augmented salt intake in the brain 11βHSD2$^{-/-}$ mice.

Interestingly, in salt deprived rats fitted with a gastric fistula to prevent sodium reabsorption, sodium intake activated neurons in the nucleus acccumbens. Since the beneficial effects of sodium intake were prevented in this model, it was postulated that nucleus accumbens activation is involved in motivation to seek and ingest salt during sodium depletion. Indeed, increased Fos-immuoreactivity in the nucleus accumbens was not found in sodium deprived rats without a gastric fistula. In these

rats ingestion of sodium resulted in the normalisation of plasma sodium levels; consequently, the continued drive to consume salt was not necessary (Voorhies and Bernstein, 2006). Dopaminergic pathways, which project to the nucleus accumbens, are central in the rewarding and reinforcing effects of drug abuse (Koob, 1992). These data raise the possibility that common neuropathways drive the motivation to seek salt. In accord with this, repeated sodium deprivation and repletion induced morphological changes in the nucleus accumbens (Roitman *et al*., 2002), similar to the effects observed following repeated cocaine administration (Robinson *et al*., 2001). Such morphological changes are involved in sensitization, the increased response to a stimulus following its repeated administration. Indeed, prior sodium deprivation challenges have been shown to increase salt appetite (Sakai *et al*., 1987, Sakai *et al*., 1989) and need free sodium consumption (Sakai *et al*., 1989) in rats. Sensitization to salt raises the possibility of salt addiction. Microarray analysis demonstrated that many of the genes enriched in drug addiction models were also increased by sodium depletion and the resultant salt appetite. Notably, dopaminergic pathways were implicated in both salt appetite and drug addiction. The physiological relevance of this finding was illustrated by the demonstration that dopamine receptor-1 antagonism selectively reduced salt intake in deplete rats (Liedtke *et al*., 2011). The demonstration that mutisynaptic pathways project from the NTS to the nucleus accumbens (Shekhtman *et al*., 2007) add further support to the hypothesis that during salt appetite, NTS mediated activation of the nucleus accumbens is involved in the motivation to consume salt.

4.4.2.3. Activation of MR contributes to the increased salt appetite in brain 11βHSD2$^{-/-}$ mice

The antagonism of MR resulted in an approximately 40% reduction in sodium intake in the brain 11βHSD2$^{-/-}$ mice. These results were specific for salt appetite since spironolactone had no effect on water intake in either group of mice, or on NaCl consumption in the floxed 11βHSD2 control mice. These data suggested that the increased salt appetite was partly driven by the loss 11βHSD2 protection of MR in NTS.

MR has been previously implicated in the drive to consume sodium. Following coronary artery ligation, to induce chronic heart failure, rats developed an increased salt appetite. Salt consumption was attenuated by the administration of spironolactone, suggesting that the increased appetite was partly driven by the over-activation of MR (Francis *et al*., 2001). These data may help explain the clinical observation that the concurrent administration of spironolactone with ACE inhibitors reduced the risk of death in severe heart failure patients (Pitt *et al*., 1999). The mechanism by which spironolactone attenuated mortality was not determined, but it is possible that a reduced salt appetite contributed to its beneficial effects.

In the brain 11βHSD2$^{-/-}$ mice spironolactone administration was unable to normalise NaCl consumption. This may have been due to incomplete MR blockade in the NTS since the spironolactone was administered s.c. The i.c.v. administration spironolactone may increase its effects on salt appetite. Conversely, it is possible

that other factors contribute to the increased sodium intake. Glucocorticoids have been shown to increase sodium intake in adrenalectomized rats (Kenyon *et al*., 1984a). Therefore, it is possible that the loss of 11βHSD2 function resulted in the overactivation of GR, which are also expressed in the NTS (Harfstrand *et al*., 1986).

4.4.2.4. The use of cre-lox technology to target 11βHSD2 in the NTS

In the studies detailed the nestin promoter was used to drive cre-recombinase expression. Since nestin is a neural stem cell marker, recombination is postulated to occur in the central nervous system, predominantly throughout neurogenesis. This is illustrated in the X-gal staining, which is widespread in the brain. Consequently, 11βHSD2 was deleted in the brain throughout prenatal development. During embryogenesis 11βHSD2 has a wide spread distribution, which restricts postnatally (Diaz *et al*., 1998, Holmes *et al*., 2006b). It is possible therefore, that the increased salt appetite might reflect prenatally programmed changes in the brain rather than adult deletion of 11βHSD2 in the NTS. Programmed changes in MR and GR within the brain have been observed in models of prenatal glucocorticoid overexposure, such as prenatal dexamethasone (Welberg *et al*., 2001) or carbenoxolone (Welberg *et al*., 2000) treated rats, however, such changes in receptor expression were not observed in the brains of global 11βHSD2$^{-/-}$ mice (Holmes *et al*., 2006a). In this context, MR and GR expression in the NTS would be of particular relevance.

In addition, overexposure to glucocorticoids can have detrimental effects on the development of the brain. Development of the cerebellum, which continues

postnatally, was attenuated in 11βHSD2$^{-/-}$ mice (Holmes *et al*., 2006b). Cerebellum size was reduced in the null mice, which correlated with an impaired ability to perform the behavioural tests used to assess neurodevelopment. It is therefore possible that the increased salt appetite observed in the brain 11βHSD2$^{-/-}$ mice resulted from altered neurodevelopment rather than the loss of 11βHSD2 function in the NTS. To evaluate this further, a temporally inducible cre could be used, such as a tamoxifen-dependent cre recombinase. This would enable the activation of cre recombinase in adult mice (for discussion of the technique see (Feil et al., 1996). This would not only ensure specific deletion of 11βHSD2 in the NTS, but it would also eliminate the confounding effects of altered neurodevelopment.

Enzyme activity analysis demonstrated that 11βHSD2 activity was reduced by ~75% in the foetal brain at E13.5. Therefore the data from the adult mice should be interpreted in the context that the activity of 11βHSD2 in the NTS was substantially reduced, rather than entirely eliminated. Nestin driven recombination has also been characterised systemically, notably in the murine kidney at E15.5 (Dubois *et al*., 2006). This raises the possibility of renal targeting of 11βHSD2 in the brain 11βHSD2$^{-/-}$ mice. However, in view of the normal enzyme activity, and the absence of X-gal staining in the adult kidney, it is unlikely that a significant loss of renal 11βHSD2 function occurred in the model.

Chapter 5: Conclusions and Perspectives

The studies detailed in this thesis evaluated the role of 11βHSD2 in the regulation of salt and water homeostasis. The novel findings were:

1. 11βHSD2$^{-/-}$ mice develop a severe and progressive nephrogenic diabetes insipidus like phenotype, characterized by polyuria, polydipsia and natriuresis. The increased urine flow is renal in origin, driven by an impaired renal response to vasopressin stimulation. As in other models of glucocorticoid excess, an impaired medullary concentration of urea also contributes to the polyuria.
2. In >180 day 11βHSD2$^{-/-}$ mice the exacerbated polyuria is associated with severe renal injury. The medullary atrophy observed at this age results in decreased NKCC2 mRNA abundance. Therefore, the loss of the cortico-medullary gradient augments the phenotype at this age.
3. Mice in which 11βHSD2 has been specifically targeted in the brain have normal water handling and kidney function, confirming a renal origin to the polyuria in the global null mice
4. Mice in which 11βHSD2 has been specifically targeted in the brain have an increased salt appetite. Blockade of MR significantly and selectively reduced NaCl intake. Since 11βHSD2 is exquisitely expressed in the NTS in adult mice these data implicate over-activation of MR on 11βHSD2 positive neurons in the NTS in salt appetite

In this chapter these findings will be discussed in wider context of the AME and their potential clinical implications.

5.1: Loss of 11βHSD2 in the NTS causes increased salt appetite

The demonstration of increased salt appetite driven by the selective targeting of 11βHSD2 in the NTS is novel and potentially, has wide clinical implications. Increased salt appetite has deleterious effects on the progression of many clinical conditions, including hypertension, congestive heart failure and chronic kidney disease (Strazzullo *et al*., 2009, Sanders, 2004). In ~15% of hypertensive individuals increased aldosterone is implicated in the progression of the disease (Freel and Connell, 2004). Based on the data presented in this thesis, it is likely that aldosterone excess, perceived or actual, accelerates hypertension through two mechanisms: by reducing the ability of the kidney to excrete sodium and by increasing the behavioural drive to consume sodium. This may help explain the notoriously poor compliance to low sodium diets in patients with hypertension (Ohta *et al*., 2004, Luft *et al*., 1997). It could be that the patients who would benefit most from a low salt diet have the highest innate salt appetite. Chronic heart failure is another condition in which the consumption of a low sodium diet is recommended (Hunt *et al*., 2005). Notably, the RALES trial demonstrated that the administration of spironolactone resulted in a 30% reduction in the risk of death from all cardiac causes (Pitt *et al*., 1999). The mechanism by which spironolactone reduced mortality was not determined, however in the context of the data presented here it is possible that a reduced salt appetite was contributory to its salubrious effects. In support of this hypothesis is the demonstration that spironolactone reduced salt appetite in the rat model of congestive heart failure (Francis *et al*., 2001).

5.2: Nephrogenic diabetes insipidus like phenotype in 11βHSD2$^{-/-}$ mice

A key finding from the current studies is the nephrogenic diabetes inspidus like phenotype in the 11βHSD2$^{-/-}$ mice. In the null mice the increased water turnover was postulated to be the result of reduced AQP2 abundance, which may have been secondary to a renal insensitivity to AVP stimulation. At >180 days exacerbated polyuria was associated with extensive medullary atrophy. Although the overarching cause of the phenotype was not determined, it is postulated that hypokalemia has a central role.

A cardinal feature of AME, and the 11βHSD2$^{-/-}$ mice, is hypokalemia (Bailey *et al*., 2008, Kotelevtsev *et al*., 1999, Ferrari, 2010). Indeed much of the phenotype described in the null mice can be attributed to low plasma potassium. As discussed in section 3.4.1.1 the administration of a low potassium diet to rats resulted in the development of polyuria and polydipsia. The increased water turnover was the result of reduced AQP2 abundance, in accordance with the phenotype observed in the 11βHSD2$^{-/-}$ mice. The restoration of plasma potassium resulted in the normalisation of urine flow in the hypokalemic rats (Marples *et al*., 1996). Low plasma potassium is also associated with renal injury, with the induction of hypokalemia resulting in tubular dilation, hypertrophy, hyperplasia and local inflammation in rats (Suga *et al*., 2001, Reungjui *et al*., 2008). Renal injury was most pronounced within the medulla, possibly driven by reduced renal oxygenation. Indeed, since pertitubular capillary loss correlated with the extent of hypokalemia impaired angiogenesis and local hypoxia were implicated in the nephropathy (Reungjui *et al*., 2008, Suga *et al*., 2001). It is possible therefore, that hypokalemia induced hypoxia contributed to the

development medullary atrophy in the >180 day 11βHSD2$^{-/-}$ mice. Notably, in humans, low plasma potassium alone may not be sufficient to induce nephropathy. Severe hypokalemia occurs in both Gitelman's and Barrter's syndromes, however, only in the latter is impaired renal function observed (Walsh *et al*., 2011). Consequently, it was postulated that clinically "hypokalemic nephropathy" may be dependent on hyperaldosteronism. Whether hypokalemia, and the perceived hyperaldosteronism, result in nephropathy in AME has not been extensively studied.

Finally, plasma potassium is receiving increasing attention as a key determinant of blood pressure, with low potassium diets implicated in the development of hypertension (Adrogue and Madias, 2007). Moreover, there is clinical evidence that potassium supplementation can reduce blood pressure in both normotensive and hypertensive subjects (Braschi and Naismith, 2008, Geleijnse *et al*., 2003). The mechanisms underlying potassium's beneficial effects are undetermined, however the demonstration that potassium reduces vascular endothelium stiffness and induces nitric oxide release suggests that increased vascular compliance may be contributory (Oberleithner *et al*., 2009). In the context of these data, whether the normalisation of plasma potassium would rescue the phenotype in the 11βHSD2$^{-/-}$ mice is of interest.

In view of their hypokalemia, it is surprising that urinary potassium excretion was not significantly lower in the 11βHSD2$^{-/-}$ mice than aged-matched controls, and indeed suggests that renal losses may contribute to the potassium depletion. There are two possible causes for renal potassium loss, which are not mutually exclusive:

impaired reabsorption and increased secretion. The cause for the relatively high potassium excretion in 11βHSD2$^{-/-}$ mice is undetermined.

Potassium is reabsorbed in the proximal tubule and thick ascending limb, and secreted in the ASDN. The demonstration that NKCC2 mRNA abundance was not significantly different in 11βHSD2$^{-/-}$ and C57Bl/6 mice at <100 days suggests that impaired potassium reabsorption in the thick ascending limb was not causative, at least at this age. This implicates increased potassium secretion in the phenotype. In Type II Bartter's syndrome the persistent kaliuresis, in the face of severe hypokalemia, is attributed to increased BK mediated potassium secretion in the distal nephron (Bailey *et al*., 2006). Notably, the calcium-dependent, BK-mediated potassium secretion is stimulated by increased flow rates (Liu *et al*., 2007). Therefore, it is postulated that in the 11βHSD2$^{-/-}$ mice the sustained hypokalemia and normal potassium excretion may be due to flow stimulated potassium secretion in the distal nephron. Hypertrophy and hyperplasia have been reported in the distal convoluted tubules of 11βHSD2$^{-/-}$ mice (Bailey *et al*., 2008): whether the structural changes are associated with altered function, namely potassium handling, is therefore of interest. The paradox of this hypothesis is that hypokalemia is postulated to be involved in the initiation of polyuria, which itself, through the stimulation of BK, may augment renal potassium losses. In view of the complexity of the phenotype, the evaluation of isolated perfused tubules from 11βHSD2$^{-/-}$ mice would help dissect the function of renal potassium handling in the model.

5.3: Central and renal components to the phenotype in 11βHSD2$^{-/-}$ mice

Severe polyuria and natriuresis were observed in the 11βHSD2$^{-/-}$ mice at <100 and >180 days. In view of the sustained hypertension reported in the model (Bailey *et al*., 2008, Kotelevtsev *et al*., 1999), these data suggest that mechanisms other than sodium and water retention are involved in the maintenance of the elevated blood pressure

Indirect evidence of increased sympathetic nerve activity has been documented in the 11βHSD2$^{-/-}$ mice. Urinary catecholamine excretion was approximately doubled in the null mice, and α_1-adrenoreceptor antagonism normalised blood pressure (Bailey *et al*., 2008). Consequently, sympathetic overdrive was implicated in the hypertension. As reviewed (Grassi, 2009) sympathetic overdrive is a key component of hypertension. Evaluation of neuroadrenergic function in hypertensive patients has demonstrated the association between increased sympathetic nerve activity and augmented blood pressure. Moreover, the degree of hypertension has been shown to directly correlate with the extent of sympathetic nerve activity, supporting a cause/effect relationship between the two factors (Grassi, 2009, Grassi *et al*., 1998). Whether sympathetic overdrive is a component of both essential and secondary hypertension is contentious. Although sympathetic overdrive has been consistently documented in essential hypertension, it has not been robustly demonstrated in secondary forms (Grassi, 2009, Grassi *et al*., 1998). Despite this, anti-adrenergics have been shown to reduce blood pressure in AME, in situations where MR blockade and cortisol suppression were not effective (Morineau *et al*., 2006). Clearly, the kidneys have a pivotal role in the control of blood pressure, however, it has recently

been postulated that there is a centrally determined set point which is implicated in its long term regulation. Since the NTS receives afferent inputs from both arterial chemoreceptors and baroreceptors it is proposed to be a central site of blood pressure regulation (Zanutto *et al*., 2010).

Increased blood pressure causes the activation of baroreceptors located in the aortic arch and carotid sinuses. Afferents from these regions project to the NTS, which though activation of GABAergic neurons in the *caudal ventrolateral medulla* (CVLM), cause the inhibition of the sympathetic premoter neurons in the *rostral ventrolateral medulla* (RVLM) that promote vasoconstriction (Schreihofer and Guyenet, 2002). Therefore, NTS mediated activation of this sympathoinhibitory pathway results in a depressor response. Accordingly, bilateral carotid occlusions to induce hypertension have been shown to result in reduced adrenaline and noradrenaline release from the rostral NTS (Philippu *et al*., 1991). Similarly, noradrenaline infusion to induce blood pressure increases resulted in reduced adrenaline release from the NTS (Singewald *et al*., 1992). These data suggest that in response to increased blood pressure, the NTS mediates a reduction in sympathetic nerve activity, in an attempt to normalise blood pressure. In contrast chemoreceptors located in the carotid and aortic bodies respond to reductions in blood pressure. Afferents from these regions also project to the NTS. In this instance it is proposed that afferents from the commissural NTS project to the RVLM and activate the vasoconstrictor sympathetic premoter neurons, therefore eliciting a pressor response. In line with this hypothesis, inhibition of neurons within the commissural NTS resulted in reduced sympathetic nerve activity and subsequently arterial blood

pressure in SHR rats (Koshiya and Guyenet, 1996, Sato *et al*., 2002). Together these data support the hypothesis that the NTS is a site of integration, responding to, and counteracting peripherally detected changes in blood pressure.

In view of the increased urinary catecholamine excretion in the 11βHSD2$^{-/-}$ mice (Bailey *et al*., 2008), it is postulated that the loss of 11βHSD2 in the NTS results in an inappropriate sympathetic response to augmented blood pressure. In this context the following hypotheses are proposed: in the 11βHSD2$^{-/-}$ mice hypertension is primarily renal in origin, driven by the increased retention of sodium and water, occurring at time points prior to those investigated. The loss of 11βHSD2 function in the NTS results in an impaired countervailing response to the initial blood pressure increase, such that an augmented centrally determined set point is established. Subsequently, inappropriate NTS driven sympathetic output and the resultant vasoconstriction may promote the maintenance of the hypertension. This would explain the acute hypotensive response to α_1-adrenoreceptor blockade in the 11βHSD2$^{-/-}$ mice (Bailey *et al*., 2008). At <100 days, polyuria and natriuresis may be a renal compensatory response to the increased blood pressure, in line with the Guytonian hypothesis (Figure 5.1). Whether renal sympathetic nerve activity is augmented in the 11βHSD2$^{-/-}$ mice is of interest, in view of the fact that increased activity would promote renal sodium and water retention (DiBona, 2000). By >180 days the augmented water turnover is associated with severe renal damage, which no doubt contributes to the exacerbation of polyuria at this age. Given that the NTS is implicated in the response to blood pressure perturbations this could explain the

normal blood pressure in the brain 11βHSD2$^{-/-}$ mice, in which there is no renal insufficiency.

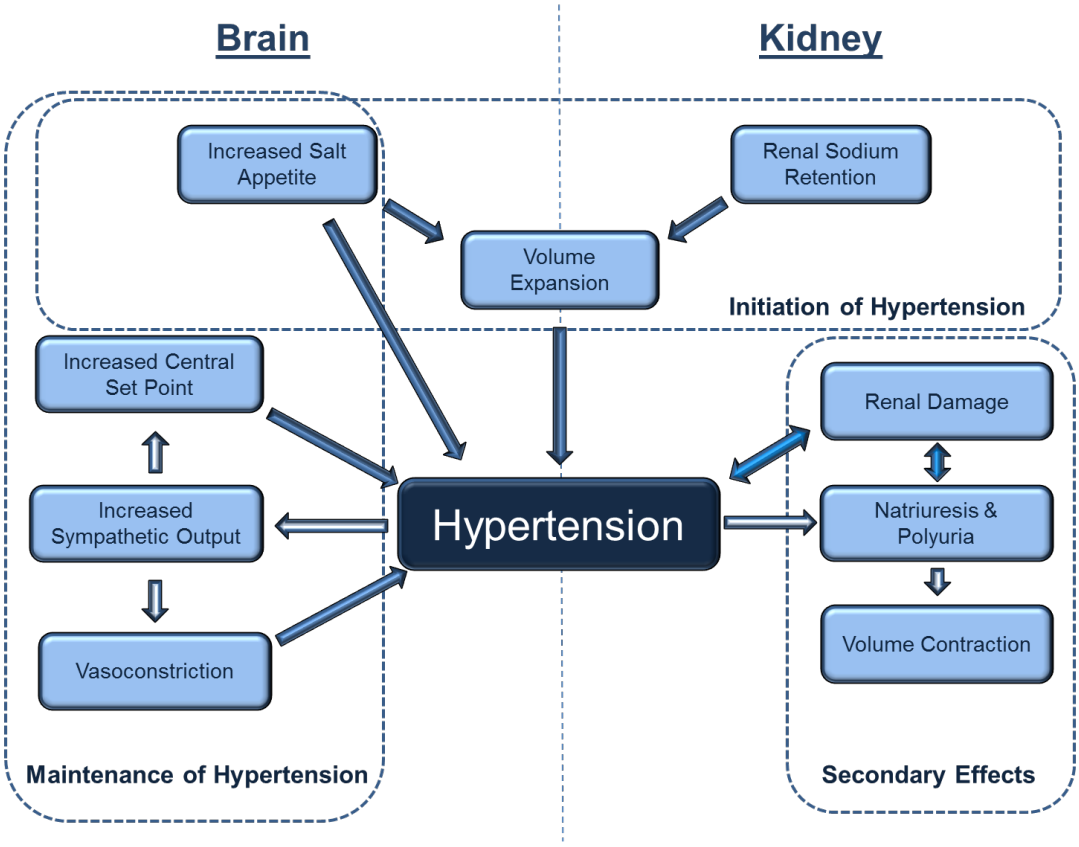

Figure 5.1: Proposed mechanism of hypertension in 11βHSD2$^{-/-}$ mice

Although basal blood pressure was not altered by the deletion of 11βHSD2 in the NTS, these data must be considered in the context of the increased salt appetite, and the impaired renal sodium handling, driven by the loss of 11βHSD2 in the brain and kidney respectively. During augmented sodium intake, the brain 11βHSD2$^{-/-}$ mice were able to remain in a normal balance because of their ability to excrete the

increased levels of sodium. In line with the Guytonian view of blood pressure regulation, this prevented the development of hypertension. However, the long term consequences of the increased salt intake are unknown. Chronic studies in chimpanzees have demonstrated that the prolonged consumption of a high salt diet resulted in increased blood pressure (Denton *et al*., 1995). These data provide a link between increased salt appetite/intake and the development of hypertension. Moreover, in the global 11βHSD2$^{-/-}$ mice renal sodium handling is impaired. This suggests that in the 11βHSD2$^{-/-}$ mice, the renal ability to handle the increased sodium intake would be diminished: which in turn could exacerbate the observed hypertension. In this context the effect of an increased salt appetite on blood pressure in the global 11βHSD2$^{-/-}$ mice is of interest. Additionally, in view of the role of the NTS in the modulation of blood pressure, it is likely that the loss of 11βHSD2 in this region would result in an impaired central regulatory response to such a challenge. In line with these hypotheses is the demonstration that blood pressure was exacerbated by a high salt appetite in a patient with a partial loss of 11βHSD2 function (Ingram *et al*., 1996). Therefore, the tissue specific targeting of 11βHSD2 in the kidney and brain can provide valuable insights into the complexity of the phenotype observed in the global 11βHSD2$^{-/-}$ mice and patients with AME.

References

ACKERMANN, D., GRESKO, N., CARREL, M., LOFFING-CUENI, D., HABERMEHL, D., GOMEZ-SANCHEZ, C., ROSSIER, B. C. & LOFFING, J. (2010) In vivo nuclear translocation of mineralocorticoid and glucocorticoid receptors in rat kidney: differential effect of corticosteroids along the distal tubule. *Am J Physiol Renal Physiol,* 299**,** F1473-85.

ADACHI, S., UCHIDA, S., ITO, H., HATA, M., HIROE, M., MARUMO, F. & SASAKI, S. (1994) Two isoforms of a chloride channel predominantly expressed in thick ascending limb of Henle's loop and collecting ducts of rat kidney. *J Biol Chem,* 269**,** 17677-83.

ADROGUE, H. J. & MADIAS, N. E. (2007) Sodium and potassium in the pathogenesis of hypertension. *N Engl J Med,* 356**,** 1966-78.

AGARWAL, A. K., ROGERSON, F. M., MUNE, T. & WHITE, P. C. (1995) Gene structure and chromosomal localization of the human HSD11K gene encoding the kidney (type 2) isozyme of 11 beta-hydroxysteroid dehydrogenase. *Genomics,* 29**,** 195-9.

AGUS, Z. S. & GOLDBERG, M. (1971) Role of antidiuretic hormone in the abnormal water diuresis of anterior hypopituitarism in man. *J Clin Invest,* 50**,** 1478-89.

AL-DUJAILI, E. A., MULLINS, L. J., BAILEY, M. A. & KENYON, C. J. (2009) Development of a highly sensitive ELISA for aldosterone in mouse urine: validation in physiological and pathophysiological states of aldosterone excess and depletion. *Steroids,* 74**,** 456-62.

ALBISTON, A. L., OBEYESEKERE, V. R., SMITH, R. E. & KROZOWSKI, Z. S. (1994) Cloning and tissue distribution of the human 11 beta-hydroxysteroid dehydrogenase type 2 enzyme. *Mol Cell Endocrinol,* 105**,** R11-7.

AMLAL, H., KRANE, C. M., CHEN, Q. & SOLEIMANI, M. (2000) Early polyuria and urinary concentrating defect in potassium deprivation. *Am J Physiol Renal Physiol,* 279**,** F655-63.

AMORIM, J. B., BAILEY, M. A., MUSA-AZIZ, R., GIEBISCH, G. & MALNIC, G. (2003) Role of luminal anion and pH in distal tubule potassium secretion. *Am J Physiol Renal Physiol,* 284**,** F381-8.

ARMOUR, D. L. (2010) Role of 11β-hydroxysteroid dehydrogenase type 2 in protection against inflammation during atherogenesis: studies in the Apoe-/-/11βHSD2-/- double knockout mouse., The University of Edinburgh.

ARRIZA, J. L., WEINBERGER, C., CERELLI, G., GLASER, T. M., HANDELIN, B. L., HOUSMAN, D. E. & EVANS, R. M. (1987) Cloning of human

mineralocorticoid receptor complementary DNA: structural and functional kinship with the glucocorticoid receptor. *Science,* 237**,** 268-75.

BAILEY, M. A., CANTONE, A., YAN, Q., MACGREGOR, G. G., LENG, Q., AMORIM, J. B., WANG, T., HEBERT, S. C., GIEBISCH, G. & MALNIC, G. (2006) Maxi-K channels contribute to urinary potassium excretion in the ROMK-deficient mouse model of Type II Bartter's syndrome and in adaptation to a high-K diet. *Kidney Int,* 70**,** 51-9.

BAILEY, M. A., CRAIGIE, E., LIVINGSTONE, D. E., KOTELEVTSEV, Y. V., AL-DUJAILI, E. A., KENYON, C. J. & MULLINS, J. J. (2011) Hsd11b2 haploinsufficiency in mice causes salt sensitivity of blood pressure. *Hypertension,* 57**,** 515-20.

BAILEY, M. A., MULLINS, J. J. & KENYON, C. J. (2009) Mineralocorticoid and glucocorticoid receptors stimulate epithelial sodium channel activity in a mouse model of Cushing syndrome. *Hypertension,* 54**,** 890-6.

BAILEY, M. A., PATERSON, J. M., HADOKE, P. W., WROBEL, N., BELLAMY, C. O., BROWNSTEIN, D. G., SECKL, J. R. & MULLINS, J. J. (2008) A switch in the mechanism of hypertension in the syndrome of apparent mineralocorticoid excess. *J Am Soc Nephrol,* 19**,** 47-58.

BALL, S. G. (2007) Vasopressin and disorders of water balance: the physiology and pathophysiology of vasopressin. *Ann Clin Biochem,* 44**,** 417-31.

BECHTOLD, A. G., PATEL, G., HOCHHAUS, G. & SCHEUER, D. A. (2009) Chronic blockade of hindbrain glucocorticoid receptors reduces blood pressure responses to novel stress and attenuates adaptation to repeated stress. *Am J Physiol Regul Integr Comp Physiol,* 296**,** R1445-54.

BECKER, A. M., ZHANG, J., GOYAL, S., DWARAKANATH, V., ARONSON, P. S., MOE, O. W. & BAUM, M. (2007) Ontogeny of NHE8 in the rat proximal tubule. *Am J Physiol Renal Physiol,* 293**,** F255-61.

BERG, J. M., TYMOCZKO, J. L. & STRYER, L. (2002) *Biochemistry,* New York, W.H. Freeman.

BERGER, S., BLEICH, M., SCHMID, W., COLE, T. J., PETERS, J., WATANABE, H., KRIZ, W., WARTH, R., GREGER, R. & SCHUTZ, G. (1998) Mineralocorticoid receptor knockout mice: pathophysiology of Na+ metabolism. *Proc Natl Acad Sci U S A,* 95**,** 9424-9.

BERL, T., LINAS, S. L., AISENBREY, G. A. & ANDERSON, R. J. (1977) On the mechanism of polyuria in potassium depletion. The role of polydipsia. *J Clin Invest,* 60**,** 620-5.

BHARGAVA, A., FULLERTON, M. J., MYLES, K., PURDY, T. M., FUNDER, J. W., PEARCE, D. & COLE, T. J. (2001) The serum- and glucocorticoid-

induced kinase is a physiological mediator of aldosterone action. *Endocrinology,* 142**,** 1587-94.

BIBER, J., CUSTER, M., MAGAGNIN, S., HAYES, G., WERNER, A., LOTSCHER, M., KAISSLING, B. & MURER, H. (1996) Renal Na/Pi-cotransporters. *Kidney Int,* 49**,** 981-5.

BICHET, D. G. (1996) Vasopressin receptors in health and disease. *Kidney Int,* 49**,** 1706-11.

BIEWENGA, W. J., RIJNBERK, A. & MOL, J. A. (1991) Osmoregulation of systemic vasopressin release during long-term glucocorticoid excess: a study in dogs with hyperadrenocorticism. *Acta Endocrinol (Copenh),* 124**,** 583-8.

BONGARTZ, L. G., CRAMER, M. J., DOEVENDANS, P. A., JOLES, J. A. & BRAAM, B. (2005) The severe cardiorenal syndrome: 'Guyton revisited'. *Eur Heart J,* 26**,** 11-7.

BONVALET, J. P., DOIGNON, I., BLOT-CHABAUD, M., PRADELLES, P. & FARMAN, N. (1990) Distribution of 11 beta-hydroxysteroid dehydrogenase along the rabbit nephron. *J Clin Invest,* 86**,** 832-7.

BOONE, M. & DEEN, P. M. (2008) Physiology and pathophysiology of the vasopressin-regulated renal water reabsorption. *Pflugers Arch,* 456**,** 1005-24.

BOSCAN, P., PICKERING, A. E. & PATON, J. F. (2002) The nucleus of the solitary tract: an integrating station for nociceptive and cardiorespiratory afferents. *Exp Physiol,* 87**,** 259-66.

BOSTANJOGLO, M., REEVES, W. B., REILLY, R. F., VELAZQUEZ, H., ROBERTSON, N., LITWACK, G., MORSING, P., DORUP, J., BACHMANN, S. & ELLISON, D. H. (1998) 11Beta-hydroxysteroid dehydrogenase, mineralocorticoid receptor, and thiazide-sensitive Na-Cl cotransporter expression by distal tubules. *J Am Soc Nephrol,* 9**,** 1347-58.

BOURDEAU, J. E. & BURG, M. B. (1979) Voltage dependence of calcium transport in the thick ascending limb of Henle's loop. *Am J Physiol,* 236**,** F357-64.

BOURQUE, C. W. (2008) Central mechanisms of osmosensation and systemic osmoregulation. *Nat Rev Neurosci,* 9**,** 519-31.

BOYKIN, J., DETORRENTE, A., ERICKSON, A., ROBERTSON, G. & SCHRIER, R. W. (1978) Role of plasma vasopressin in impaired water excretion of glucocorticoid deficiency. *J Clin Invest,* 62**,** 738-44.

BRASCHI, A. & NAISMITH, D. J. (2008) The effect of a dietary supplement of potassium chloride or potassium citrate on blood pressure in predominantly normotensive volunteers. *Br J Nutr,* 99**,** 1284-92.

BRENNER, B. M. & RECTOR, F. C. (2004) Brenner & Rector's the kidney. 7th ed. Philadelphia, PA, Saunders.

BRIMBLE, M. J. & DYBALL, R. E. (1977) Characterization of the responses of oxytocin- and vasopressin-secreting neurones in the supraoptic nucleus to osmotic stimulation. *J Physiol,* 271**,** 253-71.

BROWN, R. W., DIAZ, R., ROBSON, A. C., KOTELEVTSEV, Y. V., MULLINS, J. J., KAUFMAN, M. H. & SECKL, J. R. (1996) The ontogeny of 11 beta-hydroxysteroid dehydrogenase type 2 and mineralocorticoid receptor gene expression reveal intricate control of glucocorticoid action in development. *Endocrinology,* 137**,** 794-7.

BUJALSKA, I., SHIMOJO, M., HOWIE, A. & STEWART, P. M. (1997) Human 11 beta-hydroxysteroid dehydrogenase: studies on the stably transfected isoforms and localization of the type 2 isozyme within renal tissue. *Steroids,* 62**,** 77-82.

BURG, M., STONER, L., CARDINAL, J. & GREEN, N. (1973) Furosemide effect on isolated perfused tubules. *Am J Physiol,* 225**,** 119-24.

BURG, M. B. (1982) Thick ascending limb of Henle's loop. *Kidney Int,* 22**,** 454-64.

CACERES, P. S., ARES, G. R. & ORTIZ, P. A. (2009) cAMP stimulates apical exocytosis of the renal Na(+)-K(+)-2Cl(-) cotransporter NKCC2 in the thick ascending limb: role of protein kinase A. *J Biol Chem,* 284**,** 24965-71.

CAI, Q., FERRARIS, J. D. & BURG, M. B. (2005) High NaCl increases TonEBP/OREBP mRNA and protein by stabilizing its mRNA. *Am J Physiol Renal Physiol,* 289**,** F803-7.

CAMACHO, A. & PHILLIPS, M. I. (1981) Horseradish peroxidase study in rat of the neural connections of the organum vasculosum of the lamina terminalis. *Neurosci Lett,* 25**,** 201-4.

CAMPEAN, V., KRICKE, J., ELLISON, D., LUFT, F. C. & BACHMANN, S. (2001) Localization of thiazide-sensitive Na(+)-Cl(-) cotransport and associated gene products in mouse DCT. *Am J Physiol Renal Physiol,* 281**,** F1028-35.

CHEN, S. Y., BHARGAVA, A., MASTROBERARDINO, L., MEIJER, O. C., WANG, J., BUSE, P., FIRESTONE, G. L., VERREY, F. & PEARCE, D. (1999) Epithelial sodium channel regulated by aldosterone-induced protein sgk. *Proc Natl Acad Sci U S A,* 96**,** 2514-9.

CIURA, S. & BOURQUE, C. W. (2006) Transient receptor potential vanilloid 1 is required for intrinsic osmoreception in organum vasculosum lamina terminalis neurons and for normal thirst responses to systemic hyperosmolality. *J Neurosci,* 26**,** 9069-75.

COONEY, A. S. & FITZSIMONS, J. T. (1996) Increased sodium appetite and thirst in rat induced by the ingredients of liquorice, glycyrrhizic acid and glycyrrhetinic acid. *Regul Pept,* 66**,** 127-33.

COOPER, M. & STEWART, P. M. (1998) The syndrome of apparent mineralocorticoid excess. *QJM,* 91**,** 453-5.

COUETTE, B., JALAGUIER, S., HELLAL-LEVY, C., LUPO, B., FAGART, J., AUZOU, G. & RAFESTIN-OBLIN, M. E. (1998) Folding requirements of the ligand-binding domain of the human mineralocorticoid receptor. *Mol Endocrinol,* 12**,** 855-63.

CURTIS, K. S. & STRICKER, E. M. (1997) Enhanced fluid intake by rats after capsaicin treatment. *Am J Physiol,* 272**,** R704-9.

D'AMICO, G. & BAZZI, C. (2003) Pathophysiology of proteinuria. *Kidney Int,* 63**,** 809-25.

DAGAN, A., GATTINENI, J., COOK, V. & BAUM, M. (2007) Prenatal programming of rat proximal tubule Na+/H+ exchanger by dexamethasone. *Am J Physiol Regul Integr Comp Physiol,* 292**,** R1230-5.

DAHLSTRAND, J., LARDELLI, M. & LENDAHL, U. (1995) Nestin mRNA expression correlates with the central nervous system progenitor cell state in many, but not all, regions of developing central nervous system. *Brain Res Dev Brain Res,* 84**,** 109-29.

DAVE-SHARMA, S., WILSON, R. C., HARBISON, M. D., NEWFIELD, R., AZAR, M. R., KROZOWSKI, Z. S., FUNDER, J. W., SHACKLETON, C. H., BRADLOW, H. L., WEI, J. Q., HERTECANT, J., MORAN, A., NEIBERGER, R. E., BALFE, J. W., FATTAH, A., DANEMAN, D., AKKURT, H. I., DE SANTIS, C. & NEW, M. I. (1998) Examination of genotype and phenotype relationships in 14 patients with apparent mineralocorticoid excess. *J Clin Endocrinol Metab,* 83**,** 2244-54.

DAWBORN, J. K. & ROSS, E. J. (1967) The effect of prolonged administration of aldosterone on sodium and potassium turnover in the rabbit. *Clin Sci,* 32**,** 559-70.

DE SEIGNEUX, S., NIELSEN, J., OLESEN, E. T., DIMKE, H., KWON, T. H., FROKIAER, J. & NIELSEN, S. (2007) Long-term aldosterone treatment induces decreased apical but increased basolateral expression of AQP2 in CCD of rat kidney. *Am J Physiol Renal Physiol,* 293**,** F87-99.

DEBONNEVILLE, C., FLORES, S. Y., KAMYNINA, E., PLANT, P. J., TAUXE, C., THOMAS, M. A., MUNSTER, C., CHRAIBI, A., PRATT, J. H., HORISBERGER, J. D., PEARCE, D., LOFFING, J. & STAUB, O. (2001) Phosphorylation of Nedd4-2 by Sgk1 regulates epithelial Na(+) channel cell surface expression. *EMBO J,* 20**,** 7052-9.

DENTON, D., WEISINGER, R., MUNDY, N. I., WICKINGS, E. J., DIXSON, A., MOISSON, P., PINGARD, A. M., SHADE, R., CAREY, D., ARDAILLOU, R. & ET AL. (1995) The effect of increased salt intake on blood pressure of chimpanzees. *Nat Med,* 1**,** 1009-16.

DEUCHAR, G. A., MCLEAN, D., HADOKE, P. W., BROWNSTEIN, D. G., WEBB, D. J., MULLINS, J. J., CHAPMAN, K., SECKL, J. R. & KOTELEVTSEV, Y. V. (2011) 11beta-hydroxysteroid dehydrogenase type 2 deficiency accelerates atherogenesis and causes proinflammatory changes in the endothelium in apoe-/- mice. *Endocrinology,* 152**,** 236-46.

DIAZ, R., BROWN, R. W. & SECKL, J. R. (1998) Distinct ontogeny of glucocorticoid and mineralocorticoid receptor and 11beta-hydroxysteroid dehydrogenase types I and II mRNAs in the fetal rat brain suggest a complex control of glucocorticoid actions. *J Neurosci,* 18**,** 2570-80.

DIBONA, G. F. (2000) Neural control of the kidney: functionally specific renal sympathetic nerve fibers. *Am J Physiol Regul Integr Comp Physiol,* 279**,** R1517-24.

DICKINSON, H., WALKER, D. W., WINTOUR, E. M. & MORITZ, K. (2007) Maternal dexamethasone treatment at midgestation reduces nephron number and alters renal gene expression in the fetal spiny mouse. *Am J Physiol Regul Integr Comp Physiol,* 292**,** R453-61.

DRAPER, N. & STEWART, P. M. (2005) 11beta-hydroxysteroid dehydrogenase and the pre-receptor regulation of corticosteroid hormone action. *J Endocrinol,* 186**,** 251-71.

DUBOIS, N. C., HOFMANN, D., KALOULIS, K., BISHOP, J. M. & TRUMPP, A. (2006) Nestin-Cre transgenic mouse line Nes-Cre1 mediates highly efficient Cre/loxP mediated recombination in the nervous system, kidney, and somite-derived tissues. *Genesis,* 44**,** 355-60.

DUDLEY, H. F., BOLING, E. A., LEQUESNE, L. P. & MOORE, F. D. (1954) Studies on antidiuresis in surgery: effects of anesthesia, surgery and posterior pituitary antidiuretic hormone on water metabolism in man. *Ann Surg,* 140**,** 354-67.

DUNBAR, D. R., KHALED, H., EVANS, L. C., AL-DUJAILI, E. A., MULLINS, L. J., MULLINS, J. J., KENYON, C. J. & BAILEY, M. A. (2010) Transcriptional and physiological responses to chronic ACTH treatment by the mouse kidney. *Physiol Genomics,* 40**,** 158-66.

DUNN, F. L., BRENNAN, T. J., NELSON, A. E. & ROBERTSON, G. L. (1973) The role of blood osmolality and volume in regulating vasopressin secretion in the rat. *J Clin Invest,* 52**,** 3212-9.

ECELBARGER, C. A., KIM, G. H., WADE, J. B. & KNEPPER, M. A. (2001a) Regulation of the abundance of renal sodium transporters and channels by vasopressin. *Exp Neurol,* 171**,** 227-34.

ECELBARGER, C. A., KNEPPER, M. A. & VERBALIS, J. G. (2001b) Increased abundance of distal sodium transporters in rat kidney during vasopressin escape. *J Am Soc Nephrol,* 12**,** 207-17.

ECELBARGER, C. A., NIELSEN, S., OLSON, B. R., MURASE, T., BAKER, E. A., KNEPPER, M. A. & VERBALIS, J. G. (1997) Role of renal aquaporins in escape from vasopressin-induced antidiuresis in rat. *J Clin Invest,* 99**,** 1852-63.

ECELBARGER, C. A., TERRIS, J., FRINDT, G., ECHEVARRIA, M., MARPLES, D., NIELSEN, S. & KNEPPER, M. A. (1995) Aquaporin-3 water channel localization and regulation in rat kidney. *Am J Physiol,* 269**,** F663-72.

EDWARDS, D. P. (2000) The role of coactivators and corepressors in the biology and mechanism of action of steroid hormone receptors. *J Mammary Gland Biol Neoplasia,* 5**,** 307-24.

EGAN, G., SILK, T., ZAMARRIPA, F., WILLIAMS, J., FEDERICO, P., CUNNINGTON, R., CARABOTT, L., BLAIR-WEST, J., SHADE, R., MCKINLEY, M., FARRELL, M., LANCASTER, J., JACKSON, G., FOX, P. & DENTON, D. (2003) Neural correlates of the emergence of consciousness of thirst. *Proc Natl Acad Sci U S A,* 100**,** 15241-6.

ERKUT, Z. A., POOL, C. & SWAAB, D. F. (1998) Glucocorticoids suppress corticotropin-releasing hormone and vasopressin expression in human hypothalamic neurons. *J Clin Endocrinol Metab,* 83**,** 2066-73.

FEIL, R., BROCARD, J., MASCREZ, B., LEMEUR, M., METZGER, D. & CHAMBON, P. (1996) Ligand-activated site-specific recombination in mice. *Proc Natl Acad Sci U S A,* 93**,** 10887-90.

FEJES-TOTH, G., PEARCE, D. & NARAY-FEJES-TOTH, A. (1998) Subcellular localization of mineralocorticoid receptors in living cells: effects of receptor agonists and antagonists. *Proc Natl Acad Sci U S A,* 95**,** 2973-8.

FENTON, R. A., CHOU, C. L., STEWART, G. S., SMITH, C. P. & KNEPPER, M. A. (2004) Urinary concentrating defect in mice with selective deletion of phloretin-sensitive urea transporters in the renal collecting duct. *Proc Natl Acad Sci U S A,* 101**,** 7469-74.

FENTON, R. A., COTTINGHAM, C. A., STEWART, G. S., HOWORTH, A., HEWITT, J. A. & SMITH, C. P. (2002) Structure and characterization of the mouse UT-A gene (Slc14a2). *Am J Physiol Renal Physiol,* 282**,** F630-8.

FENTON, R. A., SMITH, C. P. & KNEPPER, M. A. (2006) Role of collecting duct urea transporters in the kidney--insights from mouse models. *J Membr Biol,* 212**,** 119-31.

FERRARI, P. (2010) The role of 11beta-hydroxysteroid dehydrogenase type 2 in human hypertension. *Biochim Biophys Acta,* 1802**,** 1178-87.

FERRARI, P. & KROZOWSKI, Z. (2000) Role of the 11beta-hydroxysteroid dehydrogenase type 2 in blood pressure regulation. *Kidney Int,* 57**,** 1374-81.

FLUHARTY, S. J. & EPSTEIN, A. N. (1983) Sodium appetite elicited by intracerebroventricular infusion of angiotensin II in the rat: II. Synergistic interaction with systemic mineralocorticoids. *Behav Neurosci,* 97**,** 746-58.

FRANCIS, J., WEISS, R. M., WEI, S. G., JOHNSON, A. K., BELTZ, T. G., ZIMMERMAN, K. & FELDER, R. B. (2001) Central mineralocorticoid receptor blockade improves volume regulation and reduces sympathetic drive in heart failure. *Am J Physiol Heart Circ Physiol,* 281**,** H2241-51.

FREEL, E. M. & CONNELL, J. M. (2004) Mechanisms of hypertension: the expanding role of aldosterone. *J Am Soc Nephrol,* 15**,** 1993-2001.

FREGLY, M. J. & WATERS, I. W. (1966) Effect of mineralocorticoids on spontaneous sodium chloride appetite of adrenalectomized rats. *Physiology and Behavior,* 1**,** 65-74.

FROKIAER, J., MARPLES, D., VALTIN, H., MORRIS, J. F., KNEPPER, M. A. & NIELSEN, S. (1999) Low aquaporin-2 levels in polyuric DI +/+ severe mice with constitutively high cAMP-phosphodiesterase activity. *Am J Physiol,* 276**,** F179-90.

FUNDER, J. W., PEARCE, P. T., SMITH, R. & SMITH, A. I. (1988) Mineralocorticoid action: target tissue specificity is enzyme, not receptor, mediated. *Science,* 242**,** 583-5.

FUSHIMI, K., SASAKI, S. & MARUMO, F. (1997) Phosphorylation of serine 256 is required for cAMP-dependent regulatory exocytosis of the aquaporin-2 water channel. *J Biol Chem,* 272**,** 14800-4.

FUSHIMI, K., UCHIDA, S., HARA, Y., HIRATA, Y., MARUMO, F. & SASAKI, S. (1993) Cloning and expression of apical membrane water channel of rat kidney collecting tubule. *Nature,* 361**,** 549-52.

GAINER, H., SARNE, Y. & BROWNSTEIN, M. J. (1977) Biosynthesis and axonal transport of rat neurohypophysial proteins and peptides. *J Cell Biol,* 73**,** 366-81.

GALL, G., USHER, P., MELBY, J. C. & KLEIN, R. (1971) Effects of aldosterone and cortisol on human erythrocyte Na efflux. *J Clin Endocrinol Metab,* 32**,** 555-61.

GEERLING, J. C., ENGELAND, W. C., KAWATA, M. & LOEWY, A. D. (2006a) Aldosterone target neurons in the nucleus tractus solitarius drive sodium appetite. *J Neurosci,* 26**,** 411-7.

GEERLING, J. C., KAWATA, M. & LOEWY, A. D. (2006b) Aldosterone-sensitive neurons in the rat central nervous system. *J Comp Neurol,* 494**,** 515-27.

GEERLING, J. C. & LOEWY, A. D. (2006) Aldosterone-sensitive NTS neurons are inhibited by saline ingestion during chronic mineralocorticoid treatment. *Brain Res,* 1115**,** 54-64.

GEERLING, J. C. & LOEWY, A. D. (2008) Central regulation of sodium appetite. *Exp Physiol,* 93**,** 177-209.

GELEIJNSE, J. M., KOK, F. J. & GROBBEE, D. E. (2003) Blood pressure response to changes in sodium and potassium intake: a metaregression analysis of randomised trials. *J Hum Hypertens,* 17**,** 471-80.

GERTNER, R. A., KLEIN, J. D., BAILEY, J. L., KIM, D. U., LUO, X. H., BAGNASCO, S. M. & SANDS, J. M. (2004) Aldosterone decreases UT-A1 urea transporter expression via the mineralocorticoid receptor. *J Am Soc Nephrol,* 15**,** 558-65.

GIMENEZ, I. & FORBUSH, B. (2003) Short-term stimulation of the renal Na-K-Cl cotransporter (NKCC2) by vasopressin involves phosphorylation and membrane translocation of the protein. *J Biol Chem,* 278**,** 26946-51.

GIRI, S. N. & PEOPLES, S. A. (1965) Antidiuretic effects of inactin and pentobarbital in chickens. *Proc Soc Exp Biol Med,* 120**,** 864-5.

GLASS, C. K. & ROSENFELD, M. G. (2000) The coregulator exchange in transcriptional functions of nuclear receptors. *Genes Dev,* 14**,** 121-41.

GOMEZ-SANCHEZ, E. P. (1986) Intracerebroventricular infusion of aldosterone induces hypertension in rats. *Endocrinology,* 118**,** 819-23.

GOMEZ-SANCHEZ, E. P. & GOMEZ-SANCHEZ, C. E. (1986) A reevaluation of the mineralocorticoid and hypertensinogenic potential of 19-hydroxyandrostenedione. *Endocrinology,* 118**,** 2582-7.

GOMEZ-SANCHEZ, E. P. & GOMEZ-SANCHEZ, C. E. (1992) Central hypertensinogenic effects of glycyrrhizic acid and carbenoxolone. *Am J Physiol,* 263**,** E1125-30.

GRASSI, G. (2009) Assessment of sympathetic cardiovascular drive in human hypertension: achievements and perspectives. *Hypertension,* 54**,** 690-7.

GRASSI, G., CATTANEO, B. M., SERAVALLE, G., LANFRANCHI, A. & MANCIA, G. (1998) Baroreflex control of sympathetic nerve activity in essential and secondary hypertension. *Hypertension,* 31**,** 68-72.

GREKIN, R. J., TERRIS, J. M. & BOHR, D. F. (1980) Electrolyte and hormonal effects of deoxycorticosterone acetate in young pigs. *Hypertension,* 2**,** 326-32.

GUYTON, A. C. & HALL, J. E. (2000) *Textbook of medical physiology,* Philadelphia, Saunders.

GUYTON, A. C., MANNING, R. D., JR., HALL, J. E., NORMAN, R. A., JR., YOUNG, D. B. & PAN, Y. J. (1984) The pathogenic role of the kidney. *J Cardiovasc Pharmacol,* 6 Suppl 1**,** S151-61.

HAACK, D., MOHRING, J., MOHRING, B., PETRI, M. & HACKENTHAL, E. (1977) Comparative study on development of corticosterone and DOCA hypertension in rats. *Am J Physiol,* 233**,** F403-11.

HADOKE, P. W., CHRISTY, C., KOTELEVTSEV, Y. V., WILLIAMS, B. C., KENYON, C. J., SECKL, J. R., MULLINS, J. J. & WALKER, B. R. (2001) Endothelial cell dysfunction in mice after transgenic knockout of type 2, but not type 1, 11beta-hydroxysteroid dehydrogenase. *Circulation,* 104**,** 2832-7.

HANSSON, G. K. (2007) The 2007 Nobel Prize in Physiology or Medicine-Advanced Information. Nobelprize.org.

HARDING, A. J., NG, J. L., HALLIDAY, G. M. & OLIVER, J. (1995) Comparison of the number of vasopressin-producing hypothalamic neurons in rats and humans. *J Neuroendocrinol,* 7**,** 629-36.

HARFSTRAND, A., FUXE, K., CINTRA, A., AGNATI, L. F., ZINI, I., WIKSTROM, A. C., OKRET, S., YU, Z. Y., GOLDSTEIN, M., STEINBUSCH, H. & ET AL. (1986) Glucocorticoid receptor immunoreactivity in monoaminergic neurons of rat brain. *Proc Natl Acad Sci U S A,* 83**,** 9779-83.

HARTLEY, C. J., REDDY, A. K., MADALA, S., MARTIN-MCNULTY, B., VERGONA, R., SULLIVAN, M. E., HALKS-MILLER, M., TAFFET, G. E., MICHAEL, L. H., ENTMAN, M. L. & WANG, Y. X. (2000) Hemodynamic changes in apolipoprotein E-knockout mice. *Am J Physiol Heart Circ Physiol,* 279**,** H2326-34.

HASLER, U., MORDASINI, D., BIANCHI, M., VANDEWALLE, A., FERAILLE, E. & MARTIN, P. Y. (2003) Dual influence of aldosterone on AQP2 expression in cultured renal collecting duct principal cells. *J Biol Chem,* 278**,** 21639-48.

HENDLER, E. D., TORRETTI, J., KUPOR, L. & EPSTEIN, F. H. (1972) Effects of adrenalectomy and hormone replacement on Na- K-ATPase in renal tissue. *Am J Physiol,* 222**,** 754-60.

HENN, V., EDEMIR, B., STEFAN, E., WIESNER, B., LORENZ, D., THEILIG, F., SCHMITT, R., VOSSEBEIN, L., TAMMA, G., BEYERMANN, M.,

KRAUSE, E., HERBERG, F. W., VALENTI, G., BACHMANN, S., ROSENTHAL, W. & KLUSSMANN, E. (2004) Identification of a novel A-kinase anchoring protein 18 isoform and evidence for its role in the vasopressin-induced aquaporin-2 shuttle in renal principal cells. *J Biol Chem,* 279**,** 26654-65.

HERMANSON, O., GLASS, C. K. & ROSENFELD, M. G. (2002) Nuclear receptor coregulators: multiple modes of modification. *Trends Endocrinol Metab,* 13**,** 55-60.

HILL, P., SHUKLA, D., TRAN, M. G., ARAGONES, J., COOK, H. T., CARMELIET, P. & MAXWELL, P. H. (2008) Inhibition of hypoxia inducible factor hydroxylases protects against renal ischemia-reperfusion injury. *J Am Soc Nephrol,* 19**,** 39-46.

HINWOOD, B. G. (1992) *A textbook of science for health professions*.

HIRASAWA, G., SASANO, H., TAKAHASHI, K., FUKUSHIMA, K., SUZUKI, T., HIWATASHI, N., TOYOTA, T., KROZOWSKI, Z. S. & NAGURA, H. (1997) Colocalization of 11 beta-hydroxysteroid dehydrogenase type II and mineralocorticoid receptor in human epithelia. *J Clin Endocrinol Metab,* 82**,** 3859-63.

HOLMES, M. C., ABRAHAMSEN, C. T., FRENCH, K. L., PATERSON, J. M., MULLINS, J. J. & SECKL, J. R. (2006a) The mother or the fetus? 11beta-hydroxysteroid dehydrogenase type 2 null mice provide evidence for direct fetal programming of behavior by endogenous glucocorticoids. *J Neurosci,* 26**,** 3840-4.

HOLMES, M. C., SANGRA, M., FRENCH, K. L., WHITTLE, I. R., PATERSON, J., MULLINS, J. J. & SECKL, J. R. (2006b) 11beta-Hydroxysteroid dehydrogenase type 2 protects the neonatal cerebellum from deleterious effects of glucocorticoids. *Neuroscience,* 137**,** 865-73.

HOORN, E. J., HOFFERT, J. D. & KNEPPER, M. A. (2005) Combined proteomics and pathways analysis of collecting duct reveals a protein regulatory network activated in vasopressin escape. *J Am Soc Nephrol,* 16**,** 2852-63.

HULT, M., JORNVALL, H. & OPPERMANN, U. C. (1998) Selective inhibition of human type 1 11beta-hydroxysteroid dehydrogenase by synthetic steroids and xenobiotics. *FEBS Lett,* 441**,** 25-8.

HULTMAN, M. L., KRASNOPEROVA, N. V., LI, S., DU, S., XIA, C., DIETZ, J. D., LALA, D. S., WELSCH, D. J. & HU, X. (2005) The ligand-dependent interaction of mineralocorticoid receptor with coactivator and corepressor peptides suggests multiple activation mechanisms. *Mol Endocrinol,* 19**,** 1460-73.

HUNT, S. A., ABRAHAM, W. T., CHIN, M. H., FELDMAN, A. M., FRANCIS, G. S., GANIATS, T. G., JESSUP, M., KONSTAM, M. A., MANCINI, D. M., MICHL, K., OATES, J. A., RAHKO, P. S., SILVER, M. A., STEVENSON, L. W., YANCY, C. W., ANTMAN, E. M., SMITH, S. C., JR., ADAMS, C. D., ANDERSON, J. L., FAXON, D. P., FUSTER, V., HALPERIN, J. L., HIRATZKA, L. F., JACOBS, A. K., NISHIMURA, R., ORNATO, J. P., PAGE, R. L. & RIEGEL, B. (2005) ACC/AHA 2005 Guideline Update for the Diagnosis and Management of Chronic Heart Failure in the Adult: a report of the American College of Cardiology/American Heart Association Task Force on Practice Guidelines (Writing Committee to Update the 2001 Guidelines for the Evaluation and Management of Heart Failure): developed in collaboration with the American College of Chest Physicians and the International Society for Heart and Lung Transplantation: endorsed by the Heart Rhythm Society. *Circulation,* 112**,** e154-235.

INGRAM, M. C., WALLACE, A. M., COLLIER, A., FRASER, R. & CONNELL, J. M. (1996) Sodium status, corticosteroid metabolism and blood pressure in normal human subjects and in a patient with abnormal salt appetite. *Clin Exp Pharmacol Physiol,* 23**,** 375-8.

JARD, S. (1991) *Vasopressin*, John Libbey Eurotext.

KAJI, D. M., THAKKAR, U. & KAHN, T. (1981) Glucocorticoid-induced alterations in the sodium potassium pump of the human erythrocyte. *J Clin Invest,* 68**,** 422-30.

KAMSTEEG, E. J., HEIJNEN, I., VAN OS, C. H. & DEEN, P. M. (2000) The subcellular localization of an aquaporin-2 tetramer depends on the stoichiometry of phosphorylated and nonphosphorylated monomers. *J Cell Biol,* 151**,** 919-30.

KATSURA, T., GUSTAFSON, C. E., AUSIELLO, D. A. & BROWN, D. (1997) Protein kinase A phosphorylation is involved in regulated exocytosis of aquaporin-2 in transfected LLC-PK1 cells. *Am J Physiol,* 272**,** F817-22.

KAUFMAN, S. (1984) Role of right atrial receptors in the control of drinking in the rat. *J Physiol,* 349**,** 389-96.

KENYON, C. J., SACCOCCIO, N. A. & MORRIS, D. J. (1984a) Aldosterone effects on water and electrolyte metabolism. *J Endocrinol,* 100**,** 93-100.

KENYON, C. J., SACCOCCIO, N. A. & MORRIS, D. J. (1984b) Glucocorticoid inhibition of mineralocorticoid action in the rat. *Clin Sci (Lond),* 67**,** 329-35.

KIM, G. H., MASILAMANI, S., TURNER, R., MITCHELL, C., WADE, J. B. & KNEPPER, M. A. (1998) The thiazide-sensitive Na-Cl cotransporter is an aldosterone-induced protein. *Proc Natl Acad Sci U S A,* 95**,** 14552-7.

KIM, J. K., SUMMER, S. N., WOOD, W. M. & SCHRIER, R. W. (2001) Role of glucocorticoid hormones in arginine vasopressin gene regulation. *Biochem Biophys Res Commun,* 289**,** 1252-6.

KNEPPER, M. A., DANIELSON, R. A., SAIDEL, G. M. & JOHNSTON, K. H. (1975) Effects of dietary protein restriction and glucocorticoid administration on urea excretion in rats. *Kidney Int,* 8**,** 303-15.

KNEPPER, M. A. & NIELSEN, S. (1993) Kinetic model of water and urea permeability regulation by vasopressin in collecting duct. *Am J Physiol,* 265**,** F214-24.

KNOEPFELMACHER, M., PRADAL, M. J., DIO, R. D., SALGADO, L. R., SEMER, M., WAJCHENBERG, B. L. & LIBERMAN, B. (1997) Resistance to vasopressin action on the kidney in patients with Cushing's disease. *Eur J Endocrinol,* 137**,** 162-6.

KNOPS, N. B., MONNENS, L. A., LENDERS, J. W. & LEVTCHENKO, E. N. (2011) Apparent mineralocorticoid excess: time of manifestation and complications despite treatment. *Pediatrics,* 127**,** e1610-4.

KNOWLTON, A. I. & LOEB, E. N. (1957) Depletion of carcass potassium in rats made hypertensive with desoxycorticosterone acetate (DCA) and with cortisone. *J Clin Invest,* 36**,** 1295-300.

KOOB, G. F. (1992) Drugs of abuse: anatomy, pharmacology and function of reward pathways. *Trends Pharmacol Sci,* 13**,** 177-84.

KOS, C. H. (2004) Cre/loxP system for generating tissue-specific knockout mouse models. *Nutr Rev,* 62**,** 243-6.

KOSHIYA, N. & GUYENET, P. G. (1996) NTS neurons with carotid chemoreceptor inputs arborize in the rostral ventrolateral medulla. *Am J Physiol,* 270**,** R1273-8.

KOTELEVTSEV, Y., BROWN, R. W., FLEMING, S., KENYON, C., EDWARDS, C. R., SECKL, J. R. & MULLINS, J. J. (1999) Hypertension in mice lacking 11beta-hydroxysteroid dehydrogenase type 2. *J Clin Invest,* 103**,** 683-9.

KUWAHARA, M. & VERKMAN, A. S. (1989) Pre-steady-state analysis of the turn-on and turn-off of water permeability in the kidney collecting tubule. *J Membr Biol,* 110**,** 57-65.

KWON, M. S., LIM, S. W. & KWON, H. M. (2009) Hypertonic stress in the kidney: a necessary evil. *Physiology (Bethesda),* 24**,** 186-91.

KYOSSEV, Z., WALKER, P. D. & REEVES, W. B. (1996) Immunolocalization of NAD-dependent 11 beta-hydroxysteroid dehydrogenase in human kidney and colon. *Kidney Int,* 49**,** 271-81.

LAVIN, N. (2009) *Manual of endocrinology and metabolism,* Philadelphia, Wolters Kluwer/Lippincott Williams & Wilkins Health.

LAYCOCK, J. F. (2010) *Perspectives on vasopressin,* London
Hackensack, NJ, Imperial College Press ;
Distributed by World Scientific.

LEECH, M., HUANG, X. R., MORAND, E. F. & HOLDSWORTH, S. R. (2000) Endogenous glucocorticoids modulate experimental anti-glomerular basement membrane glomerulonephritis. *Clin Exp Immunol,* 119**,** 161-8.

LEHR, D., MALLOW, J. & KRUKOWSKI, M. (1967) Copious drinking and simultaneous inhibition of urine flow elicited by beta-adrenergic stimulation and contrary effect of alpha-adrenergic stimulation. *J Pharmacol Exp Ther,* 158**,** 150-63.

LENDAHL, U., ZIMMERMAN, L. B. & MCKAY, R. D. (1990) CNS stem cells express a new class of intermediate filament protein. *Cell,* 60**,** 585-95.

LI, A., TEDDE, R., KROZOWSKI, Z. S., PALA, A., LI, K. X., SHACKLETON, C. H., MANTERO, F., PALERMO, M. & STEWART, P. M. (1998) Molecular basis for hypertension in the "type II variant" of apparent mineralocorticoid excess. *Am J Hum Genet,* 63**,** 370-9.

LI, C., WANG, W., SUMMER, S. N., FALK, S. & SCHRIER, R. W. (2008) Downregulation of UT-A1/UT-A3 is associated with urinary concentrating defect in glucocorticoid-excess state. *J Am Soc Nephrol,* 19**,** 1975-81.

LIEDTKE, W. B., MCKINLEY, M. J., WALKER, L. L., ZHANG, H., PFENNING, A. R., DRAGO, J., HOCHENDONER, S. J., HILTON, D. L., LAWRENCE, A. J. & DENTON, D. A. (2011) Relation of addiction genes to hypothalamic gene changes subserving genesis and gratification of a classic instinct, sodium appetite. *Proc Natl Acad Sci U S A,* 108**,** 12509-14.

LIU, W., MORIMOTO, T., WODA, C., KLEYMAN, T. R. & SATLIN, L. M. (2007) Ca2+ dependence of flow-stimulated K secretion in the mammalian cortical collecting duct. *Am J Physiol Renal Physiol,* 293**,** F227-35.

LOPEZ-RODRIGUEZ, C., ANTOS, C. L., SHELTON, J. M., RICHARDSON, J. A., LIN, F., NOVOBRANTSEVA, T. I., BRONSON, R. T., IGARASHI, P., RAO, A. & OLSON, E. N. (2004) Loss of NFAT5 results in renal atrophy and lack of tonicity-responsive gene expression. *Proc Natl Acad Sci U S A,* 101**,** 2392-7.

LORENZ, J. N. (2002) A practical guide to evaluating cardiovascular, renal, and pulmonary function in mice. *Am J Physiol Regul Integr Comp Physiol,* 282**,** R1565-82.

LOTE, C. J. (2000) *Principles of renal physiology,* London, Croom Helm.

LU, M., WANG, T., YAN, Q., WANG, W., GIEBISCH, G. & HEBERT, S. C. (2004) ROMK is required for expression of the 70-pS K channel in the thick ascending limb. *Am J Physiol Renal Physiol,* 286**,** F490-5.

LUFT, F. C., MORRIS, C. D. & WEINBERGER, M. H. (1997) Compliance to a low-salt diet. *Am J Clin Nutr,* 65**,** 698S-703S.

LUND, U., RIPPE, A., VENTUROLI, D., TENSTAD, O., GRUBB, A. & RIPPE, B. (2003) Glomerular filtration rate dependence of sieving of albumin and some neutral proteins in rat kidneys. *Am J Physiol Renal Physiol,* 284**,** F1226-34.

MA, L. Y., MCEWEN, B. S., SAKAI, R. R. & SCHULKIN, J. (1993) Glucocorticoids facilitate mineralocorticoid-induced sodium intake in the rat. *Horm Behav,* 27**,** 240-50.

MA, T., SONG, Y., YANG, B., GILLESPIE, A., CARLSON, E. J., EPSTEIN, C. J. & VERKMAN, A. S. (2000) Nephrogenic diabetes insipidus in mice lacking aquaporin-3 water channels. *Proc Natl Acad Sci U S A,* 97**,** 4386-91.

MA, T., YANG, B., GILLESPIE, A., CARLSON, E. J., EPSTEIN, C. J. & VERKMAN, A. S. (1997) Generation and phenotype of a transgenic knockout mouse lacking the mercurial-insensitive water channel aquaporin-4. *J Clin Invest,* 100**,** 957-62.

MA, T., YANG, B., GILLESPIE, A., CARLSON, E. J., EPSTEIN, C. J. & VERKMAN, A. S. (1998) Severely impaired urinary concentrating ability in transgenic mice lacking aquaporin-1 water channels. *J Biol Chem,* 273**,** 4296-9.

MADDOX, D. A., PRICE, D. C. & RECTOR, F. C., JR. (1977) Effects of surgery on plasma volume and salt and water excretion in rats. *Am J Physiol,* 233**,** F600-6.

MANNING, J. R., BAILEY, M. A., SOARES, D. C., DUNBAR, D. R. & MULLINS, J. J. (2010) In silico structure-function analysis of pathological variation in the HSD11B2 gene sequence. *Physiol Genomics,* 42**,** 319-30.

MANTERO, F., PALERMO, M., PETRELLI, M. D., TEDDE, R., STEWART, P. M. & SHACKLETON, C. H. (1996) Apparent mineralocorticoid excess: type I and type II. *Steroids,* 61**,** 193-6.

MARPLES, D., FROKIAER, J., DORUP, J., KNEPPER, M. A. & NIELSEN, S. (1996) Hypokalemia-induced downregulation of aquaporin-2 water channel expression in rat kidney medulla and cortex. *J Clin Invest,* 97**,** 1960-8.

MATSUMURA, Y., UCHIDA, S., RAI, T., SASAKI, S. & MARUMO, F. (1997) Transcriptional regulation of aquaporin-2 water channel gene by cAMP. *J Am Soc Nephrol,* 8**,** 861-7.

MCCORMICK, J. A., BHALLA, V., PAO, A. C. & PEARCE, D. (2005) SGK1: a rapid aldosterone-induced regulator of renal sodium reabsorption. *Physiology (Bethesda),* 20**,** 134-9.

MCDILL, B. W., LI, S. Z., KOVACH, P. A., DING, L. & CHEN, F. (2006) Congenital progressive hydronephrosis (cph) is caused by an S256L mutation in aquaporin-2 that affects its phosphorylation and apical membrane accumulation. *Proc Natl Acad Sci U S A,* 103**,** 6952-7.

MCTAVISH, N., GETTY, J., BURCHELL, A. & WILSON, S. M. (2009) Glucocorticoids can activate the alpha-ENaC gene promoter independently of SGK1. *Biochem J,* 423**,** 189-97.

MENETON, P., LOFFING, J. & WARNOCK, D. G. (2004) Sodium and potassium handling by the aldosterone-sensitive distal nephron: the pivotal role of the distal and connecting tubule. *Am J Physiol Renal Physiol,* 287**,** F593-601.

MIYAKAWA, H., WOO, S. K., DAHL, S. C., HANDLER, J. S. & KWON, H. M. (1999) Tonicity-responsive enhancer binding protein, a rel-like protein that stimulates transcription in response to hypertonicity. *Proc Natl Acad Sci U S A,* 96**,** 2538-42.

MOBASHERI, A., WRAY, S. & MARPLES, D. (2005) Distribution of AQP2 and AQP3 water channels in human tissue microarrays. *J Mol Histol,* 36**,** 1-14.

MOELLER, H. B., PRAETORIUS, J., RUTZLER, M. R. & FENTON, R. A. (2010) Phosphorylation of aquaporin-2 regulates its endocytosis and protein-protein interactions. *Proc Natl Acad Sci U S A,* 107**,** 424-9.

MORINEAU, G., SULMONT, V., SALOMON, R., FIQUET-KEMPF, B., JEUNEMAITRE, X., NICOD, J. & FERRARI, P. (2006) Apparent mineralocorticoid excess: report of six new cases and extensive personal experience. *J Am Soc Nephrol,* 17**,** 3176-84.

MUTIG, K., PALIEGE, A., KAHL, T., JONS, T., MULLER-ESTERL, W. & BACHMANN, S. (2007) Vasopressin V2 receptor expression along rat, mouse, and human renal epithelia with focus on TAL. *Am J Physiol Renal Physiol,* 293**,** F1166-77.

MUTIG, K., SARITAS, T., UCHIDA, S., KAHL, T., BOROWSKI, T., PALIEGE, A., BOHLICK, A., BLEICH, M., SHAN, Q. & BACHMANN, S. (2010) Short-term stimulation of the thiazide-sensitive Na+-Cl- cotransporter by vasopressin involves phosphorylation and membrane translocation. *Am J Physiol Renal Physiol,* 298**,** F502-9.

NARAY-FEJES-TOTH, A. & FEJES-TOTH, G. (2007) Novel mouse strain with Cre recombinase in 11beta-hydroxysteroid dehydrogenase-2-expressing cells. *Am J Physiol Renal Physiol,* 292**,** F486-94.

NARUSE, M., KLEIN, J. D., ASHKAR, Z. M., JACOBS, J. D. & SANDS, J. M. (1997) Glucocorticoids downregulate the vasopressin-regulated urea transporter in rat terminal inner medullary collecting ducts. *J Am Soc Nephrol,* 8**,** 517-23.

NEW, M. I., LEVINE, L. S., BIGLIERI, E. G., PAREIRA, J. & ULICK, S. (1977) Evidence for an unidentified steroid in a child with apparent mineralocorticoid hypertension. *J Clin Endocrinol Metab,* 44**,** 924-33.

NGUYEN DINH CAT, A., OUVRARD-PASCAUD, A., TRONCHE, F., CLEMESSY, M., GONZALEZ-NUNEZ, D., FARMAN, N. & JAISSER, F. (2009) Conditional transgenic mice for studying the role of the glucocorticoid receptor in the renal collecting duct. *Endocrinology,* 150**,** 2202-10.

NIELSEN, S., CHOU, C. L., MARPLES, D., CHRISTENSEN, E. I., KISHORE, B. K. & KNEPPER, M. A. (1995a) Vasopressin increases water permeability of kidney collecting duct by inducing translocation of aquaporin-CD water channels to plasma membrane. *Proc Natl Acad Sci U S A,* 92**,** 1013-7.

NIELSEN, S., DIGIOVANNI, S. R., CHRISTENSEN, E. I., KNEPPER, M. A. & HARRIS, H. W. (1993a) Cellular and subcellular immunolocalization of vasopressin-regulated water channel in rat kidney. *Proc Natl Acad Sci U S A,* 90**,** 11663-7.

NIELSEN, S., KWON, T. H., FROKIAER, J. & AGRE, P. (2007) Regulation and dysregulation of aquaporins in water balance disorders. *J Intern Med,* 261**,** 53-64.

NIELSEN, S., PALLONE, T., SMITH, B. L., CHRISTENSEN, E. I., AGRE, P. & MAUNSBACH, A. B. (1995b) Aquaporin-1 water channels in short and long loop descending thin limbs and in descending vasa recta in rat kidney. *Am J Physiol,* 268**,** F1023-37.

NIELSEN, S., SMITH, B. L., CHRISTENSEN, E. I., KNEPPER, M. A. & AGRE, P. (1993b) CHIP28 water channels are localized in constitutively water-permeable segments of the nephron. *J Cell Biol,* 120**,** 371-83.

NISHIMOTO, G., ZELENINA, M., LI, D., YASUI, M., APERIA, A., NIELSEN, S. & NAIRN, A. C. (1999) Arginine vasopressin stimulates phosphorylation of aquaporin-2 in rat renal tissue. *Am J Physiol,* 276**,** F254-9.

NISSEN, R., BOURQUE, C. W. & RENAUD, L. P. (1993) Membrane properties of organum vasculosum lamina terminalis neurons recorded in vitro. *Am J Physiol,* 264**,** R811-5.

NOGUEIRA, B. V., PEOTTA, V. A., MEYRELLES, S. S. & VASQUEZ, E. C. (2007) Evaluation of aortic remodeling in apolipoprotein E-deficient mice and renovascular hypertensive mice. *Arch Med Res,* 38**,** 816-21.

NORGREN, R. & SMITH, G. P. (1988) Central distribution of subdiaphragmatic vagal branches in the rat. *J Comp Neurol,* 273**,** 207-23.

OBEID, J. & WHITE, P. C. (1992) Tyr-179 and Lys-183 are essential for enzymatic activity of 11 beta-hydroxysteroid dehydrogenase. *Biochem Biophys Res Commun,* 188**,** 222-7.

OBERLEITHNER, H., CALLIES, C., KUSCHE-VIHROG, K., SCHILLERS, H., SHAHIN, V., RIETHMULLER, C., MACGREGOR, G. A. & DE WARDENER, H. E. (2009) Potassium softens vascular endothelium and increases nitric oxide release. *Proc Natl Acad Sci U S A,* 106**,** 2829-34.

OBEYESEKERE, V. R., LI, K. X., FERRARI, P. & KROZOWSKI, Z. (1997) Truncation of the N- and C-terminal regions of the human 11beta-hydroxysteroid dehydrogenase type 2 enzyme and effects on solubility and bidirectional enzyme activity. *Mol Cell Endocrinol,* 131**,** 173-82.

ODERMATT, A., ARNOLD, P. & FREY, F. J. (2001) The intracellular localization of the mineralocorticoid receptor is regulated by 11beta-hydroxysteroid dehydrogenase type 2. *J Biol Chem,* 276**,** 28484-92.

ODERMATT, A., ARNOLD, P., STAUFFER, A., FREY, B. M. & FREY, F. J. (1999) The N-terminal anchor sequences of 11beta-hydroxysteroid dehydrogenases determine their orientation in the endoplasmic reticulum membrane. *J Biol Chem,* 274**,** 28762-70.

OHTA, Y., TSUCHIHASHI, T., UENO, M., KAJIOKA, T., ONAKA, U., TOMINAGA, M. & ETO, K. (2004) Relationship between the awareness of salt restriction and the actual salt intake in hypertensive patients. *Hypertens Res,* 27**,** 243-6.

OKUNO, T., SUZUKI, H. & SARUTA, T. (1981) Dexamethasone hypertension in rats. *Clin Exp Hypertens,* 3**,** 1075-86.

OPPERMANN, M., HANSEN, P. B., CASTROP, H. & SCHNERMANN, J. (2007) Vasodilatation of afferent arterioles and paradoxical increase of renal vascular resistance by furosemide in mice. *Am J Physiol Renal Physiol,* 293**,** F279-87.

ORLOWSKI, J. (1993) Heterologous expression and functional properties of amiloride high affinity (NHE-1) and low affinity (NHE-3) isoforms of the rat Na/H exchanger. *J Biol Chem,* 268**,** 16369-77.

ORTIZ, L. A., QUAN, A., ZARZAR, F., WEINBERG, A. & BAUM, M. (2003) Prenatal dexamethasone programs hypertension and renal injury in the rat. *Hypertension,* 41**,** 328-34.

PALERMO, M., DELITALA, G., SORBA, G., COSSU, M., SATTA, R., TEDDE, R., PALA, A. & SHACKLETON, C. H. (2000) Does kidney transplantation

normalise cortisol metabolism in apparent mineralocorticoid excess syndrome? *J Endocrinol Invest,* 23**,** 457-62.

PAN, Y. J. & YOUNG, D. B. (1982) Experimental aldosterone hypertension in the dog. *Hypertension,* 4**,** 279-87.

PASCUAL-LE TALLEC, L. & LOMBES, M. (2005) The mineralocorticoid receptor: a journey exploring its diversity and specificity of action. *Mol Endocrinol,* 19**,** 2211-21.

PATERSON, J. M., SECKL, J. R. & MULLINS, J. J. (2005) Genetic manipulation of 11beta-hydroxysteroid dehydrogenases in mice. *Am J Physiol Regul Integr Comp Physiol,* 289**,** R642-52.

PEARCE, D., VERREY, F., CHEN, S. Y., MASTROBERARDINO, L., MEIJER, O. C., WANG, J. & BHARGAVA, A. (2000) Role of SGK in mineralocorticoid-regulated sodium transport. *Kidney Int,* 57**,** 1283-9.

PEDERSEN, N. B., HOFMEISTER, M. V., ROSENBAEK, L. L., NIELSEN, J. & FENTON, R. A. (2010) Vasopressin induces phosphorylation of the thiazide-sensitive sodium chloride cotransporter in the distal convoluted tubule. *Kidney Int,* 78**,** 160-9.

PENG, T., SANDS, J. M. & BAGNASCO, S. M. (2002) Glucocorticoids inhibit transcription and expression of the UT-A urea transporter gene. *Am J Physiol Renal Physiol,* 282**,** F853-8.

PHILIPPU, A., PFITSCHER, A. & SINGEWALD, N. (1991) Involvement of catecholaminergic neurones of the nucleus of the solitary tract (NTS) in blood pressure regulation. *J Neural Transm Suppl,* 34**,** 107-12.

PIPPAL, J. B. & FULLER, P. J. (2008) Structure-function relationships in the mineralocorticoid receptor. *J Mol Endocrinol,* 41**,** 405-13.

PITT, B., ZANNAD, F., REMME, W. J., CODY, R., CASTAIGNE, A., PEREZ, A., PALENSKY, J. & WITTES, J. (1999) The effect of spironolactone on morbidity and mortality in patients with severe heart failure. Randomized Aldactone Evaluation Study Investigators. *N Engl J Med,* 341**,** 709-17.

PULKKANEN, K. J., LAUKKANEN, M. O., NAARALA, J. & YLA-HERTTUALA, S. (2000) False-positive apoptosis signal in mouse kidney and liver detected with TUNEL assay. *Apoptosis,* 5**,** 329-33.

QUAMME, G. A. (1981) Effect of furosemide on calcium and magnesium transport in the rat nephron. *Am J Physiol,* 241**,** F340-7.

QUILLEN, E. W., JR., KEIL, L. C. & REID, I. A. (1990) Effects of baroreceptor denervation on endocrine and drinking responses to caval constriction in dogs. *Am J Physiol,* 259**,** R618-26.

RABER, J., AKANA, S. F., BHATNAGAR, S., DALLMAN, M. F., WONG, D. & MUCKE, L. (2000) Hypothalamic-pituitary-adrenal dysfunction in Apoe(-/-) mice: possible role in behavioral and metabolic alterations. *J Neurosci,* 20**,** 2064-71.

REED, B., VARON, J., CHAIT, B. T. & KREEK, M. J. (2009) Carbon dioxide-induced anesthesia results in a rapid increase in plasma levels of vasopressin. *Endocrinology,* 150**,** 2934-9.

REUNGJUI, S., RONCAL, C. A., SATO, W., GLUSHAKOVA, O. Y., CROKER, B. P., SUGA, S., OUYANG, X., TUNGSANGA, K., NAKAGAWA, T., JOHNSON, R. J. & MU, W. (2008) Hypokalemic nephropathy is associated with impaired angiogenesis. *J Am Soc Nephrol,* 19**,** 125-34.

RICHTER, C. P. (1936) Increased salt appetite in adrenalectomized rats. *Am J Physiol,* 115**,** 155-161.

ROBINSON, T. E., GORNY, G., MITTON, E. & KOLB, B. (2001) Cocaine self-administration alters the morphology of dendrites and dendritic spines in the nucleus accumbens and neocortex. *Synapse,* 39**,** 257-66.

ROBSON, A. C., LECKIE, C. M., SECKL, J. R. & HOLMES, M. C. (1998) 11 Beta-hydroxysteroid dehydrogenase type 2 in the postnatal and adult rat brain. *Brain Res Mol Brain Res,* 61**,** 1-10.

ROITMAN, M. F., NA, E., ANDERSON, G., JONES, T. A. & BERNSTEIN, I. L. (2002) Induction of a salt appetite alters dendritic morphology in nucleus accumbens and sensitizes rats to amphetamine. *J Neurosci,* 22**,** RC225.

ROLAND, B. L., LI, K. X. & FUNDER, J. W. (1995) Hybridization histochemical localization of 11 beta-hydroxysteroid dehydrogenase type 2 in rat brain. *Endocrinology,* 136**,** 4697-700.

RONZAUD, C., LOFFING, J., BLEICH, M., GRETZ, N., GRONE, H. J., SCHUTZ, G. & BERGER, S. (2007) Impairment of sodium balance in mice deficient in renal principal cell mineralocorticoid receptor. *J Am Soc Nephrol,* 18**,** 1679-87.

RONZAUD, C., LOFFING, J., GRETZ, N., SCHUTZ, G. & BERGER, S. (2011) Inducible renal principal cell-specific mineralocorticoid receptor gene inactivation in mice. *Am J Physiol Renal Physiol,* 300**,** F756-60.

ROZANSKY, D. J., CORNWALL, T., SUBRAMANYA, A. R., ROGERS, S., YANG, Y. F., DAVID, L. L., ZHU, X., YANG, C. L. & ELLISON, D. H. (2009) Aldosterone mediates activation of the thiazide-sensitive Na-Cl cotransporter through an SGK1 and WNK4 signaling pathway. *J Clin Invest,* 119**,** 2601-12.

SAITO, T., HIGASHIYAMA, M., NAGASAKA, S., SASAKI, S. & ISHIKAWA, S. E. (2001) Role of aquaporin-2 gene expression in hyponatremic rats with chronic vasopressin-induced antidiuresis. *Kidney Int,* 60**,** 1266-76.

SAITO, T., ISHIKAWA, S. E., ANDO, F., HIGASHIYAMA, M., NAGASAKA, S. & SASAKI, S. (2000) Vasopressin-dependent upregulation of aquaporin-2 gene expression in glucocorticoid-deficient rats. *Am J Physiol Renal Physiol,* 279**,** F502-8.

SAKAI, R. R., FINE, W. B., EPSTEIN, A. N. & FRANKMANN, S. P. (1987) Salt appetite is enhanced by one prior episode of sodium depletion in the rat. *Behav Neurosci,* 101**,** 724-31.

SAKAI, R. R., FRANKMANN, S. P., FINE, W. B. & EPSTEIN, A. N. (1989) Prior episodes of sodium depletion increase the need-free sodium intake of the rat. *Behav Neurosci,* 103**,** 186-92.

SANDERS, P. W. (2004) Salt intake, endothelial cell signaling, and progression of kidney disease. *Hypertension,* 43**,** 142-6.

SATO, M. A., COLOMBARI, E. & MORRISON, S. F. (2002) Inhibition of neurons in commissural nucleus of solitary tract reduces sympathetic nerve activity in SHR. *Am J Physiol Heart Circ Physiol,* 282**,** H1679-84.

SCHAFFLHUBER, M., VOLPI, N., DAHLMANN, A., HILGERS, K. F., MACCARI, F., DIETSCH, P., WAGNER, H., LUFT, F. C., ECKARDT, K. U. & TITZE, J. (2007) Mobilization of osmotically inactive Na+ by growth and by dietary salt restriction in rats. *Am J Physiol Renal Physiol,* 292**,** F1490-500.

SCHEUER, D. A., BECHTOLD, A. G. & VERNON, K. A. (2007) Chronic activation of dorsal hindbrain corticosteroid receptors augments the arterial pressure response to acute stress. *Hypertension,* 49**,** 127-33.

SCHNEIDER, E. G., STRANDHOY, J. W., WILLIS, L. R. & KNOX, F. G. (1973) Relationship between proximal sodium reabsorption and excretion of calcium, magnesium and phosphate. *Kidney Int,* 4**,** 369-76.

SCHNERMANN, J., CHOU, C. L., MA, T., TRAYNOR, T., KNEPPER, M. A. & VERKMAN, A. S. (1998) Defective proximal tubular fluid reabsorption in transgenic aquaporin-1 null mice. *Proc Natl Acad Sci U S A,* 95**,** 9660-4.

SCHREIHOFER, A. M. & GUYENET, P. G. (2002) The baroreflex and beyond: control of sympathetic vasomotor tone by GABAergic neurons in the ventrolateral medulla. *Clin Exp Pharmacol Physiol,* 29**,** 514-21.

SCHREIHOFER, A. M., STRICKER, E. M. & SVED, A. F. (1994) Chronic nucleus tractus solitarius lesions do not prevent hypovolemia-induced vasopressin secretion in rats. *Am J Physiol,* 267**,** R965-73.

SCHRIER, R. W. (2003) *Renal and electrolyte disorders,* Boston, Little, Brown.

SHAREGHI, G. R. & AGUS, Z. S. (1982) Magnesium transport in the cortical thick ascending limb of Henle's loop of the rabbit. *J Clin Invest,* 69**,** 759-69.

SHEKHTMAN, E., GEERLING, J. C. & LOEWY, A. D. (2007) Aldosterone-sensitive neurons of the nucleus of the solitary tract: multisynaptic pathway to the nucleus accumbens. *J Comp Neurol,* 501**,** 274-89.

SHI, H., CUI, H., ALAM, G., GUNNING, W. T., NESTOR, A., GIOVANNUCCI, D., ZHANG, M. & DING, H. F. (2008) Nestin expression defines both glial and neuronal progenitors in postnatal sympathetic ganglia. *J Comp Neurol,* 508**,** 867-78.

SINGEWALD, N., KLAUSMAIR, A. & PHILIPPU, A. (1992) Blood pressure changes modify the release rates of catecholamines in the intermediate nucleus of the solitary tract. *Naunyn Schmiedebergs Arch Pharmacol,* 345**,** 176-80.

SINGH, R. R., MORITZ, K. M., BERTRAM, J. F. & CULLEN-MCEWEN, L. A. (2007) Effects of dexamethasone exposure on rat metanephric development: in vitro and in vivo studies. *Am J Physiol Renal Physiol,* 293**,** F548-54.

SOHARA, E., RAI, T., MIYAZAKI, J., VERKMAN, A. S., SASAKI, S. & UCHIDA, S. (2005) Defective water and glycerol transport in the proximal tubules of AQP7 knockout mice. *Am J Physiol Renal Physiol,* 289**,** F1195-200.

SPELLER, A. M. & MOFFAT, D. B. (1977) Tubulo-vascular relationships in the developing kidney. *J Anat,* 123**,** 487-500.

STANTON, B. A. (1986) Regulation by adrenal corticosteroids of sodium and potassium transport in loop of Henle and distal tubule of rat kidney. *J Clin Invest,* 78**,** 1612-20.

STAUB, O., DHO, S., HENRY, P., CORREA, J., ISHIKAWA, T., MCGLADE, J. & ROTIN, D. (1996) WW domains of Nedd4 bind to the proline-rich PY motifs in the epithelial Na+ channel deleted in Liddle's syndrome. *EMBO J,* 15**,** 2371-80.

STEWART, P. M., CORRIE, J. E., SHACKLETON, C. H. & EDWARDS, C. R. (1988) Syndrome of apparent mineralocorticoid excess. A defect in the cortisol-cortisone shuttle. *J Clin Invest,* 82**,** 340-9.

STEWART, P. M., KROZOWSKI, Z. S., GUPTA, A., MILFORD, D. V., HOWIE, A. J., SHEPPARD, M. C. & WHORWOOD, C. B. (1996) Hypertension in the syndrome of apparent mineralocorticoid excess due to mutation of the 11 beta-hydroxysteroid dehydrogenase type 2 gene. *Lancet,* 347**,** 88-91.

STEWART, P. M., ROGERSON, F. M. & MASON, J. I. (1995) Type 2 11 beta-hydroxysteroid dehydrogenase messenger ribonucleic acid and activity in human placenta and fetal membranes: its relationship to birth weight and putative role in fetal adrenal steroidogenesis. *J Clin Endocrinol Metab,* 80**,** 885-90.

STEWART, P. M., WALLACE, A. M., VALENTINO, R., BURT, D., SHACKLETON, C. H. & EDWARDS, C. R. (1987) Mineralocorticoid activity of liquorice: 11-beta-hydroxysteroid dehydrogenase deficiency comes of age. *Lancet,* 2**,** 821-4.

STRAZZULLO, P., D'ELIA, L., KANDALA, N. B. & CAPPUCCIO, F. P. (2009) Salt intake, stroke, and cardiovascular disease: meta-analysis of prospective studies. *BMJ,* 339**,** b4567.

STRICKER, E. M. & SVED, A. F. (2000) Thirst. *Nutrition,* 16**,** 821-6.

STRICKLER, J. C., THOMPSON, D. D., KLOSE, R. M. & GIEBISCH, G. (1964) Micropuncture Study of Inorganic Phosphate Excretion in the Rat. *J Clin Invest,* 43**,** 1596-607.

SUGA, S. I., PHILLIPS, M. I., RAY, P. E., RALEIGH, J. A., VIO, C. P., KIM, Y. G., MAZZALI, M., GORDON, K. L., HUGHES, J. & JOHNSON, R. J. (2001) Hypokalemia induces renal injury and alterations in vasoactive mediators that favor salt sensitivity. *Am J Physiol Renal Physiol,* 281**,** F620-9.

SUN, T. X., VAN HOEK, A., HUANG, Y., BOULEY, R., MCLAUGHLIN, M. & BROWN, D. (2002) Aquaporin-2 localization in clathrin-coated pits: inhibition of endocytosis by dominant-negative dynamin. *Am J Physiol Renal Physiol,* 282**,** F998-1011.

TCHAPYJNIKOV, D., LI, Y., PISITKUN, T., HOFFERT, J. D., YU, M. J. & KNEPPER, M. A. Proteomic profiling of nuclei from native renal inner medullary collecting duct cells using LC-MS/MS. *Physiol Genomics,* 40**,** 167-83.

TERRIS, J., ECELBARGER, C. A., NIELSEN, S. & KNEPPER, M. A. (1996) Long-term regulation of four renal aquaporins in rats. *Am J Physiol,* 271**,** F414-22.

THOMAS, N. (2008) *Renal nursing,* Edinburgh ; New York, Baillière Tindall Elsevier.

THRASHER, T. N., KEIL, L. C. & RAMSAY, D. J. (1982) Lesions of the organum vasculosum of the lamina terminalis (OVLT) attenuate osmotically-induced drinking and vasopressin secretion in the dog. *Endocrinology,* 110**,** 1837-9.

THRASHER, T. N., NISTAL-HERRERA, J. F., KEIL, L. C. & RAMSAY, D. J. (1981) Satiety and inhibition of vasopressin secretion after drinking in dehydrated dogs. *Am J Physiol,* 240**,** E394-401.

TIAN, Y., SANDBERG, K., MURASE, T., BAKER, E. A., SPETH, R. C. & VERBALIS, J. G. (2000) Vasopressin V2 receptor binding is down-regulated during renal escape from vasopressin-induced antidiuresis. *Endocrinology,* 141**,** 307-14.

TIERNEY, L. M. (2004) *Current medical diagnosis & treatment 2004,* New York, Lange Medical/McGraw-Hill.

TRONCHE, F., KELLENDONK, C., KRETZ, O., GASS, P., ANLAG, K., ORBAN, P. C., BOCK, R., KLEIN, R. & SCHUTZ, G. (1999) Disruption of the glucocorticoid receptor gene in the nervous system results in reduced anxiety. *Nat Genet,* 23**,** 99-103.

TSIGELNY, I. & BAKER, M. E. (1995) Structures important in mammalian 11 beta- and 17 beta-hydroxysteroid dehydrogenases. *J Steroid Biochem Mol Biol,* 55**,** 589-600.

UCHIDA, S., SASAKI, S., FURUKAWA, T., HIRAOKA, M., IMAI, T., HIRATA, Y. & MARUMO, F. (1993) Molecular cloning of a chloride channel that is regulated by dehydration and expressed predominantly in kidney medulla. *J Biol Chem,* 268**,** 3821-4.

ULICK, S., LEVINE, L. S., GUNCZLER, P., ZANCONATO, G., RAMIREZ, L. C., RAUH, W., ROSLER, A., BRADLOW, H. L. & NEW, M. I. (1979) A syndrome of apparent mineralocorticoid excess associated with defects in the peripheral metabolism of cortisol. *J Clin Endocrinol Metab,* 49**,** 757-64.

ULICK, S., TEDDE, R. & MANTERO, F. (1990) Pathogenesis of the type 2 variant of the syndrome of apparent mineralocorticoid excess. *J Clin Endocrinol Metab,* 70**,** 200-6.

UNWIN, R. J., LUFT, F. C. & SHIRLEY, D. G. (2011) Pathophysiology and management of hypokalemia: a clinical perspective. *Nat Rev Nephrol,* 7**,** 75-84.

VAN LIEBURG, A. F., KNOERS, N. V. & MONNENS, L. A. (1999) Clinical presentation and follow-up of 30 patients with congenital nephrogenic diabetes insipidus. *J Am Soc Nephrol,* 10**,** 1958-64.

VAN UUM, S. H., HERMUS, A. R., SMITS, P., THIEN, T. & LENDERS, J. W. (1998) The role of 11 beta-hydroxysteroid dehydrogenase in the pathogenesis of hypertension. *Cardiovasc Res,* 38**,** 16-24.

VELAZQUEZ, H., BARTISS, A., BERNSTEIN, P. & ELLISON, D. H. (1996) Adrenal steroids stimulate thiazide-sensitive NaCl transport by rat renal distal tubules. *Am J Physiol,* 270**,** F211-9.

VIENGCHAREUN, S., LE MENUET, D., MARTINERIE, L., MUNIER, M., PASCUAL-LE TALLEC, L. & LOMBES, M. (2007) The mineralocorticoid receptor: insights into its molecular and (patho)physiological biology. *Nucl Recept Signal,* 5**,** e012.

VOORHIES, A. C. & BERNSTEIN, I. L. (2006) Induction and expression of salt appetite: effects on Fos expression in nucleus accumbens. *Behav Brain Res,* 172**,** 90-6.

WALL, S. M., HAN, J. S., CHOU, C. L. & KNEPPER, M. A. (1992) Kinetics of urea and water permeability activation by vasopressin in rat terminal IMCD. *Am J Physiol,* 262**,** F989-98.

WALSH, S. B., UNWIN, E., VARGAS-POUSSOU, R., HOUILLIER, P. & UNWIN, R. (2011) Does hypokalaemia cause nephropathy? an observational study of renal function in patients with Bartter or Gitelman syndrome. *QJM*.

WALTHER, R. F., ATLAS, E., CARRIGAN, A., ROULEAU, Y., EDGECOMBE, A., VISENTIN, L., LAMPRECHT, C., ADDICKS, G. C., HACHE, R. J. & LEFEBVRE, Y. A. (2005) A serine/threonine-rich motif is one of three nuclear localization signals that determine unidirectional transport of the mineralocorticoid receptor to the nucleus. *J Biol Chem,* 280**,** 17549-61.

WANG, L., FLANNERY, P. J., ATHIRAKUL, K., DUNN, S. R., KOURANY, W. M. & SPURNEY, R. F. (2006) Galphaq-dependent signaling cascades stimulate water-seeking behavior. *Am J Physiol Renal Physiol,* 291**,** F781-9.

WANG, W. H. (1994) Two types of K+ channel in thick ascending limb of rat kidney. *Am J Physiol,* 267**,** F599-605.

WEINER, H. & HURLEY, T. D. (2005) NAD(P)+ Binding to Dehydrogenases. *eLS*.

WELBERG, L. A., SECKL, J. R. & HOLMES, M. C. (2000) Inhibition of 11beta-hydroxysteroid dehydrogenase, the foeto-placental barrier to maternal glucocorticoids, permanently programs amygdala GR mRNA expression and anxiety-like behaviour in the offspring. *Eur J Neurosci,* 12**,** 1047-54.

WELBERG, L. A., SECKL, J. R. & HOLMES, M. C. (2001) Prenatal glucocorticoid programming of brain corticosteroid receptors and corticotrophin-releasing hormone: possible implications for behaviour. *Neuroscience,* 104**,** 71-9.

WERDER E, ZACHMANN M, VOLLMIN, J. A., VEYRAT, R. & PRADER, A. (1974) Unusual steroid excretion in a child with low renin hypertension. *Res Steroids,* 6**,** 385-359.

WILKINS, L. & RICHTER, C. P. (1940) A great craving for salt by a child with cortico-adrenal insufficiency. *JAMA,* 144**,** 866-868.

WILSON, F. H., KAHLE, K. T., SABATH, E., LALIOTI, M. D., RAPSON, A. K., HOOVER, R. S., HEBERT, S. C., GAMBA, G. & LIFTON, R. P. (2003)

Molecular pathogenesis of inherited hypertension with hyperkalemia: the Na-Cl cotransporter is inhibited by wild-type but not mutant WNK4. *Proc Natl Acad Sci U S A,* 100**,** 680-4.

WOO, S. K., LEE, S. D. & KWON, H. M. (2002) TonEBP transcriptional activator in the cellular response to increased osmolality. *Pflugers Arch,* 444**,** 579-85.

WULFF, P., VALLON, V., HUANG, D. Y., VOLKL, H., YU, F., RICHTER, K., JANSEN, M., SCHLUNZ, M., KLINGEL, K., LOFFING, J., KAUSELMANN, G., BOSL, M. R., LANG, F. & KUHL, D. (2002) Impaired renal Na(+) retention in the sgk1-knockout mouse. *J Clin Invest,* 110**,** 1263-8.

YAMAGUCHI, H., AKITAYA, T., YU, T., KIDACHI, Y., KAMIIE, K., NOSHITA, T., UMETSU, H. & RYOYAMA, K. (2011a) Homology modeling and structural analysis of 11beta-hydroxysteroid dehydrogenase type 2. *Eur J Med Chem,* 46**,** 1325-30.

YAMAGUCHI, H., AKITAYA, T., YU, T., KIDACHI, Y., KAMIIE, K., NOSHITA, T., UMETSU, H. & RYOYAMA, K. (2011b) Molecular docking and structural analysis of cofactor-protein interaction between NAD(+) and 11beta-hydroxysteroid dehydrogenase type 2. *J Mol Model*.

YANG, B., GILLESPIE, A., CARLSON, E. J., EPSTEIN, C. J. & VERKMAN, A. S. (2001) Neonatal mortality in an aquaporin-2 knock-in mouse model of recessive nephrogenic diabetes insipidus. *J Biol Chem,* 276**,** 2775-9.

YANG, B., ZHAO, D., QIAN, L. & VERKMAN, A. S. (2006) Mouse model of inducible nephrogenic diabetes insipidus produced by floxed aquaporin-2 gene deletion. *Am J Physiol Renal Physiol,* 291**,** F465-72.

YANG, C. L., ANGELL, J., MITCHELL, R. & ELLISON, D. H. (2003) WNK kinases regulate thiazide-sensitive Na-Cl cotransport. *J Clin Invest,* 111**,** 1039-45.

YANG, K. (1997) Placental 11 beta-hydroxysteroid dehydrogenase: barrier to maternal glucocorticoids. *Rev Reprod,* 2**,** 129-32.

YANG, M., TRETTEL, L. B., ADAMS, D. J., HARRISON, J. R., CANALIS, E. & KREAM, B. E. (2010) Col3.6-HSD2 transgenic mice: a glucocorticoid loss-of-function model spanning early and late osteoblast differentiation. *Bone,* 47**,** 573-82.

YOO, T. H., RYU, D. R., SONG, Y. S., LEE, S. C., KIM, H. J., KIM, J. S., CHOI, H. Y. & KANG, S. W. (2006) Congenital nephrogenic diabetes insipidus presented with bilateral hydronephrosis: genetic analysis of V2R gene mutations. *Yonsei Med J,* 47**,** 126-30.

YOUNG, D. B. (1988) Quantitative analysis of aldosterone's role in potassium regulation. *Am J Physiol,* 255**,** F811-22.

YOUNG, D. B. & JACKSON, T. E. (1982) Effects of aldosterone on potassium distribution. *Am J Physiol,* 243**,** R526-30.

YUN, C. H., TSE, C. M., NATH, S. K., LEVINE, S. A., BRANT, S. R. & DONOWITZ, M. (1995) Mammalian Na+/H+ exchanger gene family: structure and function studies. *Am J Physiol,* 269**,** G1-11.

YUN, J., SCHONEBERG, T., LIU, J., SCHULZ, A., ECELBARGER, C. A., PROMENEUR, D., NIELSEN, S., SHENG, H., GRINBERG, A., DENG, C. & WESS, J. (2000) Generation and phenotype of mice harboring a nonsense mutation in the V2 vasopressin receptor gene. *J Clin Invest,* 106**,** 1361-71.

ZANUTTO, B. S., VALENTINUZZI, M. E. & SEGURA, E. T. (2010) Neural set point for the control of arterial pressure: role of the nucleus tractus solitarius. *Biomed Eng Online,* 9**,** 4.

ZHANG, X., ZHENG, X., SUN, H., FENG, B., CHEN, G., VLADAU, C., LI, M., CHEN, D., SUZUKI, M., MIN, L., LIU, W., GARCIA, B., ZHONG, R. & MIN, W. P. (2006) Prevention of renal ischemic injury by silencing the expression of renal caspase 3 and caspase 8. *Transplantation,* 82**,** 1728-32.

ZHAO, D., BANKIR, L., QIAN, L., YANG, D. & YANG, B. (2006) Urea and urine concentrating ability in mice lacking AQP1 and AQP3. *Am J Physiol Renal Physiol,* 291**,** F429-38.

ZHAO, D. Q. & AI, H. B. (2011) Oxytocin and vasopressin involved in restraint water-immersion stress mediated by oxytocin receptor and vasopressin 1b receptor in rat brain. *PLoS One,* 6**,** e23362.

ZINGG, H. H., LEFEBVRE, D. & ALMAZAN, G. (1986) Regulation of vasopressin gene expression in rat hypothalamic neurons. Response to osmotic stimulation. *J Biol Chem,* 261**,** 12956-9.